EXPERIMENTAL STUDY OF NATURAL COMPOSITE DESICCANT-BASED DEHUMIDIFICATION SYSTEM

Thesis

Submitted in partial fulfilment of the requirement for the degree of

DOCTOR OF PHILOSOPHY

by

SANGAPPA R. DASAR

(Reg. No. 177022ME015)

DEPARTMENT OF MECHANICAL ENGINEERING

NATIONAL INSTITUTE OF TECHNOLOGY KARNATAKA

SURATHKAL, MANGALURU – 575025

FEBRUARY, 2024

EXPERIMENTAL STUDY OF NATURAL COMPOSITE DESICCANT-BASED DEHUMIDIFICATION SYSTEM

Thesis

Submitted in partial fulfilment of the requirement for the degree of

DOCTOR OF PHILOSOPHY

by

SANGAPPA R. DASAR

(Reg. No. 177022ME015)

Under the guidance of

Dr. ANISH S. & Dr. AJAY KUMAR YADAV

DEPARTMENT OF MECHANICAL ENGINEERING

NATIONAL INSTITUTE OF TECHNOLOGY KARNATAKA

SURATHKAL, MANGALURU – 575025

FEBRUARY, 2024

DECLARATION

I hereby declare that the Research Thesis entitled **"EXPERIMENTAL STUDY OF NATURAL COMPOSITE DESICCANT-BASED DEHUMIDIFICATION SYSTEM"** which is being submitted to the **National Institute of Technology Karnataka, Surathkal** in partial fulfillment of the requirements for the award of the degree of **Doctor of Philosophy** in **Mechanical Engineering** is a *bonafide report of the research work carried out by me*. The material contained in this thesis has not been submitted to any University or Institution for the award of any degree.

Register Number: **177022ME015**

Name of the Research Scholar: **SANGAPPA R. DASAR**

Signature of the Research Scholar: S. R. Dasar

Department of Mechanical Engineering

Place: NITK, Surathkal

Date: 16.02.2024

CERTIFICATE

This is to certify that the Research Thesis entitled **"EXPERIMENTAL STUDY OF NATURAL COMPOSITE DESICCANT-BASED DEHUMIDIFICATION SYSTEM"** submitted by **Mr. SANGAPPA R. DASAR (Register Number: 177022ME015)** as the record of the research work carried out by him, *is accepted as the Research Thesis submission* in partial fulfilment of the requirements for the award of the degree of **Doctor of Philosophy**.

Research Guides

20/2/2024

Dr. Anish S.
Department of Mechanical Engineering
NITK Suarthkal

Dr. Ajay Kumar Yadav
Department of Mechanical Engineering
NITK Surathkal
Presently on-lien:
Department of Mechanical Engineering
IIT Patna

राष्ट्रीय प्रौद्योगिकी संस्थान, कर्नाटक
यांत्रिकी अभियांत्रिकी विभाग
Dept. of Mechanical Engineering
National Institute of Technology

16/2/2024

Chairman-DRPC
Department of Mechanical Engineering
National Institute of Technology Karnataka
Surathkal, Mangaluru - 575025

Dedicated
to
my
Beloved Parents
and
Teachers
Whose Love and Support
Sustained Me Throughout

ACKNOWLEDGEMENT

The journey of completing my PhD has been head over heels, with failures and learning. But amid all the lows, few people stood by me and kept motivating me to step further. This thesis will be incomplete without expressing my gratitude to all those who have been my strength and left an affirmative mark on this journey. I would like to begin with my warmest thanks and acknowledgement to my supervisors, **Dr. Anish S.** and **Dr. Ajay Kumar Yadav** for their guidance, patience, and support. I have been benefited greatly from their wealth of knowledge and fastidious editing. I am extremely grateful that they took me as a research scholar and continued to have faith in me over the years that I will never forget.

I am thankful to **Dr. S. M. Murigendrappa**, Professor and Head, Department of Mechanical Engineering, for the support and providing facilities required to complete this research work successfully. Furthermore, I take this opportunity to acknowledge the former heads of mechanical engineering, **Dr. Ravikiran Kadoli, Dr. Narendranath S., Dr. Shrikantha S. Rao, Dr. Satyabodh M. Kulkarni and Dr. Gangadharan K.V.,** for their support and encouragement. I would also wish to express my gratitude to my RPAC members, **Dr. Ranjith M.** and **Dr. Preetham Kumar G. V.**, for their extended discussions and valuable suggestions, which have contributed greatly to the improvement of this thesis. I am thankfull to **Dr. Bhawana Rudra** and her research scholar, **Dr. Swathi Mummadi** and my friend, **Dr. Ram Babu**, who helped me in thesis type setting in LaTeX. I am thankful to **Dr. Vasudeva M. & Dr. Veershetty G.,** for the financial support and an opportunity to work as project associate at Maire Tecnimont Centre for Clean Energy Transition.

A very special word of thanks goes to my father **Ramanna J. Pujari** (not in my official records), and my mother, **Rangavva**, for their endless supports and unwavering belief in me. Avva, thank you for making number of untold sacrifices for the entire family. Appa, you are a great inspiration to me; thank you for all of your love, and without you, I would not be the person I am today. The Deepest thanks to my younger brother, **Ayyappa R. Dasar** and younger sister **Giravva R. Dasar (Girija)**, always supported my educational journey and letting me be vulnerable about sharing my dark and damaged past and leaving such wonderful, heartfelt comments. My thanks are extended to my maternal uncles **Shasappa G. Dasar, Hanamantha G. Dasar, Srinivas G. Dasar and their family,** and my cousins and all my relatives for their support and love. I hope that I have made all of them proud.

A warm word for my co-research scholar and great friend **Manu J.** always made me feel special and shared moments of deep anxiety and immense excitement. I would like to thank all my Ph.D. colleagues, Dr. Nidhul K., Dr. Mukund Patil, Dr. Prakash, Dr. Anteneh Wogasso, Dr. Santosh K., Dr. Arun Kumar D. S., Mr. Ranjan Yadav, Dr. Vishwanth Bajanthri, Mr. Nethrananda Behra, and my seniors Dr. Lokesh B. Paradeshi (NITC), Dr. Rajesh Kana (NITC), Dr. Prashantha B., Dr. SushanLal Babu, Dr. Deepak Nararayanan, Dr. Madagonda Biradar, Dr. Shankar Kodate, Dr. Thippeswamy L. R., Dr.Venkatesh T. Lamani, Dr. Tabish Wahidi, Dr. Rudramurty, Dr. Mithun Kumar Kanchan, Dr. Abdul Buradi, Mr. Deepak Kolke, Mr. Chandramouli, Mr. Lakshman Nayak, Mr. Shanegouda T. G., Mr. Rakesh, list seems to be endless. Many others have been instrumental in this process. I would like to appreciate the generous assistance from Yathin Devadiga, Vishal Kumar, Vinayaraj M. K., Yashpal, Krishna, and Ashok staffs of IC engine lab at various stages in the completion of my work.

I feel immense gratitude for being granted the privilege of studying at the esteemed National Institute of Technology Karnataka, Surathkal. I am extremely grateful to the Mechanical Engineering department NITK Surathkal, the faculties and the non-teaching staffs for providing all the facilities for my research work. I earnestly regret to numerous

others whom I forgot to cite. However, their contributions are also equally significant to me for completing my thesis successfully.

SANGAPPA R. DASAR
FEBRUARY, 2024
NITK, SURATHKAL

ABSTRACT

This study investigates the sorption and desorption characteristics of a natural composite desiccant based on dried cow dung (DCD). The first part of the study focuses on finding out an effective binding material for DCD. For this Polyvinyl Pyrrolidone (PVP) and clay are selected as binders. The moisture uptake capacity of composite desiccants is measured with an isotherm experiment under different DCD-to-binder ratios. Based on their isotherms, composite desiccants are chosen for the study under different humid conditions and compared with available literature data. Brunauer-Emmett-Teller and Barrett-Joyner-Halenda analyses are carried out to understand the physical properties of DCD, DCD+PVP (3:1 ratio) and DCD+Clay (3:1 ratio). Total heat load reduction, exergy efficiency and power required for these dehumidification systems are calculated for different inlet conditions. Desorption characteristics are tested at 328 K and 6% RH. Results show the maximum moisture uptake capacity of DCD and DCD+PVP as 9.87 and 9.01 g/100 g, respectively. The maximum exergy efficiency of the DCD+PVP dehumidification system is found to be 55%. The desorption time for DCD+PVP desiccant is 17 minutes, which is 4 and 2 minutes higher compared to DCD, and DCD+Clay, respectively.

In the second phase of the study, a natural composite desiccant, in which the unutilized portion of the spherical desiccant material is replaced with a metallic ball, is proposed. Stainless steel balls with a diameter of 4.75 and 6.35 mm are used to make different thickness ratios (TR = 1, 0.525, and 0.365) of metal-embedded natural composite desiccants (MENCDs). The natural composite desiccant is prepared from dried cow dung and polyvinyl pyrrolidone with a ratio of 3:1. Experiments are conducted to

find the optimum thickness ratio of MENCDs. The total moisture sorption, moisture sorption rate, total heat load reduction, and exergy efficiency of these dehumidification systems are investigated under different relative humidities (RH = 65%, 75% and 85%), and at a constant temperature and velocity. Desorption characteristics are tested at 328 K and 5% RH. The maximum moisture upatake capacity of MENCDs with a TR of 0.365 is found to be 11.84 g/100 g, which is 17% higher compared to natural composite desiccants (i.e., TR = 1) at 85% RH, whereas, the total moisture sorption rate is 0.4 g/100 g·min, which is 20.57% higher for TR of 0.365 compared to TR = 1. The moisture desorption rate for TR = 0.365 is 16.66% higher compared to TR = 1. The systems exhibit an average exergy efficiency of 60%. However, when employing composite desiccants with a TR of 0.365, their average exergy efficiency improves by 9.6% compared to the systems operating with TR = 1. Furthermore, the average reduction in total heat load with TR = 0.365 is 24% higher compared to those utilizing TR = 1.

Further studies are carried out to reduce the pressure loss across the dehumidification bed and increase the moisture sorption capacity. To achieve this the dehumidification bed is designed with staggered hexagonal aluminium channels (SHACs). The natural composite desiccant (NCD) was prepared by coating the mixture onto the channels with a 2:1 ratio of DCD:PVP due to better coatability. The results of the study show that the NCD-coated SHACs dehumidification system had a high moisture sorption capacity, with maximum moisture sorption values ranging from 8.34 to 14.31 g/100 g at different RH and temperature conditions. The system also shows an average moisture sorption rate of 0.26 g/100 g·min and a desorption rate of 0.51 g/100 g·min. Furthermore, the moisture flow design of the NCD-coated SHACs bed results in a low-pressure drop of 0.13 kPa, which is significantly lower than the NCD-packed bed.

Keywords: Natural composite desiccants, Metal embedded natural composites, Staggered hexagonal aluminium channels, Dehumidification system, Total heat load reduction, Exergetic analysis.

TABLE OF CONTENTS

LIST OF TABLES

LIST OF FIGURES

CHAPTER 1

INTRODUCTION

1.1 Need of desiccant based air conditioning system

According to International Energy Agency, the demand for air conditioners (ACs) and the energy consumption of these systems will be tripled by 2050. This will lead to increased emissions of greenhouse gases (Birol 2018). The United Nations estimate that if hydrofluorocarbons are not phased out, they could cause global temperatures to rise up to an extra 0.4 K by 2100 (Davis *et al.* 2021). Statistics show that ACs are concentrated in very few countries. In fact 66.66% of all AC systems are in just three countries viz., China, United States, and Japan (Fig.1.1). The demand will grow to 5.6 billion by 2050, which amounts to 10 new ACs sold every second for the next 30 years. It is estimated that by 2050, around 67% of the world's households will have an air conditioner (Strobel *et al.* 2023; Birol 2018). In this China, India and Indonesia will together account for half of the total number. The use of air conditioners and electric fans accounts about a fifth of the total electricity in buildings around the world, which is 10% of all global electricity consumption. During 1990, the energy consumption of these systems was just 2%, in 2016 it rose to 6% (Dhawan *et al.* 2023; Birol 2018). The percentage of households equipped with AC in selected countries as of 2018 is shown in Fig.1.2. Houses in Japan, the United States, and Korea are equipped with ACs is about 91%, 90%, and 86% respectively. The total energy consumed by these 1.6 billion systems is about 11,675 GW as of 2016. As of 2018, only 5% Indian houses are equipped with air conditioning systems (Birol 2018).

India is one of the fastest growing economy in the world. With the economic progress in the country there can be a surge in the Indian market for ACs in the coming year. This may lead to more energy consumption and create additional load on the energy sector. In this scenario alternate air conditioning systems which use less energy and more environment friendly are of great significance. Desiccant based evaporative cooling is one such method.

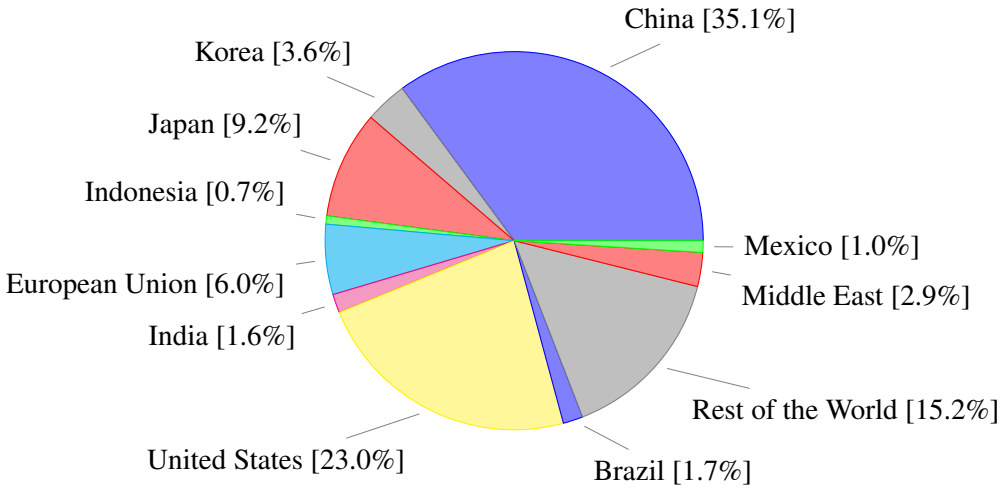

Figure 1.1: Stock of ACs by country/region end of 2016 (Birol 2018)

1.2 How desiccant based air-conditioning system works?

Desiccant dehumidification is entirely a low-grade thermal energy process and can be utilized in both in industrial air conditioning and dehumidification applications. According to research conducted on human comfort, indoor air conditioning is most comfortable within the range of 45 - 60% relative humidity (RH) and 21 - 27 °C temperature (Arens *et al.* 2017; Dai *et al.* 2017). The air conditioning systems mainly consists of two heat load components. One is sensible heat load and another one is latent heat load. In conventional air conditioning systems, to remove the latent heat, vapour compression systems (VCS) are used to cool the air below its dew point to condense out water vapour contained within. The dehumidified air is then warmed to have the desired indoor conditions. Cooling of air below dew point temperature reduces the coefficient

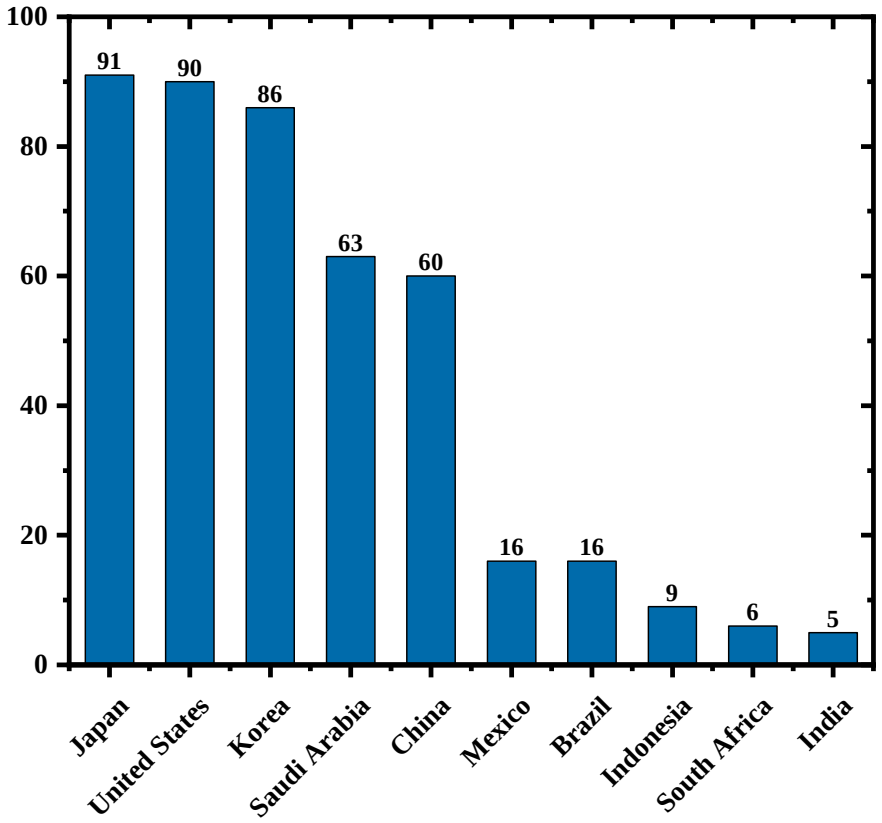

Figure 1.2: Percentage of households equipped with AC in selected countries as of 2018 (Birol 2018)

of performance (COP) of air conditioning system. The energy required for dehumidification, or latent cooling, increases the power input while the refrigeration capacity remains relatively constant. Since the power input increases while the refrigeration capacity remains the same or slightly decreases, the overall COP decreases. If the latent load is handled by other methods then this deep cooling can be avoided (Cui *et al.* 2018). Desiccant-based air conditioning system has the ability to abstain from this deep cooling process with the help of desiccant materials. The schematic of desiccant based evaporative cooling system is shown in Fig. 1.3

The difference between the process of conventional air conditioning and desiccant-based cooling is shown in psychrometric chart (Fig. 1.4). The Energy consumption by the conventional air conditioning system to reach from point 1 to 3, which will be

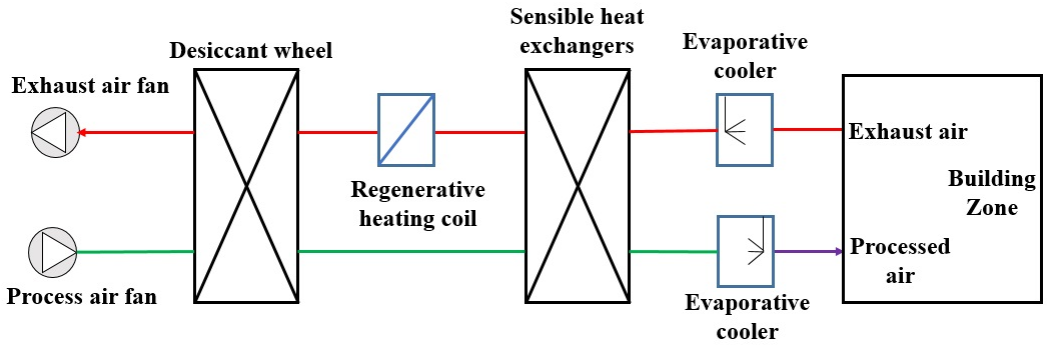

Figure 1.3: Schematic diagram of solid desiccant-based evaporative cooling system

30-40% higher compared to the desiccant-based evaporative cooling system, this can be observed from the Fig. 1.4. In hot and humid region, the relative humidity and temperature between 70-90% and 295-306 K respectively, which causes discomforts to the inhabitants. The desiccant-based evaporative cooling consists of two process one is dehumidification and another sensible cooling.

The different methods used to dehumidify the moist air are shown in Fig.1.5. Namely, first one is the refrigeration (or mechanical) dehumidification, which is based on the principles of cooling and condensation. It utilizes a refrigeration cycle similar to that of an air conditioner. Seoncd one, compression dehumidification, also known as desiccant-assisted dehumidification, combines both refrigeration and desiccant technologies to enhance dehumidification efficiency. Third one, sorption dehumidification method employs a solid or liquid desiccant material to remove moisture from the air. In this method no refrigerant and compressor is used. Since the 1920's desiccant materials have been used for dehumidification purposes including process improvement and product protection. In the past twenty years, the use of desiccant dehumidification has expanded into new areas including hospitals, hotels, ice rinks, and supermarkets (Li *et al.* 2021). Still, more recently, the possibilities of applying desiccant-based cooling technologies to office and residential buildings have been explored. The wide acceptance of desiccant-based cooling technology and the expanding markets for these materials have created a competitive production environment.

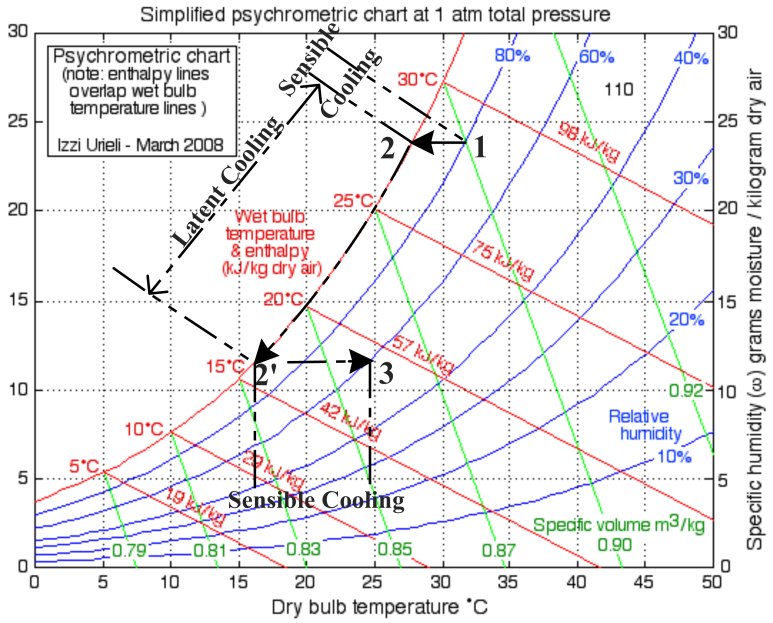

(a)

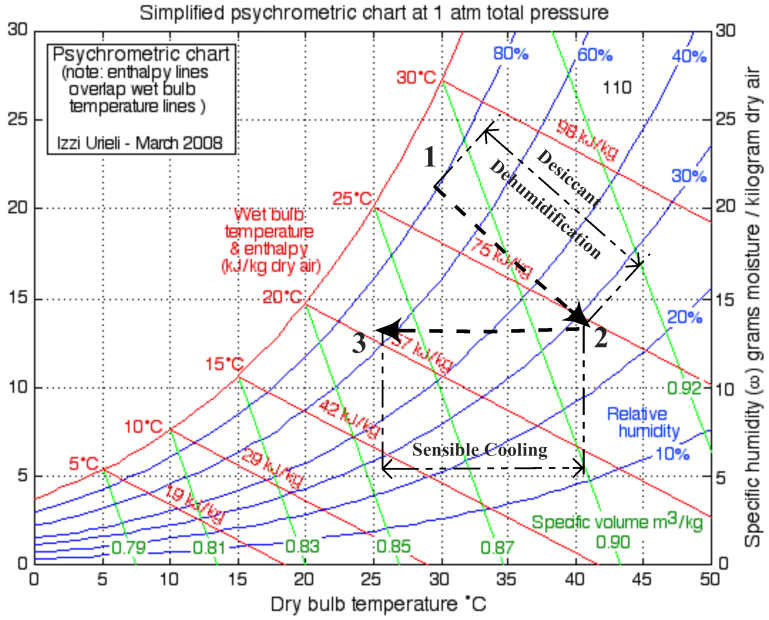

(b)

Figure 1.4: Representation of (a) conventional air conditioning and (b) desiccant-based evaporative cooling through psychrometric chart

The desiccant based-air conditioning industry is continually looking for an im-

proved desiccant material. Specifically, research within the field of air conditioning technology has focused on developing new desiccant materials capable of removing both sensible and latent energy within a single process. Compression methods and refrigeration methods are widely used till now. The current trend is shifting toward the sorption methods, due to less power consumption and being environmentally friendly. Hence, desiccant based dehumidification systems are used to control the humidity. Moreover, the utilization of advanced materials and innovative designs is being explored to enhance the performance and efficiency of desiccant-based air conditioning systems. These advancements aim to optimize the desiccant regeneration process, increase moisture removal capacity, and minimize the overall energy consumption.

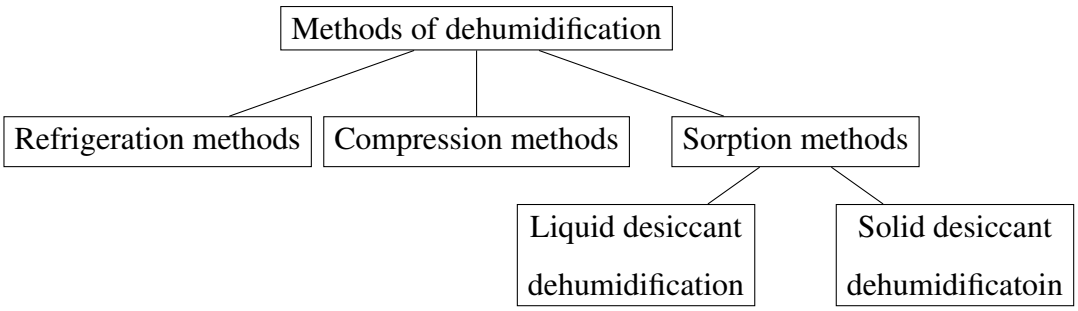

Figure 1.5: Methods of dehumidification

1.3 Types of desiccants

Desiccants are mainly classified as liquid and solid desiccants. Some of the solid desiccants are as follows:

Silica Gel: Silica gel is a popular and widely used desiccant. It is a porous, granular form of silicon dioxide that can absorb moisture effectively. Silica gel is often found in small packets in product packaging to prevent moisture-related damage.

Calcium Chloride: Calcium chloride is a hygroscopic compound that can absorb large amounts of moisture from the air. It is commonly used as a desiccant in industrial and commercial applications. Calcium chloride can also be used in pellet or powder form.

Molecular Sieve: Molecular sieves are crystalline metal aluminosilicates with a three-dimensional porous structure. They have a high affinity for water molecules and can selectively absorb moisture. Molecular sieves are often used in applications that require the removal of water vapor from gases or liquids.

Activated Carbon: Activated carbon, also known as activated charcoal, is a highly porous material with a large surface area. While its primary purpose is adsorption of gases and impurities, activated carbon can also absorb moisture from the air. It is commonly used in combination with other desiccants.

Clay Desiccants: Clay desiccants are made from natural clay minerals such as montmorillonite. They have a high water-absorption capacity and are often used in packaging to protect goods from moisture damage.

Zeolites: Zeolites are microporous minerals with a unique structure that allows them to selectively adsorb water molecules. They are commonly used as desiccants in various applications, including drying air and gases.

The solid desiccants are further classified based on the pore size distribution, which is shown in Fig. 1.6. Solid sorbents usually have the properties of a porous material with different pore sizes. These can maintain their properties if they are heated up so they can desorb the sorbed moisture or other gases and therefore regain their original state. This makes them very useful in applications like dehumidifiers. According to the international union of pure and applied chemistry (IUPAC), the pore size of a solid desiccant less than 2 nm, is called microporous, between 2 and 50 nm is called mesoporous, and above 50 nm is called macroporous.

In recent years, there has been a significant shift in research focus towards the investigation of composite desiccants, with the primary goal of enhancing the efficiency and effectiveness of humidity control systems. The conventional use of single-component desiccants has demonstrated certain limitations, including slow adsorption rates, material degradation, and limited capacity for moisture removal. To overcome these chal-

lenges, researchers have delved into the potential of composite desiccants, which involve combinations of different desiccant materials. The concept behind composite desiccants lies in the amalgamation of desiccant materials that possess complementary properties. By leveraging the synergistic effects of these materials, researchers aim to address the limitations associated with single-component desiccants. This approach has shown promising results, as composite desiccants can exhibit enhanced moisture adsorption capacities, faster adsorption and regeneration rates, and improved stability under various operating conditions.

Beyond laboratory investigations, researchers are also keen on assessing the real-world performance of composite desiccants. This evaluation encompasses aspects such as energy efficiency, cost-effectiveness, and environmental impact. By conducting comprehensive studies on the practical applications of composite desiccants, researchers can provide valuable insights into their suitability and viability in diverse humidity control scenarios. Chapter 2 provides an extensive literature review on composite desiccants, offering a comprehensive overview of the research conducted in composite desiccants, natural desiccants, natural composite desiccants, and binders used to make the composite desiccants.

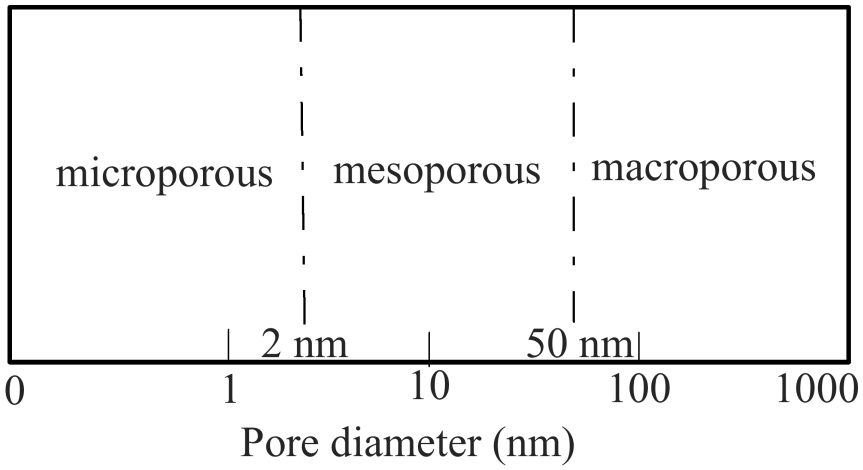

Figure 1.6: Classification of porous material as recommended by the International Union of Pure and Applied Chemistry (IUPAC)

1.4 Regeneration of the desiccants

The desiccant materials need to be regenerated to dry out the sorbed moisture by desiccant bed or wheel as energy efficient as possible. This is done by heating the air and there are a number of different ways to heat the air, viz., ground thermal sources, industrial waste heat, and solar air heaters. The regeneration temperature is often selected with respect to the desiccants and time required to regenerate the desiccant.

The desiccant wheel, also known as the rotary desiccant dehumidifier, is an important component in various applications that require humidity control. It is a rotating device designed to remove moisture from the air by using a desiccant material. This technology is widely used in industries such as air conditioning, food processing, pharmaceuticals, and drying applications.

The desiccant wheel operates on the principle of adsorption, where a solid material, known as a desiccant, attracts and holds moisture molecules from the air. During the dehumidification process, the wheel rotates continuously. The moist air from the environment enters one side of the wheel, and as it passes through the desiccant-coated surface, the desiccant adsorbs the moisture from the air. The now-dehumidified air exits the other side of the wheel, resulting in a lower humidity level. Simultaneously, a separate air stream, known as the regeneration air, is heated to a high temperature using various methods, such as electric heaters, natural gas burners, solar air heaters, and waste sources. This hot air is then passed through a section of the wheel, known as the regeneration section, to remove the moisture from the desiccant. The moisture-laden regeneration air is then exhausted outside. The schematic of desiccant wheel is showed in Fig. 1.7. While in a desiccant bed, the regeneration process takes place subsequent to the sorption process. By seamlessly transitioning between the sorption and regeneration process, the desiccant wheel provides a continuous and efficient dehumidification process. This cyclic operation enables the wheel to consistently maintain a lower humidity level in the desired environment.

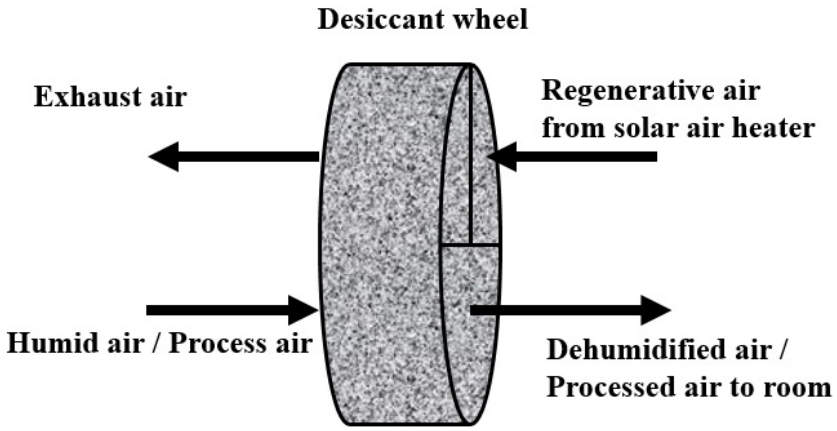

Figure 1.7: Schematic representation of desiccant dehumification wheel

1.5 Motivation for the present study

The increasing demand for air conditioners (ACs) has strained our energy resources and negatively impacted the environment. Traditional ACs heavily rely on refrigerants and energy-intensive cooling mechanisms, leading to greenhouse gas emissions and contributing to global warming. Addressing the challenges posed by climate change requires exploring innovative solutions, and a promising approach involves the use of natural composite desiccants in cooling systems.

In contrast to traditional AC units, desiccant-based cooling systems offer a compelling alternative that addresses environmental concerns. These systems operate by utilizing desiccant materials, which naturally absorb moisture from the air. This moisture removal process enables effective cooling without the extensive use of refrigerants, resulting in a significant reduction in energy requirements.

Moreover, the adoption of sustainable and natural composite desiccants enhances the dehumidification and cooling performance of these systems. To the best of the authors' knowledge, no studies have been reported on the usage of composites of dried cow dung as desiccant materials. Ongoing research and development efforts have led to the creation of natural desiccant materials such composites of dried cow dung and study the moisture sorption properties. Additionally, these materials can be regenerated

using low-grade or waste heat, further improving energy efficiency and minimizing the overall environmental impact of cooling systems.

1.6 Structure of the thesis

This thesis consist of seven chapters two appendices and a list of references.

Chapter one gives the insight about need of desiccant based air conditioning systems, difference between working principle of desiccant based air conditioning system and conventional air conditioning system, composite desiccants and their applications, and motivation for the current study.

Chapter two contains detailed literature review of literature of the composite desiccants, natural desiccants, natural composite desiccants, summary of literature review, research gap, and objectives of the present study.

Chapter three details about desiccant material preparation, metal embedded desiccant preparation, fabrication of experimental setup, desiccant material characteristics methods viz., isotherms test using moisture chamber, BET & BJH analysis, exergetic efficiency, and total heat load calculation of these desiccant-based dehumidification systems.

Chapter four presents the sorption-desorption characteristics of dried cow dung (DCD)-based composited desiccants. isotherms, exergetic efficiency and total heat load reduction of DCD-based dehumidification systems.

Chapter five deals with the sorption-desorption characteristics metal embedded natural composite desiccants; exergetic efficiency and total heat load reduction of metal embedded natural composite desiccant dehumidification systems.

Chapter six deals with the improved utilisation of natural composite desiccant, which is coated on hexagonal aluminium channels. Comparison of pressure loss, moisture sorption, and desorption with packed bed dehumidification and NCD-coated hexagonal aluminium channels bed.

Chapter seven concludes the thesis with important findings based on present experimental study, significant conclusions, and future work recommendations.

CHAPTER 2

LITERATURE REVIEW AND OBJECTIVES

In this chapter, a literature review is presented on various types of desiccants including composite desiccants, natural composite desiccants, desiccants coated on different geometries, and desiccant coated heat exchangers.

2.1 Study on composite desiccants

The concept of using desiccants dates back centuries, with early civilizations employing natural materials such as salt, charcoal, and silica gel to protect goods from moisture damage. However, it was not until more recent times that the idea of composite desiccants, combining multiple moisture-absorbing materials, came into prominence. The use of composite desiccants emerged as a result of a growing demand for improved moisture control in various industries. Traditional desiccants had limitations in terms of their absorption capacities and specific applications. Researchers and engineers began experimenting with different combinations of desiccant materials to enhance moisture absorption capabilities and address specific needs more effectively.

The development of composite desiccants gained momentum in the late 20^{th} century, as advancements in material science and industrial processes allowed for greater flexibility in creating tailored desiccant formulations. These composite desiccants often consisted of a mixture of different substances, such as silica gel, clay, molecular sieves, and activated carbon, among others, each contributing unique properties to the over-

all moisture-absorbing performance. Over time, research and development efforts have continued to refine and expand the capabilities of composite desiccants. The pursuit of more sustainable and environmentally friendly options has also driven innovations in this field, with the introduction of biodegradable or recyclable composite desiccants.

Zhang *et al.* (2006) compared the moisture removal capacity of silica gel (SG) and silica gel with calcium chloride ($CaCl_2$) composite desiccants put in corrugated paper (CP). The maximum regeneration temperature was around 393 K and results showed that CP–SG–$CaCl_2$ wheel is always higher than the CP–SG wheel with a maximum improvement of 80%. CP–SG–$CaCl_2$ composite reaches equilibrium much faster than CP-SG and CP-$CaCl_2$. In a related paper, Zhang and Qiu (2007) discussed the moisture transport model and adsorption process. This study shows the impregnation of $CaCl_2$ in the pores of silica gel is the most dominant factor deciding the vapor adsorption on the composite adsorbent. With an increase in $CaCl_2$ content, the saturated water uptake increased. However, rate of water vapor transport was slowed down by the salt inside the pores, which results in a poor mass diffusion coefficient and suggested that not to have too high salt in desiccant.

Jia *et al.* (2006) found that the composite desiccant materials, which are made with lithium chloride (LiCl) and silica gel composite desiccant wheel performs and removes moisture from air approximately 50% better than the which is silica gel. Perhaps, higher regeneration temperature results in more moisture removal capacity. Optimal regeneration temperature of silica gel desiccant wheel (373 K) is more that of composite desiccant (353 K). This show the higher power consumption and less coefficient of performance by the silica gel desiccant. LiCl implanted in the pore channels of the silica gel which have high hygroscopic property improves its moisture adsorption capacity of composite desiccant.

Normally a polymeric desiccant has sorption and regeneration capacity of 40,000 cycles (durability) compared to inorganic desiccants like silica gel, lithium chloride, and molecular sieve (Lee and Lee 2012). Desiccants like silica gel need high regenera-

tion temperature and have low sorption capacity whereas chloride based desiccants may cause corrosion due to deliquescence problem (Zhang *et al.* 2014). This necessitates the need of an alternate desiccant material which can provide good sorption capacity as well as high durability. Tso and Chao (2012) described about composite absorbent making. The preparation of composite absorbent is done through two steps. One is impregnating of hydrophilic silica and anther one is impregnating of $CaCl_2$. In impregnation of hydrophilic silica gel the 10 g of activated carbon is heated for evacuation at 383 K for about 24 hrs to get the silica activated carbon. During first and second penetration 150 ml of Na_2O - 3.3 SiO_2 and 75 ml of 3.9 N H_2SO_4 solutions respectively and filtration drying was done after both penetration at 383 K for about 24 hrs. Later, this dried product was washed with de-ionized water to remove Na_2SO_4 and dried it for about 24 hrs at 423 K. In impregnating of $CaCl_2$, 10 g of silica activated carbon mixed with 100 ml of $CaCl_2$ solution. Filtration drying was done at 423 K for about 24 hrs to composite absorbent (Silica Activated Carbon/$CaCl_2$). A composite adsorbent was prepared which was able to absorb upto 0.23 g of H_2O per gram of the dry adsorbent at 900 Pa, which was a 933% improvement over raw activated carbon. This paper also explained about characterization of composite absorbent by using X-ray photoelectron spectroscopy (XPS). XPS is a surface sensitive quantitative spectroscopic technique that measures the elemental composition part per thousand range, chemical state, empirical formula and electronic state of the elements that exist within a material.

Yu *et al.* (2014) experimented on composite desiccant materials which were also used for thermal storage. They suggested that two major key parameter to adopt the suitable desiccant materials were salt concentration and pore volume, these helps to improve sorption capacity to meet the required moisture content removal at low temperatures, from 333 to 373 K. Desiccant materials were prepared as two types of silica gels with type A and type C with an average pore diameter of 2–3 nm and 8–10 nm respectively, were applied in this study to find a suitable matrix for lithium chloride. The size of the silica gel grains was 2–3 mm. First, the silica gel was dried at 393 K in an oven to drive possible remaining water out of it. The dry silica gel was then

immersed into aqueous LiCl solutions with varied mass concentrations in the range of 10–40 wt% at an ambient temperature of about 298 K for 12 hrs, which is sufficient to make the salt well distributed inside the pores of silica gel. Yu *et al.* (2014) concluded that the SLi30 (sample prepared in 30 wt% of LiCl aqueous solution) sample prepared by impregnating the silica gel in the 30 wt% LiCl solution shows the highest and stable storage performance.

Chen *et al.* (2015) showed that the silica gel–LiCl composite sorbents could be regenerated by low-temperature heat sources as complete water desorption could be reached at relatively low temperatures in this experiments, from 333 to 373 K. Silica gel with both polyacrylic acid and sodium polyacrylate composite has sorption capacity 41% higher than silica gel. Low material cost, a longer dehumidifying time of operation, and a low pressure drop show the less energy consumption of desiccant system. In another study done by Chen *et al.* (2016) revealed that the power consumption of low pressure drop composite desiccant systems showed an improvement of 33% over packed bed systems. The molecular sieve could not regenerate at a temperature below 313 K. Polyacrylic acid had a low transient absorption rate and a high adsorption capacity. Diatomite had the same adsorption isotherm as alumina, but had lower adsorption capacity.

Zheng *et al.* (2015*b*) made composite desiccants by impregnating LiCl into pores of SBA-15 (Santa Barbara Amorphous) and MCM-41 (Mobil Composition Matter No.41) mesoporous silicates. The preparation process of composite desiccant materials was done using mesoporous silicate materials were dried in an oven at 393 K for 4 hrs, after which their masses were recorded. Dry silicates were then put into a vacuum glass container which was then evacuated by a vacuum pump for about 2 hrs to take out remaining air from the pores of the silicate. Later, a saturated aqueous solution of LiCl was poured into the container at an ambient temperature for 24 hrs. After that, composite samples separated from salt solutions by a vacuum filter. Finally, composite samples were dried at 393 K for another 4 hrs until their weight remained constant. Salt

content in each composite was obtained via weighing dry samples before and after salt impregnation.

Experimental and computational comparison done by Zheng *et al.* (2015*a*) showed that composite desiccant made of SBA-15/LiCl had more water uptake and dehumidification capacity far better than the SBA-15 and mesoporous silica gel. Cho *et al.* (2007) presented results from the testing of desiccant wheels with the FAM-Z01 zeolite material. They found that the zeolite desiccant wheel gave improved performance over a silica-gel wheel when regenerating at very low temperatures (323 K). Czanderna and Neidlinger (1990) compared the performance of a new superabsorbent polymer desiccant material with that of silica gel in a batch dehumidification regeneration desiccant process. They reported an increase in the dehumidification rate of around 20% with the superabsorbent polymer at a regeneration temperature of 333 K.

Ahmed *et al.* (2005) conducted the evaluation and optimization of a solar desiccant wheel performance. A numerical model was developed and validated with experimental data. Moreover, parametric studies were conducted to investigate the effects of the design parameters such as rotational speed, regeneration to adsorption area ratio, and the operating parameters such as air flow rate, inlet air humidity ratio, and regeneration air temperature on the wheel performance. Wheel thickness was found to be between 0.18 and 0.26 m for regeneration temperature between 333 and 363 K. The effective air flow rate was found to be between 1 and 5 kg/min for the range of temperature between 333 and 363 K, and the wheel speed range from 15 to 60 rev/hr. Enteria et al. (2010) evaluated the desiccant wheel based on its moisture removal capacity (MRC) and moisture removal regeneration (MRR). Large flow rate of air (200 m^3/hr) resulting to higher moisture adsorbed in the desiccant matrix for a short period of time. Maximum MRC was 0.016 kg/kg and optimum speed of 30 RPH for the 100 m^3/hr and 50 RPH for the 200 m^3/hr. They had also investigated several commercially available desiccant wheels, and determined the best rotational speeds for different desiccants wheels. Angrisani et al. (2013) conducted experimental tests on a silica gel desiccant wheel to high- light

the effect of rotational speed on its performance. The desiccant could be regenerated with low-temperature thermal energy (333-343 K). Optimized wheel of dehumidification performances varied in the range 6–7 revolutions per hour. The maximum DCOP (Desiccant Coefficient of Performance) is in the range 0.50–1.50 was achieved. The desiccant material was regenerated by low temperature thermal energy from a micro co-generator. Angrisani et al. (2012) conducted an experimental analysis of the desiccant wheel, which focused on the variations of the performance as a function of the process and regeneration air flow rates.

Subramanyam *et al.* (2004) designed a non-adiabatic desiccant wheel and examined its performance through mathematical models and experimental testing. The new design could increase the dehumidification level by around 45 to 53%. The effect of operating parameters on the vertically packed burnt clay – additives – $CaCl_2$ composite desiccant beds is experimentally and numerically investigated by (Hiremath et al. 2018). The theoretical results for percentage reduction in moisture content show trends similar to that of experimental results of burnt clay additive based $CaCl_2$ composite desiccants. The RMSE (Root Mean Square Error) of measured and predicted results for reduction of moisture content from the process air by composite desiccant beds are in the range of 3.26–13.2% (Hiremath *et al.* 2018). The transient heat and mass transfer in a desiccant packed bed containing varying particle diameter distribution along the axial direction had been investigated using the pseudo gas controlled approach that considers the heat conduction in the bed (Kadoli *et al.* 2012). It has been found that there is a 25.7% reduction in pressure drop with negligible reduction in the total mass adsorbed for a desiccant bed with cubic type particle size distribution when compared to the bed with uniform particle diameter of 1.0 mm. It was found that a 25.7% reduction in pressure drop with negligible reduction in the total mass adsorbed for a desiccant bed with cubic type particle size distribution when compared to the bed with uniform particle diameter of 1.0 mm. Pressure drop in the bed increased from 750 Pa to 1900 Pa for air velocity of 1.0 m/s. Proposed particle diameter distributions enhances the utilization of the trailing layers of the desiccant bed by increasing the water content of the particles

by about 50%.

Courbon *et al.* (2017) and Chua *et al.* (2018) carried out experimental studies to understand the moisture adsoprtion capacity of activated carbon, silica gel and $CaCl_2$. These studies showed the moisture uptake capacity of these desiccants is nearly 0.40 g/g. Composite desiccant with activated carbon, silica gel and lithium chloride for air dehumidification is proposed by Wang *et al.* (2022). The water vapor adsorption capacity of this composite desiccant was 0.81 g/g. The amalgamation of silica gel, polypropylene fibers, sodium polyacrylate and vinyl glue composite desiccant was proposed by De Antonellis *et al.* (2022). Process of the sorbent material preparation and its adsorption capacity, morphology and surface analysis were studied.

Composite desiccant is prepared by impregnation of activated carbon by soaking in 10 wt.% of sodium silicate solution for 48 hours and then in 30 wt.% $CaCl_2$ solution for 48 hours. The maximum adsorption capacity of this composite desiccant was found to be 0.23 kg/kg at 300 K. The influence of equilibrium and heat of sorption properties were studied by Ng *et al.* (2001) using different types of silica gels. They observed that adsorption properties depend on the pore size of the material. Adsorption performance of the zeolite 13X and $CaCl_2$ composite adsorbent were tested under vacuum conditions by Zhao *et al.* (2017). The moisture uptake capacity of composite adsorbent (CA10X), which was zeolite 13X impregnated with 10 wt.% $CaCl_2$ solution was increased by 5.7% compared with that of 13X, and the maximum moisture uptake is 0.37 g/g. Tashiro *et al.* (2004) observed that Y-type zeolite treated with hydrochloric acid could improve the adsorption characteristics of the hydrophobic surface. As $CaCl_2$ is deliquescent, this salt was used as additive to make composite desiccants. Zhang *et al.* (2016) reported the synthesis of silica gel and $CaCl_2$ composite sorbent. Its water adsorption capacity exceeded 75 g/100 g. The sorption capacity was improved compared with pure $CaCl_2$ powder and the desorption temperature was 343 K. Moisture uptake capacity of $CaCl_2$ was nearly about 40 g/100 g.

Hashemi *et al.* (2022) used CaO as CO_2 capturing sorbent and its CO_2 uptake ca-

pacity is 0.4 g/g. In a separate study, Kurlov *et al.* (2020) observed the theoretical CO_2 uptake capacity of CaO as 0.78 g/g. Barčauskaitė *et al.* (2020) found out the moisture uptake capacity of $CaSO_4$ as 0.4 g/g. Younes *et al.* (2019) studied the use of different binders like polyvinyl pyrrolidone (PVP), hydroxyethyl cellulose (HEC), gelatine and polyvinyl alcohol (PVA) for silica gel powder. With PVP, the thermal conductivity was increased by 32% and volumetric uptake was increased by 12.5% compared to silica gel powder. Chen *et al.* (2015), found the optimal composite material with mixing ratio of 10:1:1 by a mixing silica gel with sodium polyacrylate and polyacrylic acid. The average dehumidification amount reached 2.73 g/min, which was higher than the silica gel packed bed at 2.46 g/min.

Yefeng and Ruzhu (2003) were made a composite adsorbent $SiO_2 \cdot xH_2O \cdot yCaCl_2$ which was composed of macro-porous silica gel and calcium chloride. This composite adsorbent can adsorb more water than common adsorbents like macro-porous silica gel, micro-porous silica gel and synthetic zeolite 13X and also measured the adsorption isotherms at 298 K are measured. Younes *et al.* (2019) were considered the different binder like Polyvinyl pyrolidone (PVP), gelatine, Hydroxyethyl cellulose (HEC) and polyvinyl alcohol (PVA) for silica gel powder. Thermal conductivity of PVP of 2 wt.% was found to be 32 % and volumetric uptake is increase to 12.5% higher than the silica gel powder.

Chen *et al.* (2015), found the optimal composite material with mixing ratio of 10:1:1 by combining silica gel with polyacrylic acid and sodium polyacrylate. The average dehumidification amount reached 2.73 g/min, which was higher than silica gel packed bed at 2.46 g/min. Adsorption rates in which 0.23 kg/kg of adsorption capacity was recorded. Type 3A, 5A and 13X molecular sieves and the influence of the equilibrium and heat of sorption properties were studied by Ng *et al.* (2001). Adsorption performance of the 13X/$CaCl_2$ composite adsorbent under vacuum conditions was proven composite adsorbent CA10X (zeolite 13X impregnated with 10 wt.% $CaCl_2$ solution) was increased 5.7% compared with that of 13X, and the moisture uptake was 0.37 g/g

(Zhao *et al.* 2017). Adsorption properties also depends on the pore size of the material. Three types of silica gels with different pore volumes and pore size distributions, and zeolite with various molar ratios of Si/Al, 5.6, 29, 47, 91, and 220, made from a Y-type zeolite treated with hydrochloric acid, an activated carbon with silica gel added to improve the hydrophobic surface were examined.

2.2 Study on natural composite desiccants

Most of the researches are focused on chemical desiccants except very few researches like Hiremath *et al.* (2018), Lee *et al.* (2008), and Singh *et al.* (2019). This draws the attention towards researching more on natural desiccants. Natural desiccants were tested in different air conditions to know the sorption and desorption characteristics (323 K and 10% RH) by Singh *et al.* (2019). The materials' behavior in different humidity with the same temperature; and the same humidity with different temperature was also studied by Singh *et al.* (2019). The study showed that the moisture uptake capacity of cocopeat, cow dung and sawdust was 10.8, 8.64 and 7.21 g/100 g respectively at 301 K and 85% RH conditions.

To study the BET surface area, internal surface area, pore volume and pore radius of cow dung, the Brunauer-Emmett-Teller (BET) and Barrett-Joyner-Halenda (BJH) methods were used by Garba *et al.* (2019). BET surface area, internal surface area, pore radius and pore volume of cow dung were 9.37 m^2/g, 13.104 m^2/g, 21.451 Å and 0.046 m^3/g respectively. The use of potter's clay as a desiccant material with binders like sawdust and horse dung as binders was studied by (Hiremath *et al.* 2018; Hiremath and Ravikiran 2021; Hiremath and Kadoli 2022; Hiremath *et al.* 2014). Their study showed that addition of binders increase the porosity, which helped to increase the moisture uptake capacity of composite desiccants. A composite of red clay and PVP was studied by Lee *et al.* (2008). This study focused on examining how the inclusion of polymer binders influences various properties, including compressive strength, flexural strength, water absorption, pore volume, and specific surface area. The moisture uptake capacity was found to vary from 0.28 - 0.3 g/g depending upon the samples.

Hiremath *et al.* (2018), studied potter's clay as desiccant material with binders like saw dust and horse dung were used for composite desiccant preparation. Materials were characterized for pore volume and surface area. Clay was subjected to 773 K possess higher pore volume but clay-horse dung particles exhibit higher surface area were revealed by BET test. According to Tretiak and Abdallah (2009), the clay-$CaCl_2$ composite desiccant exhibited excellent sorption capacity. The desiccant material demonstrated high moisture adsorption at low relative humidity levels, making it suitable for dehumidification purposes. The desorption process was also efficient, with the desiccant absorbing moisture effectively when exposed to humid conditions. These tests were conducted at inlet air temperatures from 296-309 K with corresponding relative humidities of between 42 and 66%. This desiccant was regenerated at temperatures from 323-330 K.

2.3 Study on dehumidification system using desiccants coated on various geometries

Desiccant-based evaporative cooling systems typically use packed beds of desiccant balls. These systems, however, are known to cause high pressure loss across the desiccant bed due to the densely packed structure which creates higher inertial and viscous resistance to airflow. As a result, these systems consume more energy. To address this issue, researchers have been exploring various arrangements and coating methods of desiccants or composite desiccants on low-pressure loss arrangements. For instance, composite desiccants may be coated on metal substrates (Ge *et al.* 2017), metal-organic frameworks (Liu *et al.* 2022), heat exchangers (Sun *et al.* 2021; Valarezo *et al.* 2019; Ma and Zheng 2022; Zheng *et al.* 2020), different channel and duct geometries (Al-Sharqawi and Lior 2007; Zhang 2015; Narayanan 2017; Bhabhor and Jani 2021), etc., in order to reduce pressure loss and energy consumption.

In a study by Al-Sharqawi and Lior (2007), moisture flow was examined in triangular, circular, and square ducts. Results showed that the triangular duct had the greatest convective heat and mass transport and absorbed 11% and 42% more water vapor than

the circular and square ducts, respectively. However, the circular duct required less work input than the other two geometries. The triangular duct also had a high dehumidification performance but had an average pressure drop that was 69% and 73.5% larger than the square and circular ducts, respectively, which would lead to higher fan power consumption. Zhang (2015) conducted an analysis of the convective heat and mass transfer coefficients for ducts by examining temperature, humidity, velocity, and water content contours. Additionally, the effects of solid wall thickness and operating time were taken into account. The Nusselt and Sherwood numbers were determined for fully developed hexagonal ducts with different wall thickness ratios, which ranged from 3.6 to 4.04. These findings served as a helpful guide for designing and optimizing performance of adsorption systems that utilize hexagonal ducts.

Narayanan (2017) explored the dehumidification capabilities of different channel geometries. He found that triangular (0.495 g/g), sinusoidal-2 (0.48 g/g), and rectangular (0.49 g/g) channels performed better than hexagonal (0.435 g/g), circular (0.45 g/g), and square (0.47 g/g) shapes. Bhabhor and Jani (2021) and Gao *et al.* (2005) conducted computational studies on the performance of desiccant wheel channel geometries, including square, triangular, hexagonal, sinusoidal-1 (1:1), and sinusoidal-2 (1:2), using silica gel and various operating input parameters. They found that for a fixed inlet condition, the outlet humidity ratio for triangular, square, hexagonal, sinusoidal-1, and sinusoidal-2 geometries were 11.6, 12.8, 14.5, 8.2, and 7.9 g/kg, respectively. De Antonellis *et al.* (2021) investigated a novel humidification system utilizing silica gel-packed beds through both experimental and numerical approaches. They developed a test rig to evaluate performance and found that the humidity ratio of airflow supplied to the building varied depending on bed thickness, airflow arrangement, and velocity.

2.4 Summary of literature review and research gap

From the detailed literature review, the study on natural desiccants and natural composite desiccants is found to be scant. Very few studies have been done on natural desiccants, such as cow dung, composites of cow dung, potter's clay, coco-peat and

red clay. Majority of the studies have been done on desiccants like molecular sieve, silica gel, activated carbon, calcium chloride, lithium chloride, zeolite and polymer desiccants, and composite of these with different proportion (Tso and Chao 2012; Intini *et al.* 2015; Zhou and Chen 2016; Zheng *et al.* 2015*b*,*a*; Majumdar 1998; De Antonellis *et al.* 2021). Natural desiccants offer a safe and non-toxic solution for a wide range of applications, such as food packaging, pharmaceuticals, and electronics. Derived from renewable resources, these desiccants are environmentally friendly and biodegradable, setting them apart from chemical alternatives. In addition to their eco-friendliness, natural desiccants are often more affordable, making them a cost-effective choice. They are easily accessible and can be obtained locally, reducing transportation expenses. This makes them a practical option for various industries, including small-scale operations and budget-conscious businesses. Moreover, handling natural desiccants is generally safe, as they pose minimal health risks when used correctly. Unlike synthetic desiccants, they do not emit harmful chemicals or by-products during use, ensuring a secure working environment. Current study is focusing on identifying a natural and natural composite desiccants for the application of rural India. Based on the research gap, the following objectives have been framed.

2.5 Objectives

The specific objectives for this study are as follows.

- To identify and prepare a stable natural composite desiccant using dried cow dung, clay and Polyvinylpyrrolidone for use in a desiccant-based evaporative cooling system
- To study experimentally the sorption-desorption characteristics of natural composite desiccants and identify a suitable composition
- To identify an optimum thickness ratio of metal-embedded natural composite desiccant for a dehumidification system

- To Study the pressure drop and moisture sorption characteristics of natural composite desiccant using the staggered hexagonal aluminium channel for desiccant-based evaporative cooling system
- To carry out energy and exergetic analysis of desiccant based systems at different relative humidity and temperature

CHAPTER 3

MATERIALS AND METHODS

In this study dried cow dung (DCD) is selected as the base material for composite desiccants. Dried cow dung cakes are a common fuel source in rural India. They are burned to cook, provide heat and light source. They are being used as fertilizer, building material and a raw material for many other products. It is a cheap, renewable and widely available in rural India. Dried cow dung is hygroscopic and porous material making it suitable candidate for composite desiccants. This chapter covers the preparation of natural composite desiccants, as well as metallic ball-embedded natural composite desiccants and natural composite desiccants coated on staggered hexagonal aluminium channels. The desiccants are subject to characterization using isotherms, aided by a moisture chamber setup, thermophysical properties, and BET (Brunauer-Emmett-Teller) and BJH (Barrett-Joyner-Halenda) analysis to determine their surface area, pore size, and pore volume. A thorough explanation of the experimental rig is provided. Furthermore, the chapter includes calculations of total heat load reduction and exergy analysis in order to assess the system's performance.

3.1 Preparation of natural composite desiccants

Dried cow dung cakes are made out of raw and wet cow dung. These are dried for 48 hours under sunlight to remove the moisture. Dried cow dung cakes are crushed into powder and strained to remove any other particulates with a mesh size of 6-20 (0.841-3.36 mm). The composite desiccants are made with cow dung powder using

polyvinyl pyrrolidone (PVP) and clay as binders. These binders are selected due to ease of availability. The resultant composites are named DCD+PVP and DCD+Clay respectively. The composition of DCD and binder are varied in the ratio of 4:1, 3:1, 2:1 and 1:1 to obtain four different variants of composites. These composite variants are rolled into small spherical balls with an average size of 10 mm (Fig. 3.1). The composite desiccant balls are dried in a hot air oven at 358-373 K till their weight reaches constant (up to 2 decimal places).

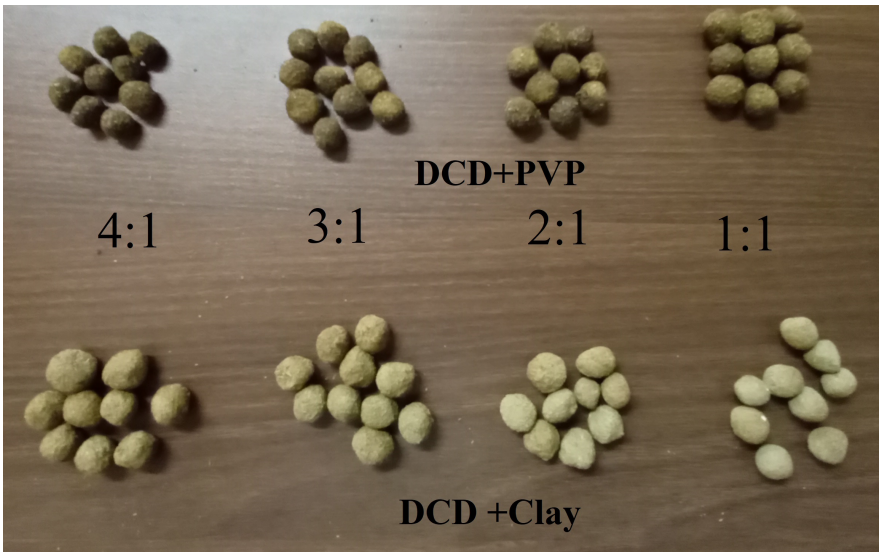

Figure 3.1: Photograph of dried cow dung based composite desiccant materials, namely DCD+Clay and DCD+PVP

3.2 Preparation of metallic ball embedded natural composite desiccants

The second part of the study consists of the usage of a metallic ball embedded in the composite desiccant. The steps involved in the making of metal-embedded natural composite desiccants are shown in Fig. 3.2. Raw and wet cow dung is collected from nearby Goshaala (Cow shelter). This cow dung is made into palm size cakes and dried for 48 hours under sunlight to remove the moisture. Dried cow dung cakes are crushed into powder using a hammer mill pulverizer. Then the powdered cow dung is sieved with a mesh size of 6-20 (0.841-3.36 mm) to remove any other particulates. The sieved powder of dried cow dung (DCD) and polyvinyl pyrrolidone (PVP) as a binder

are mixed in a ratio of 3:1. Sufficient amount of water is added and a natural composite desiccant paste is prepared. Stainless steel (SS) balls are weighed before embedding into natural composite desiccant. Metallic balls with 4.75 and 6.35 mm diameter are used to make metal-embedded natural composite desiccants (MENCDs). Table 3.1 shows the dimensions of stainless steel ball and different thickness ratio of metal embedded natural composite desiccants. The number of desiccant balls is constant for all the cases (390 balls). Each stainless steel ball is embedded in DCD+PVP (3:1) desiccant and rolled into a spherical shape with an average size of 10 mm. Photographs of MENCDs are shown in Fig. 3.3. The thickness ratios (TR) of MENCDs are 1, 0.525, and 0.365. TR equal to 1 refers to the natural composite (DCD+PVP) desiccant with a 10 mm diameter. The thicknes ratio is defined as-

$$\frac{d_{MENCD} - d_b}{d_{MENCD}} \tag{3.1}$$

where, d_{MENCD} is the diameter of metal-embedded natural composite desiccant and (d_b) is diameter of metallic ball. The details are shown in Fig. 3.4. Other details viz. total weight, diameter and thickness ratio of MENCDs are shown in Table 3.2. The thickness of metal-embedded natural composite desiccants is different for different thickness ratios. The MENCDs are dried for 24 hours inside the room. Later, dried in a hot air oven to completely remove the moisture at 373 K, till their weight becomes constant (up to 2 decimal places). This process ensures complete removal of moisture from the MENCDs, ensuring their optimal performance. The dried composite desiccants are placed in dehumidification bed to test moisture sorption and desorption characteristics.

Table 3.1: Dimensions of stainless steel ball embedded composite desiccants

Diameter of metallic ball (mm)	**Diameter of MENCDs (mm)**	**Thickness ratio**
0	10	1
4.75	10	0.525
6.35	10	0.365

Figure 3.2: Picture flow of processes involved in making of metal-embedded natural composite desiccant

Figure 3.3: Actual size of metal-embedded natural composite desiccants

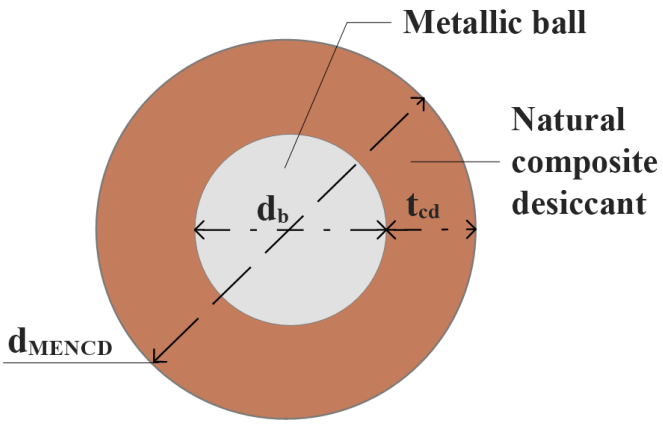

Figure 3.4: Nomenclature of metal-embedded natural composite desiccants

Table 3.2: Weight of stainless steel ball embedded composite desiccants with different thickness ratios

Parameters		**Values**	
Thickness ratio	1	0.525	0.365
Total weight of MENCDs (g); (a)	124.60	270.00	483.6
Weight of SS balls (g); (b)	0.00	177.60	408.72
Weight of plastic bag (g); (c)	5.60	5.60	5.60
Weight of desiccant (g); (a-b-c)	119.00	86.80	69.28

3.3 Preparation of natural composite desiccant coated on staggered hexagonal aluminium channels

Natural composite desiccants (NCDs) are prepared from dried cow dung (DCD) and polyvinyl pyrrolidone (PVP) with a ratio of 3:1 and 2:1. Before making a mixer of DCD and PVP, dried cow dung is prepared from raw and wet dung and PVP is procured from the market. The composite desiccant with a ratio of 2:1 and 3:1 are prepared and coated on hexagonal channels. Dried for 24 hours under room conditions. It is observed that a natural composite desiccant with a ratio of 2:1 has a better coatability after drying it for 24 hours inside the room. Coatability is confirmed by simple scratching method. With a 2:1 ratio, the natural composite desiccant is coated on 10 hexagonal frames to make a desiccant bed with 100 mm. A hexagonal channel has width of 10 mm, and a side thickness of 0.4 mm. The average thickness of the coating is 5.8 mm. Detailed

specifications and photographs of the dehumidification bed are shown in Table 3.3 and Fig. 3.5. Later, NCD-coated hexagonal frames are dried in a hot air oven at 373 K to remove the complete moisture from the desiccant material before testing at different relative humidities and temperatures in a dehumidification bed. During testing, the desiccant bed effectively removes moisture from the surrounding air at various relative humidities and temperatures. The performance of the desiccant bed is evaluated by measuring the moisture uptake capacity and moisture uptake rate.

Table 3.3: Specification of natural composite desiccant coated hexagonal channel dehumidification bed

Length of bed	Diameter of bed	Each side of hexagon	Thickness of hexagon	Avg. thickness of coating	Width of hexagon	Weight of 10 hexagons	Weight of desiccant coated
100 mm	76 mm	7.5 mm	0.4 mm	5.80 mm	10 mm	20 g	102.0 g

3.4 Experimental rig

The experimental rig consists of a screw compressor, heater, a mist producer, a mixing chamber and a cylindrical test section, made of PVC pipe. The schematic block diagram of experimental rig is shown in Fig. 3.6 and photographs are shown in Fig. 3.7. The flow to the mixing chamber is regulated by using control valves to attain constant relative humidity and temperature at constant velocity (2.5 m/s). Two openings are made to place the humidity sensor at the exit and entry of composite desiccants. The composite desiccants are placed at a distance of 1.6 m away from the entrance of the PVC pipe to attain a fully developed flow through it. The process of stabilization of inlet relative humidity and temperature takes 9 to 10 minutes, which is shown in Fig. 3.8 (a) and (b). Experiments are carried out under different relative humidities (RH = 65, 78, and 85%), and temperatures (295, 299, 301, and 304 K). The inlet velocity and temperature are kept constant at 2.5 m/s for all the tests (Florides *et al.* 2002). The desiccants are filled in between two metal meshes provided in the tubular test section, which is shown in Fig. 3.7 (c). The dehumidification bed length is fixed for all the cases.

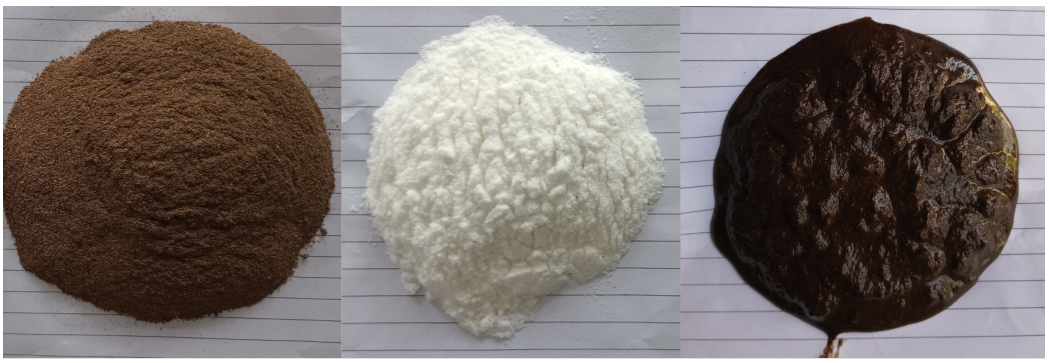

(a)

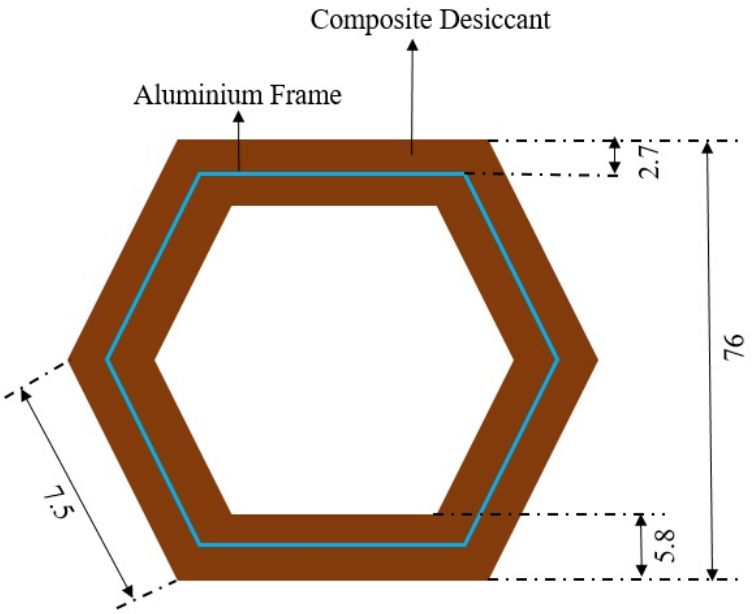

(b)

Figure 3.5: (a) Photograph of natural composite desiccant mixing ratio and (b) schematic of natural composite desiccant coated on hexagonal frame (all the dimensions are in mm)

Different humid air conditions (RH = 65, 78, and 85%) are chosen for the comparative study with constant temperature and velocity. The test conditions are chosen from the metrological data of humidity at coastal region the average condition during the day is 303 and 75% RH while at night, it is 298 K and 85% RH during April, May, June and July. The inlet moist air and outlet dehumidified air properties are measured by using Testo 605i at an interval of 2 s. Accuraccy for a relative humidity measurement

is ±3% and for temperature it is ±0.5 K with a resolution of 0.1 K. The inlet moist air velocity is measured by a digital anemometer (Work Zone AM-4202), having resolution of 0.1 m/s and accuracy of ±2%. The natural composite desiccant and MENCDs are oven-dried and weighed before putting into the test section (desiccant holder). The weight of desiccants is measured by using Con-tech CAI-234 analytical balance with an error of 0.001 g. The weight of desiccants is measured after every five minutes to check the amount of moisture adsorbed. The experiment is continued for 30-55 minutes depending upon saturation level of the desiccant. The experimental uncertainty of various equipments is shown in Table 3.4

The desorption characteristic of the materials is studied at 328 K and below 5% RH condition. This condition is achieved by closing valve 2 and opening valve 1. This particular condition is chosen as it can be easily availed by a lower level energy source such as waste heat and solar energy etc. (Singh *et al.* 2019; Florides *et al.* 2002). However, in this experiment, the heat is generated by an electric air heater to regenerate the composite desiccants. Like previously, during desorption experiment also the weight of the desiccant is recorded at an interval of 5 minutes. Measurements are repeated until there is no change in weight for two consecutive readings. This approach allows for precise measurement of the desorption process and ensures that the desiccant has reached its fully regenerated state.

Table 3.4: Uncertainty of experimental measurements

Sl. No.	Quantity	Instrument	Uncertainty
1	Temperature	Hygrometer (Testo 605i)	$\delta T = \pm 0.5$ K
2	Velocity	Anemometer	$\delta V = 0.04$ m/s
3	Relative humidity	Hygrometer (Testo 605i)	$\delta RH = \pm 3\%$
4	Mass of desiccant	Electronic weighing machine	$\delta M_d = 0.001$ g
5	Time	Stop watch	$\delta t = 0.01$ s
6	Pressure drop	Digital U-tube manometer (HTC, PM-6025)	$\delta P = \pm 0.2$ Pa

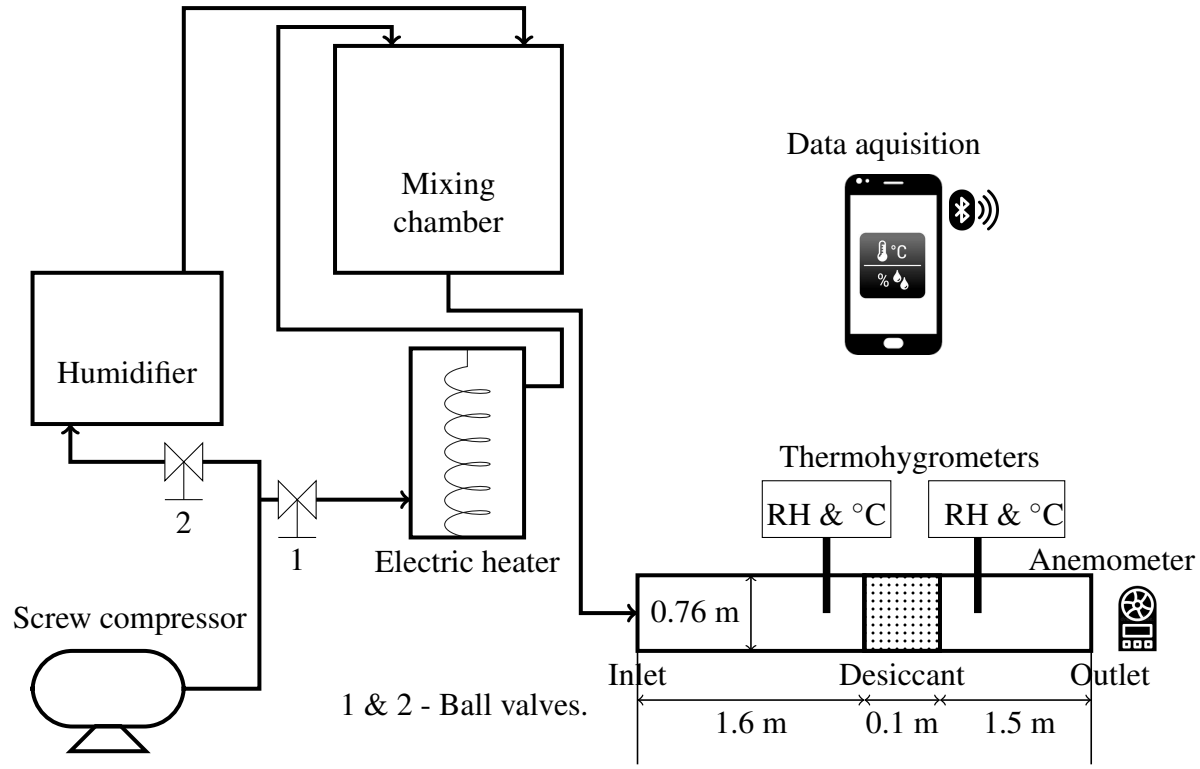

Figure 3.6: Schematic block diagram of experimental rig

3.5 Methods used to analyse the properties and performance of the natural composite desiccants

3.5.1 Isotherm tests using moisture chamber

In order to determine the optimal natural composite desiccant from a selection of eight samples, each consisting of varying ratios of dried cow dung as the base material and incorporating polyvinylpyrrolidone and clay as binders. The varying ratio all the samples is 4:1, 3:1, 2:1, and 1:1 (DCD:binder). The experiments are conducted on moisture sorption isotherms at 300 K. The photogragph and schematic diagram of experimental rig of moisture sorption isotherms is shown in Fig. 3.9 and Fig. 3.10 respectively. This experimental rig consists of nine plastic containers and nine flasks with a different salt solution to obtain constant relative humidity inside the containers. The salt solution maintains the constant humidity inside the closed container for nearly two hours. A metal mesh is used to hold the composite desiccant on top of the flask.

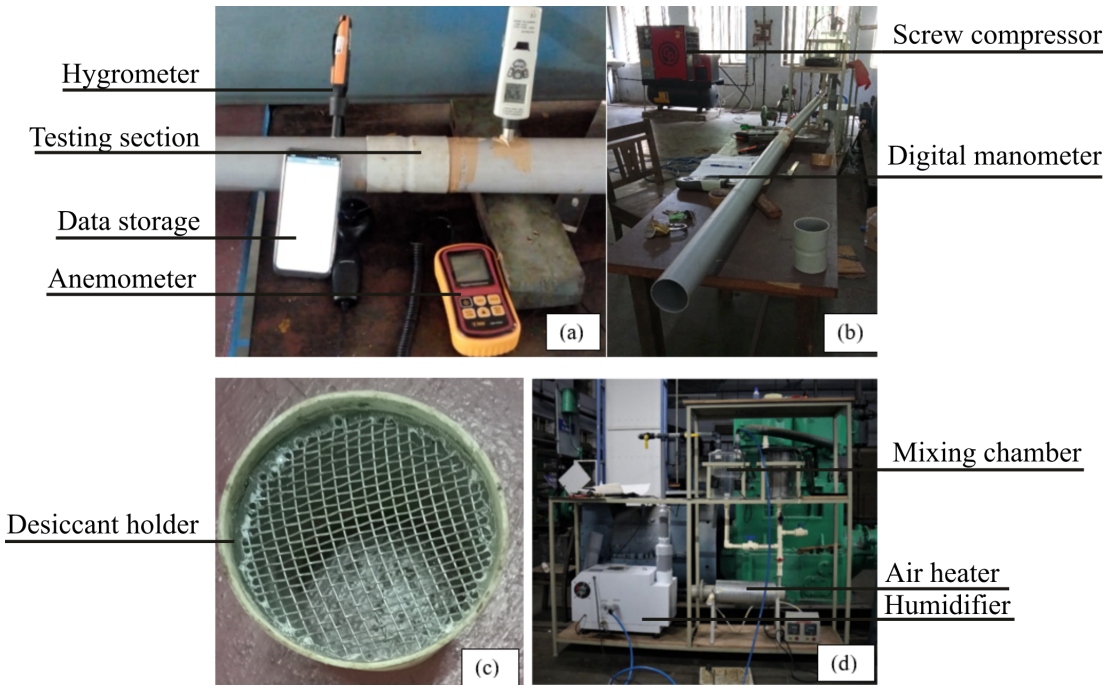

Figure 3.7: Photographs of experimental rig (a) Desiccant holder with velocity, temperature and relative humidity measuring devices, (b) Side view of experimental rig, (c) Close view of desiccant holder, and (d) Front view of experimental rig

A hygrometer is placed on the topside of the container to check the humidity inside the plastic container. The composite desiccant is kept on the metal, which is inside the containers. The moisture gained by the composite desiccant is weighed at an interval of 10 min. Then the humidities and temperatures are measured before placing the desiccant back to the container. If the humidity is changed, then the salt is added and stirred to bring back the relative humidity inside the container. This process is continued till the composite desiccants reach the saturation level. A similar procedure is adopted for all other natural composite desiccants. The salts used for this experiment are provided in Table 3.5.

3.5.2 Types of Isotherms

The adsorption isotherm describes the relationship between the equilibrium pressure of a gas and the amount of substance adsorbed at a constant temperature. Figure

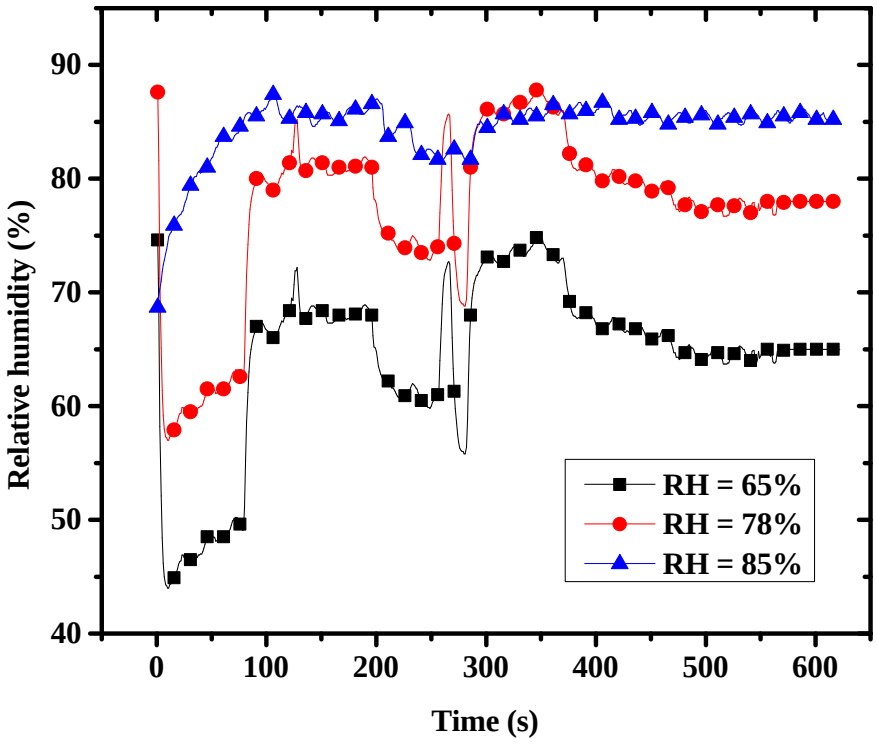

(a)

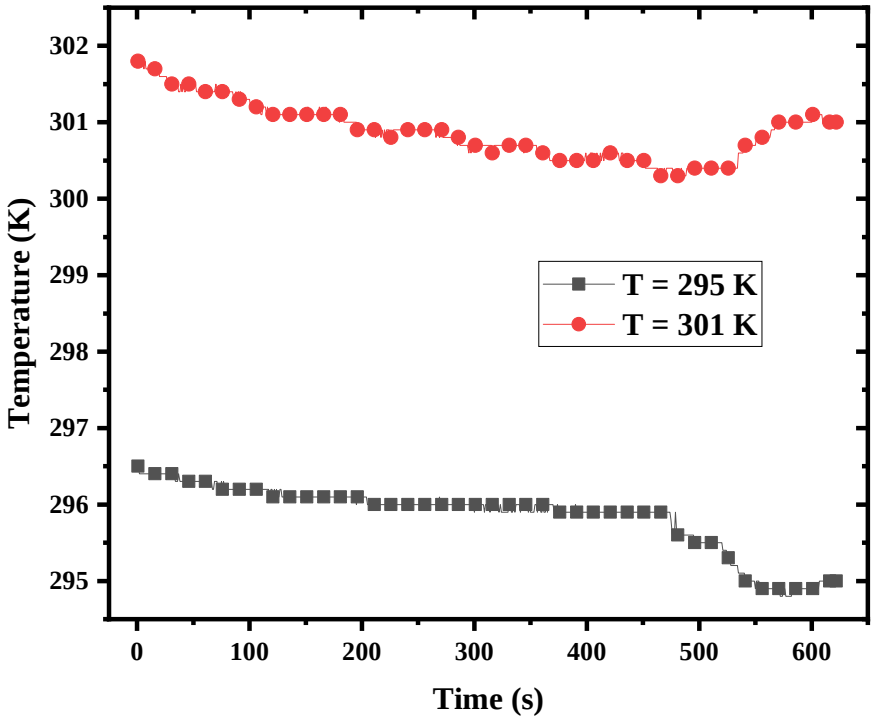

(b)

Figure 3.8: Stabilisation time for (a) relative humidity and (b) temperature

Figure 3.9: Photograph of moisture sorption isotherms rig

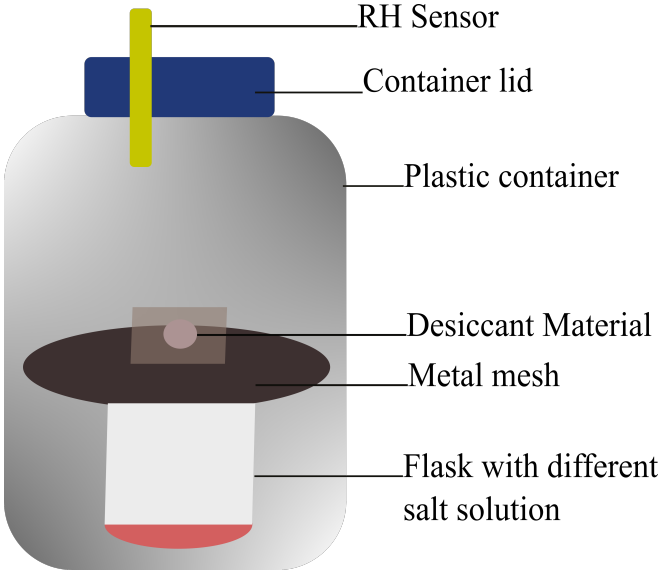

Figure 3.10: Experimental rig for moisture sorption isotherms of DCD+PVP and DCD+Clay composite desiccants at 300 K

3.11 shows a typical adsorption isotherm with different regions during the water vapour isotherm. Region A corresponds to single-layer adsorption, where the moisture content of the adsorbent increases with relative humidity until saturation is reached. Region B represents multilayer adsorption and is associated with hysteresis, where the adsorption process results in a higher adsorbed moisture content than the desorption process at the same relative humidity. Region C is the capillary domain, where water vapour molecules accumulate during multilayer adsorption and tend to form a liquid water meniscus. The Kelvin equation (p_{sat} = exp(T)) can determine the critical pore diame-

Table 3.5: Different types of salt solutions, which are used to maintaining the constant relative humidity inside the plastic container

Sl. No.	Salt solutions	Equilibrium relative humidity at 303 K (Hyland and Hurley 1983)
1	Potassium Sulphate	97.00
2	Potassium Chloride	83.62
3	Sodium Chloride	75.09
4	Sodium Bromide	56.03
5	Potassium Carbonate	43.17
6	Magnesium chloride	32.17
7	Potassium Acetate	21.61
8	Lithium Chloride	11.28
9	Lithium Bromide	06.16

ter for a given relative humidity, where water vapour can condense (Hall and Allinson 2009). Beyond region C, as the relative humidity approaches 100%, gravitational forces dominate (Hall and Allinson 2009). According to Sing (1985), there exist six primary types of physisorption isotherm. In many cases, these isotherms exhibit a linear relationship between the number of moles adsorbed ($n^a \propto p$) and the vapor pressure of the gas (p) at low surface coverage, a region commonly referred to as Henry's law region (Hall and Allinson 2009). Avogadro's number is represented by 'a', while 'n' and 'p' represent the number of moles and vapor pressure of the gas, respectively. Based on the nature of the adsorbent, there are six different types of iostherms. These are discussed below.

Type I isotherm: This type of isotherm is concave with respect to the relative humidity (X-axis). As the relative humidity approaches 100%, its adsorption capacity approaches a limiting value (Fig.3.12). This type of isotherm is observed in the case of microporous solids having relatively small external surfaces (e.g. activated carbons, molecular sieve zeolites and certain porous oxides). Here, the micropore volume is responsible for maximum water uptake rather than the internal surface area.

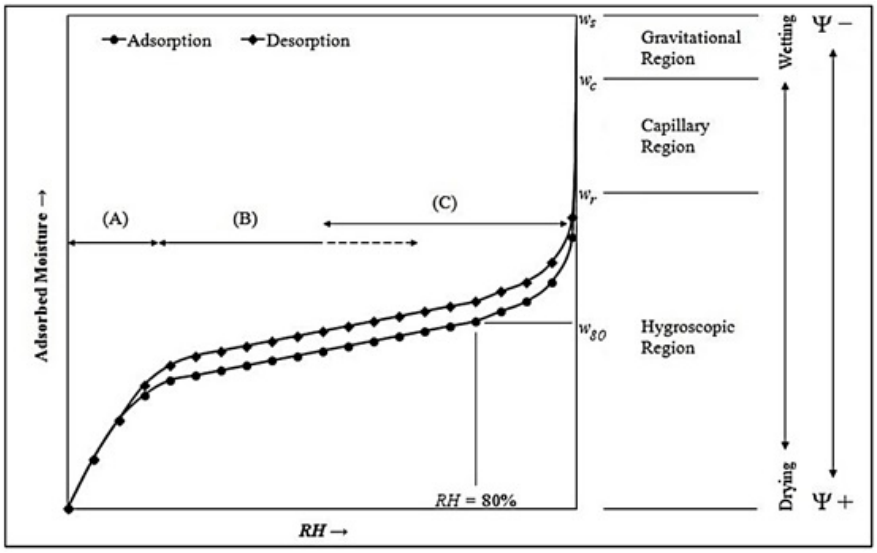

Figure 3.11: The typical water vapour isotherm with various stages (Hall and Allinson 2009)

Type II isotherm: This type of isotherm is observed with non-porous or macro-porous adsorbent. The unrestricted monolayer-multilayer adsorption is represented by this isotherm. Point B in the linear middle section of the isotherm indicates the stage where the monolayer coverage gets completed and multilayer adsorption gets started (3.12).

Type III isotherm: This type of isotherm is convex with respect to the X-axis during its entire region. It doesn't have any point as B where the monolayer adsorption gets converted into multi-layered adsorption. This kind of isotherm is possible only in some systems like nitrogen on polyethylene. In such cases, there is an important role in adsorbate and adsorbent interaction.

Type IV isotherm: The main characteristic of this type of isotherm is the hysteresis loop. The hysteresis loop is due to the capillary condensation in mesopores at the limiting uptake over the range of high humidity. The type IV isotherm and type II isotherm are the same at the initial part of isotherm and the same pattern is observed in monolayer-multilayer adsorption. Many mesoporous industrial adsorbents are governed by the type IV isotherm.

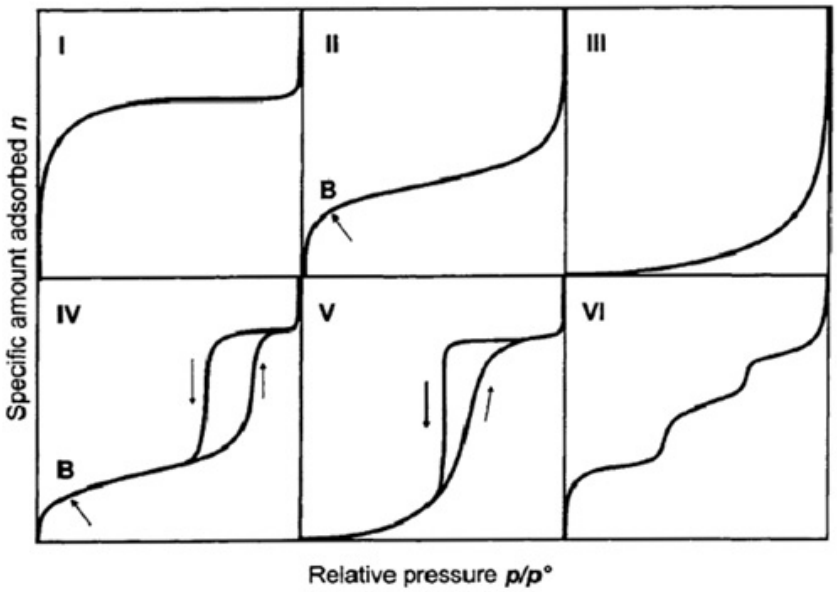

Figure 3.12: Types of adsorption isotherms (Sing 1985)

Type V isotherm: The Type V isotherm is observed in very few cases. It occurs in certain porous adsorbents where the adsorbent-adsorbate interaction is weak as observed in type III isotherms.

Type VI isotherm: The Types VI isotherm shows the stepwise multilayer adsorption on a uniform non-porous surface. The steps depend on the temperature and also on the system. For each adsorbed layer, the monolayer capacity is its step height on the graph. At liquid nitrogen temperature, Argon or Crypton on graphitised carbon blacks shows this type of isotherm.

3.5.3 BET and BJH analysis

The Physical properties of composite desiccant samples are analyzed by using the Brunauer-Emmett-Teller (BET) method. In BET analysis nitrogen is used as adsorbate. The surface area is one of the important parameters which affects the sorption capacity of a desiccant. BET is a widely used method to measure the surface area of the desiccant. Barrett-Joyner-Halenda (BJH) method is used during the desorption process for the determination of pore size distribution from the isotherms (Thommes *et al.*

2015; Touloumet *et al.* 2022; Garba *et al.* 2019; Brunauer *et al.* 1938; Fagerlund 1973; Sing 1985). BJH (Barrett *et al.* 1951; Tian *et al.* 2013; Zhang and Yang 2013; Han *et al.* 2020) model is commonly used for characterization of pore structure of porous material. Samples are kept at a temperature of 353 K in vacuum conditions for 8 h, before measurement. The adsorption and desorption experiment is conducted using the Quantachrome® Autosorb iQ with nitrogen at 77 K. The photograph of device is shown in Fig. 3.13, which is available at central research facility, National Institute of Technology Karnataka Surathkal. The N_2 adsoprtion and desorption isotherms of the samples to know the corresponding to type of isotherms as suggested by the IUPAC (International Union of Pure and Applied Chemistry) classifications (Duong *et al.* 2021). Results of BET and BJH analysis are discussed in chapter 4 under heading of physical properties.

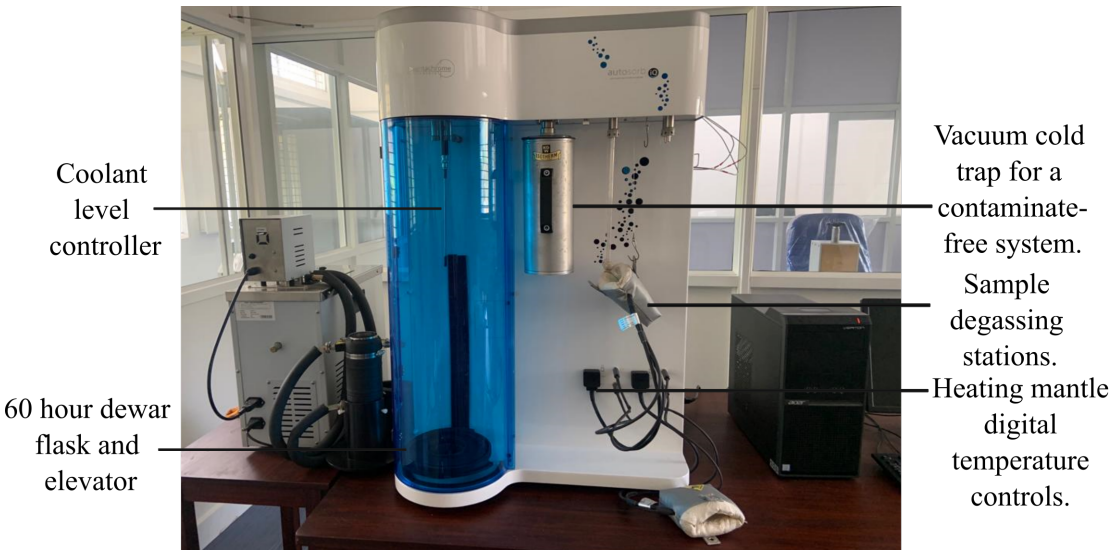

Figure 3.13: Photograph of Quantachrome® Autosorb iQ, which is available at central research facility, NITK Surathkal

3.5.4 Thermophysical properties

Thermal conductivity of DCD+PVP (3:1) is measured using Xenon Flash Analyser at different temperatures varying between 298 and 373 K at department of chemistry, Indian Institute of Technology, Hyderabad. The results are discussed in the section 4.4 of chapter 4.

3.5.5 Theory of exergetic analysis

Exergy means the theoretical maximum energy or work that can be extracted from a system when its condition reaches the defined dead state (T_0, ω_0). To calculate the exergy of desiccant systems, moist air is modelled as an ideal mixture of water vapour and dry air. In dehumidification and humidification process, the separating and mixing of dry air and water vapour takes places respectively. In the dehumidification process which requires additional work, the exergy of the process air increases during the separation of water vapour from humid air. While in humidification, water vapour content is mixed with the dry air, which reduces the exergy of processed air. The exergy of moist air per kilogram of dry air at atmospheric pressure can be calculated by Eq. 3.2 (Ge and Wang 2020; Bejan 2016).

$$\begin{aligned} X =& (c_{p,a} + \omega c_{p,v}) T_0 \left[\frac{T}{T_0} - 1 - \ln \frac{T}{T_0} \right] \\ &+ R_a T_0 \left[(1 + 1.608\omega) \ln \frac{(1 + 1.608\omega_0)}{(1 + 1.608\omega)} + 1.608\omega \ln \frac{\omega}{\omega_0} \right] \end{aligned} \tag{3.2}$$

Where, T means the thermodynamic temperature, ω means the humidity ratio, R_a is the characteristic gas constant, $c_{p,v}$ is the specific heat of water vapor, $c_{p,a}$ is the specific heat of air, and the subscripts 0 indicate the dead state. The first term on the right-hand side of Eq. 3.2 defines the thermal exergy and the second term represents the chemical exergy.

The present study aims to calculate the overall performance of natural composite desiccant dehumidification systems. It is essential to calculate the input and output work of dehumidification systems. The input work is the power required to blow the humid air through the test section, The output work is the exergy change of the humid air. The exergy efficiency of the dehumidification system (η_X), can be calculated as shown in Eq. 3.3 (Ge and Wang 2020):

$$\eta_X = \frac{m_a (X_2 - X_1)}{W} \tag{3.3}$$

$$W = \frac{m_a}{\eta_c \rho_a} \Delta P \tag{3.4}$$

$$m_a = \frac{m_w}{\Delta \omega} 1000 \tag{3.5}$$

where, ΔP flow resistance across bed is calculated using η_c, which is the efficiency of the fan (in this case it is screw compressor), the density of air, and the air pressure difference (Δp referred to as differential pressure) across the desiccant bed with the respect to the atmosphere (Pa), which is measured digital u-tube manometer.

3.5.6 Theory of total heat load calculation

Sorption is an exothermic process, which releases heat during moisture uptake and increases the temperature of outlet air. The heat released by this process is not needed in evaporative cooling becuase it will increase the air temperature which is directed to the conditioned space. This heat can be further indirectly cooled and sent to conditioned sapce (Lee and Lee 2012). The total heat load comprises sensible as well as latent heat load. An increase in sensible heat load for unit mass flow rate due to the increase in the temperature of the air can be obtained using the following relation.

Sensible heat load,

$$Q_s = c_p \Delta T \tag{3.6}$$

There is a decrease in latent heat load because of a reduction in moisture content from the moist air. For unit mass flow rate, it can be found using the following relation.

Latent heat load for unit mass flow rate,

$$Q_L = L \Delta \omega \tag{3.7}$$

Where, L is the latent heat of vaporization of water, $\Delta\omega$ is the amount of decrease in moisture content.

Total heat load,

$$Q_t = Q_s + Q_L \tag{3.8}$$

3.6 Summary

- The materials and methods chapter focuses on the experimental setup and techniques used to investigate the properties and performance of dried cow dung composite desiccants.

- Moisture chamber analysis: A moisture chamber was used to measure the sorption isotherms of the dried cow dung composite desiccants. This involved exposing the desiccants to controlled humidity conditions and measuring the amount of moisture sorbed.

- BET and BJH analysis: The desiccant samples were subjected to BET (Brunauer-Emmett-Teller) analysis to determine their specific surface area. BJH (Barrett-Joyner-Halenda) analysis is used to study the pore size distribution of the desiccants.

- Thermo-physical properties: The thermo-physical properties of the dried cow dung composite desiccants were examined. This includes the measurements such as density, thermal conductivity, specific heat capacity, and porosity.

- Total heat load reduction: The performance of the desiccants in reducing the total heat load was evaluated. This involved conducting experiments where the desiccants were used to absorb moisture from an air stream, and the corresponding reduction in latent heat load is measured.

- Exergy analysis: Exergy analysis was performed to assess the efficiency and effectiveness of the dried cow dung composite desiccants in terms of energy utilization. This analysis provides insights into the exergy destruction and exergy efficiency of the natural composite desiccant-based dehumidification system.

- Overall, the materials and methods chapter provides a detailed description of the experimental procedures employed to characterize the dried cow dung composite desiccants, including the moisture chamber and BET and BJH analysis, as well as

the evaluation of thermo-physical properties, total heat load reduction, and exergy analysis.

CHAPTER 4

NATURAL COMPOSITE DESICCANT-BASED DEHUMIDIFICATION SYSTEM

The chapter commences by investigating the isotherms of dried cow dung (DCD) and DCD-based composite desiccants, which offer valuable insights into the materials' moisture sorption and desorption behavior. By analyzing the isotherms, the study aims to comprehend the adsorption capacity and equilibrium moisture content of these desiccants at varying humidity levels. Various factors that influence the sorption-desorption characteristics are explored, including the composition, structure, binding agents, porosity, and surface area of the composite desiccants. The outcomes of this research contribute significantly to the advancement of sustainable and environmentally friendly dehumidification solutions by harnessing the potential of DCD, an abundant and renewable agricultural waste material. Through an in-depth analysis of the sorption-desorption behavior, exergetic efficiency, and total heat load reduction, this chapter seeks to provide a comprehensive understanding of the performance and potential applications of DCD and DCD-based composite desiccants in dehumidification systems.

4.1 Isotherms of DCD-based composite desiccants

Initially a study on dried cow dung (DCD) without a binder material is carried out to obtain the sorption desorption characteristics. While carrying out experiments, mass reduction of desiccant (DCD) is observed, as shown in Fig. 4.1. This mass reduction occurs due to low binding strength, which reduces the durability and moisture uptake

capacity of DCD. The main reason for the mass reduction is due to less durability of natural binder which is available in the dried cow dung. Results show that the mass reduction is increasing at every trail linearly. After six sorption-desorption cycles, the mass reduction is almost 8 g/ 100 g. The sorption test is conducted with moist air velocity at 2.5 m/s, 85% relative humidity, and temperature of 300 K. The desorption test is conducted at 323 K to regenerate the desiccant. The mass loss is measured at an interval of 5 minutes during sorption and desorption tests. To overcome the mass reduction problem, composite desiccants are made with binders PVP and clay. Moisture uptake capacity (MUC) of eight different samples of composite desiccants is shown in Fig. 4.2. Results show that the MUC is higher for composite desiccants with ratio 3:1 (DCD: binder). DCD and binder with 3:1 ratio will result in stronger bonding between the DCD particles, creating a denser composite material. The specific surface area of the composite desiccants is another crucial factor influencing moisture uptake capacity. Desiccants with a 3:1 ratio exhibits an optimized pore structure, with a balance between micropores and mesopores. DCD and binder ratio less than 3:1 ratio will lead to less binding strength and if the ratio is more 3:1 will more denser and less porous. Further, it is observed that composite desiccant with PVP performs better compared to clay. In the moisture sorption isotherm test at 96.7% RH, composite desiccant with PVP shows 77% higher moisture uptake capacity compared to composite desiccant with clay.

4.2 Study on sorption characteristics

The experimental results of moisture uptake capacity (sorption capacity) of DCD, DCD + PVP, and DCD + Clay with time at different relative humidities are shown in Fig. 4.3. The results also show how the desiccants behave at three different RH conditions, while the temperature of inlet moist air is kept constant. The moisture sorption is found to be more at a higher humidity for the same temperature. Moisture holding capacity decreases at a higher temperature because sorption is an exothermic process. According to the Le-Chatelier principle, moisture retention capacity decreases with an

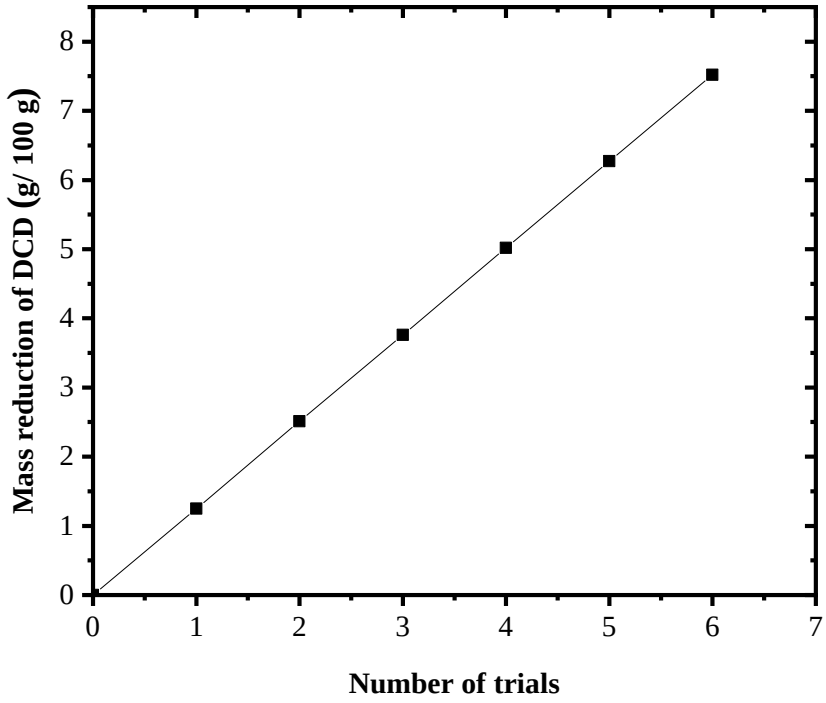

Figure 4.1: Mass reduction of dried cow dung during sorption desorption process

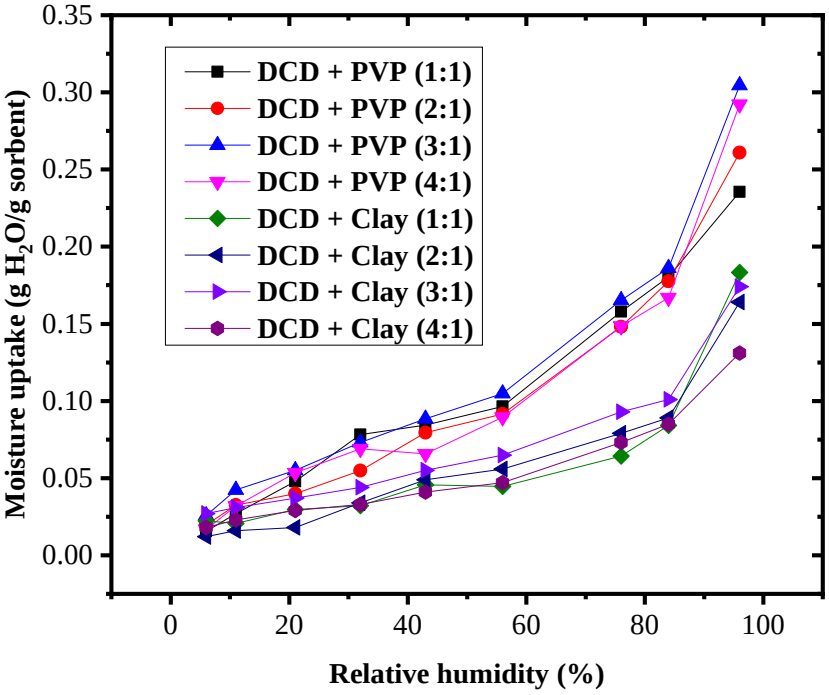

Figure 4.2: Moisture sorption Isotherms of DCD+PVP and DCD+Clay composite desiccants at 300 K

increase in temperature. This principle can also be applied to changes in temperature or pressure. For example, an increase in temperature would generally favor desorption or release of the moisture content from the desiccants, while a decrease in temperature would promote adsorption or absorption of the desiccant.

Since, the sorption is an exothermic process, the temperature of dehumidified air, which is coming out of the desiccant bed will be higher. The temperature rise of outlet dehumidified air coming through different desiccants is shown in Fig. 4.5. The increase in temperature is found significantly high for the first few minutes and later it gradually decreases due to decrease in moisture uptake capacity of desiccant. The maximum temperature rise for DCD, DCD+PVP and DCD+Clay is found to be 5, 4.8 and 3.9 K respectively. Maximum temperature rise is found in dried cow dung while minimum in DCD+Clay. With the increase in temperature of the outlet air, the sensible heat load of the evaporative cooling system will increase. However, the moisture content of the air is reduced which in turn reduces the latent heat load.

Figure 4.3 shows the comparative analysis of dried cow dung and their composite desiccants based on moisture sorption at relative humidities and temperatures. In Fig. 4.3 (c), the moisture uptake capacity of desiccants is more at the higher relative humidity due to the increased moisture content in the inlet air compared to lower relative humidity. The DCD+PVP composite has higher moisture uptake capacity and has twice the saturation time compared to DCD due to the addition of binder. The maximum moisture uptake capacity of DCD+PVP, DCD and DCD+Clay is 14.72, 14.42, and 5.53 g/100 g respectively at 95% RH, which can be observed from Fig. 4.4. Similarly, MUC is 9.01, 9.87, and 5.12 at 85% RH respectively. The trend is similar at 75% RH. Compared to its composites, DCD reaches the saturation limit quite early. The saturation time required for DCD is 18, 29 and 30.5 minutes at 75, 85 and 95% RH receptively. The moisture uptake capacity of DCD increases slightly when the PVP is used as a binder. However, DCD+Clay is proved to be a not-worthy composite in terms of moisture uptake capacity.

Figure 4.6 and Table 4.1 show the experimental results of dried cow dung, which are compared with the results obtained by Singh *et al.* (2019). They reported the moisture uptake capacity of DCD as 8.64 g/100 g at 85% RH and 299 K, whereas, the present experimental results show MUC of 9.87g /100 g, which is 14.23% higher compared to the results obtained by Singh *et al.* (2019). The experimental result comparison reveal that silica gel reaches its saturation level earlier compared to dried cow dung (DCD) and its composite desiccants. This suggests that silica gel exhibits a higher sorption-desorption rate in comparison. Despite this, it is noteworthy that the maximum moisture uptake capacity of silica gel is similar to that of DCD and its composite desiccants.

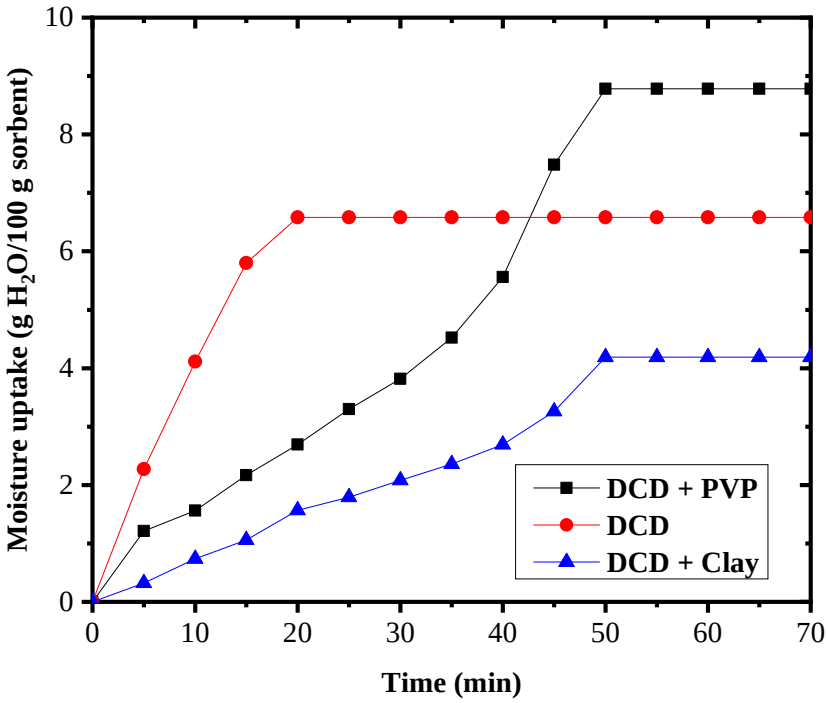

(a)

See the next page for two more figures and caption...

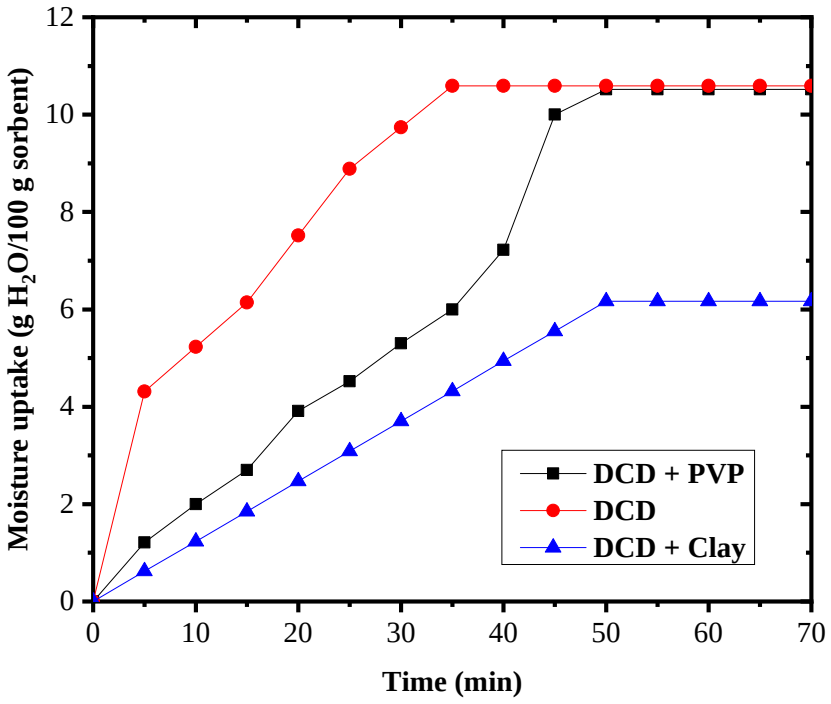

(b)

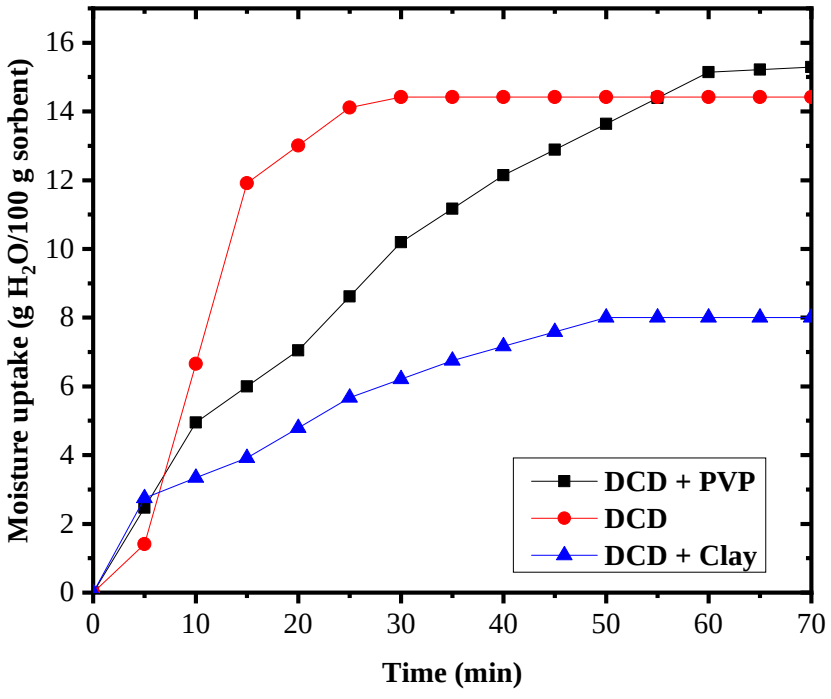

(c)

Figure 4.3: Comparative analysis of dried cow dung and their composite desiccants based on moisture sorption at (a) 299 K, 75% RH (b) 299 K, 85% RH and (c) 299 K, 95% RH conditions.

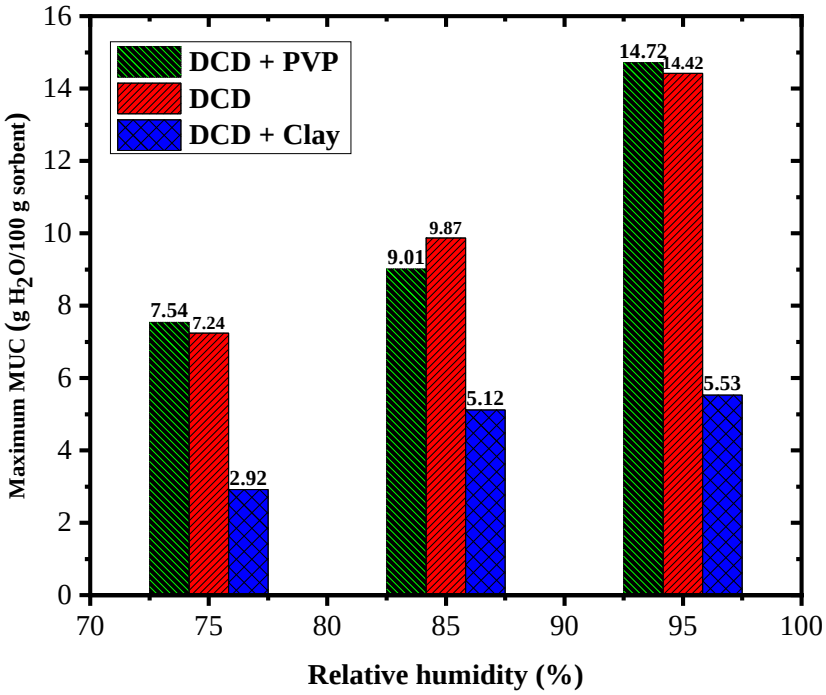

Figure 4.4: Comparative analysis of dried cow dung and their composite desiccants based on moisture sorption at 299 K three different RH (75%, 85%, and 95%)

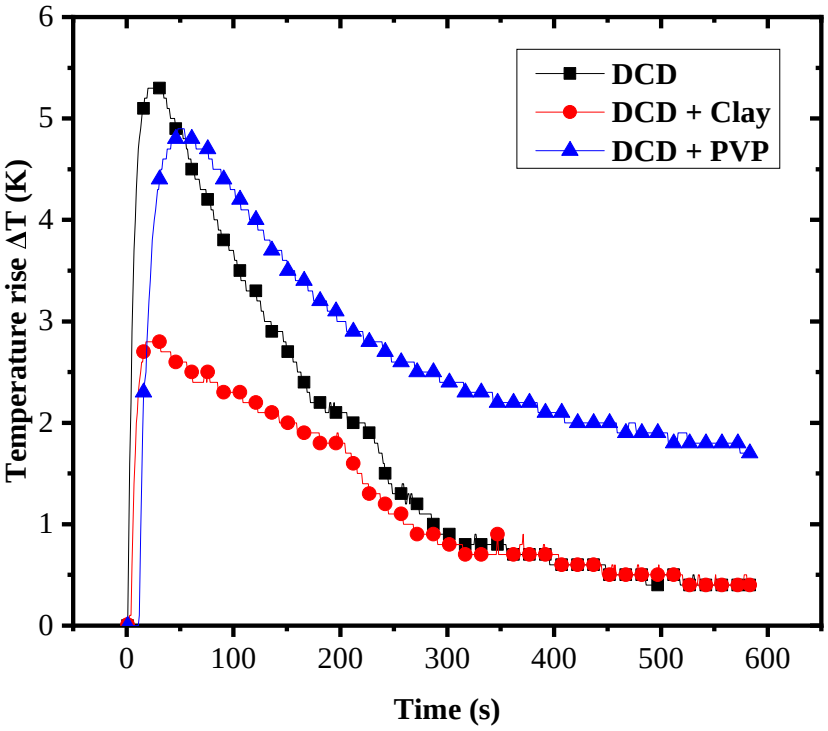

Figure 4.5: Temperature rise during sorption

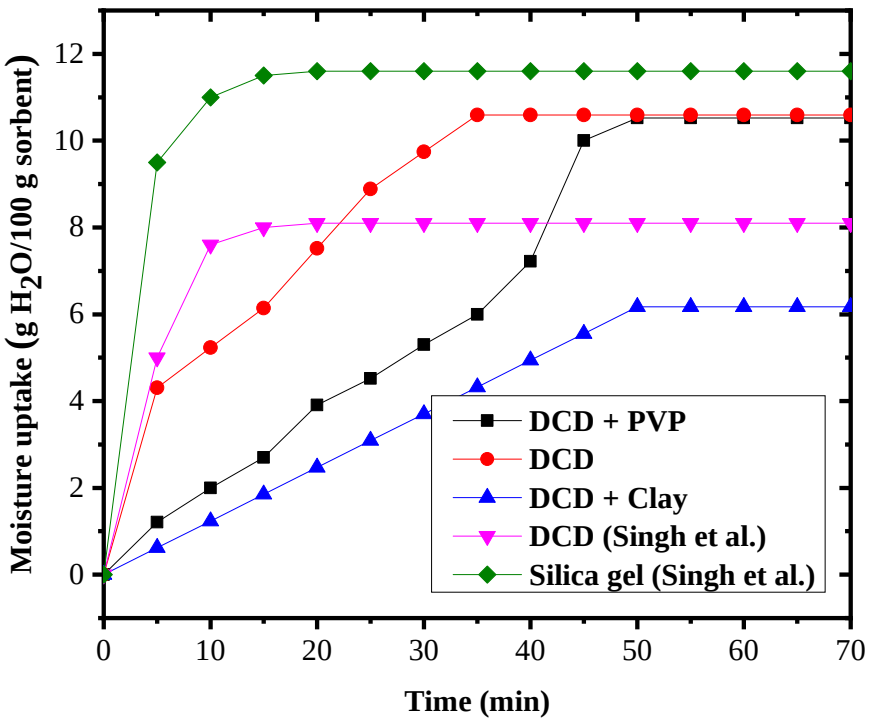

Figure 4.6: Comparison of moisture uptake capacity of current experimental values with Singh *et al.* (2019) at 85% RH and 299 K.

Table 4.1: Maximum moisture uptake capacity of different desiccants at various conditions and comparison of present study results with results obtained by Singh *et al.* (2019).

Test conditions	Desiccants	Moisture uptake capacity (g/100 g)	Moisture uptake capacity (g/100g) (Singh *et al.* 2019)
95% RH, 299 K	DCD	14.42	-
	DCD+PVP	14.72	-
	DCD+Clay	4.53	-
85% RH, 299 K	DCD	9.87	8.64
	DCD+PVP	9.01	-
	DCD+Clay	5.12	-
75% RH, 299 K	DCD	7.24	4.4 (at 60% RH)
	DCD+PVP	7.52	-
	DCD+Clay	2.9	-

4.3 Study on desorption characteristics

To analyze the moisture regeneration capacity, desorption tests are conducted for all the samples after every sorption cycle. The materials are placed in the test section (same as the sorption test), and regeneration air is sent at 328 K and 6% RH with help of temperature controlled air heater. Figure 4.7 shows the variation of moisture desorbed with respect to time. Desorption time is minimum for dried cow dung and maximum for DCD+PVP. Desorption time for DCD, DCD+PVP and DCD+Clay is 13, 17 and 15 minutes respectively. After desorption, some amount of moisture is present in the desiccant material, known as moisture locking. The moisture content at end of desorption process is found to be 11.5%, 10%, and 15.6% for DCD, DCD+PVP and DCD+Clay respectively (Table 4.2). The moisture lock is higher for DCD+Clay. However the regeneration time for DCD+Clay is higher than DCD+PVP (Fig. 4.7). The desorption experiment is repeated after every sorption process for all desiccant materials, and found that no substantial change in the sorption and desorption characteristics of DCD+PVP, but a mass reduction is observed with DCD.

Table 4.2: Percentage of moisture content remained

Desiccants	Initial moisture (g)	Final moisture (g)	% of moisture remained
DCD	9.87	1.13	11.5
DCD + PVP	9.01	0.9	10.0
DCD+Clay	5.12	0.8	15.6

4.4 Thermophysical properties of the desiccants

The physical properties of composite desiccant samples are analyzed by using the BET method. In BET analysis nitrogen is used as adsorbate. The surface area is one of the important parameters which affects the sorption capacity of a desiccant. BET is a widely used method to measure the surface area of the desiccant. BJH method is used during the desorption process for the determination of pore size distribution from the isotherms (Touloumet *et al.* 2022). The physical properties such as surface area,

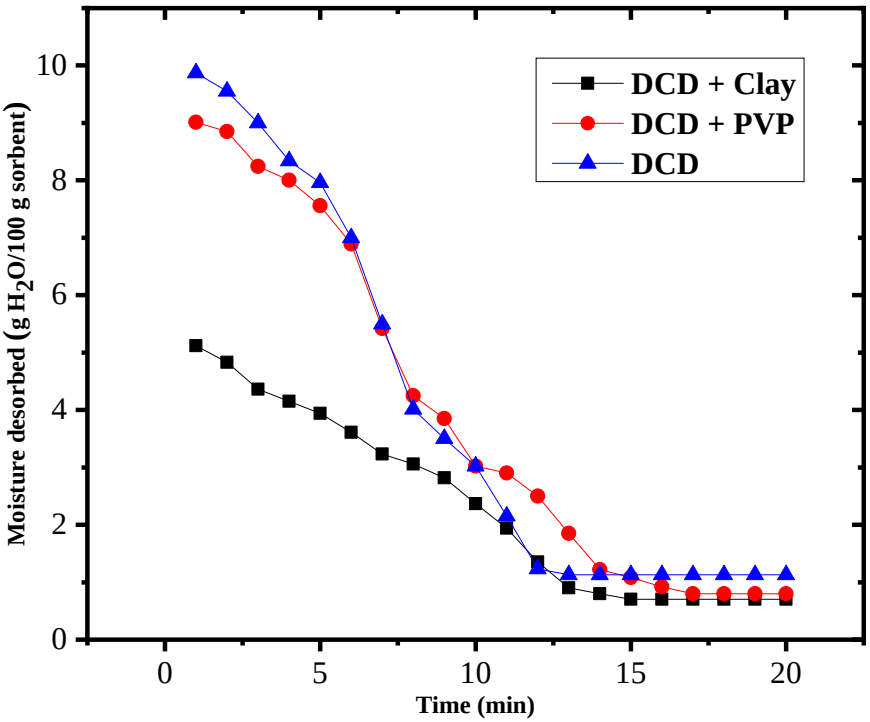

Figure 4.7: Variation of moisture content with time in different materials while desorption at 328 K and 6% RH, after sorption at 85% RH.

pore volume and average pores diameter of desiccants are shown in Table 4.3. For the DCD, it has a specific surface area (S*BET*) of 21.570 m^2/g and a micro surface area (S*micro*) of 11.408 m^2/g. The ratio of micro surface area to specific surface area is approximately 52.88%. The desiccant has a BJH pore volume of 0.022 cm^3/g and an average pore diameter (D_{avg}) of 5.02 nm.

When DCD is combined with PVP (3:1 ratio), the resulting desiccant has a specific surface area of 15.157 m^2/g and a micro surface area of 6.462 m^2/g. The micro surface area to specific surface area ratio is approximately 42.63%. The desiccant exhibits a BJH pore volume of 0.009 cm^3/g and an average pore diameter of 2.686 nm. Lastly, DCD:clay (3:1 ratio) desiccant shows a specific surface area of 10.251 m^2/g and a micro surface area of 11.672 m^2/g. The ratio of micro surface area to specific surface area is significantly higher at approximately 113.82%. The desiccant has a BJH pore volume of 0.058 cm^3/g and an average pore diameter of 22.85 nm.

Samples are kept at a temperature of 353 K in vacuum conditions for 8 hours, before measurement. The adsorption and desorption experiment is conducted using the Quantachrome® Autosorb iQ with nitrogen at 77 K. It is observed that the N_2 adsoprtion and desorption isotherms of the samples correspond to type III and type IV isotherms of the IUPAC (International Union of Pure and Applied Chemistry) classifications (Duong *et al.* 2021) (Fig.4.8). DCD and DCD+PVP desiccants follow the type IV isotherm, which indicates the formation of multilayer adsorption as the relative pressure increases. In type IV isotherms, the hysteresis loop appears as a closed loop shape, typically resembling an "S" or a sigmoid curve. The loop is formed due to the presence of capillary condensation and evaporation within the porous structure. The hysteresis loop in type IV isotherms signifies the occurrence of pore blocking and the presence of a significant volume of adsorbed material that remains trapped within the pores even at low pressures. This behavior is often associated with materials that have a complex pore structure or a hierarchical arrangement of pores. The loop indicates a large amount of irreversible adsorption-desorption, which suggests the presence of strong adsorbate-adsorbent interactions or the existence of narrow necks or tortuous paths within the pore network.

Whereas, DCD+Clay desiccant follows type III, which is non-porous or macroporous with weak interaction (Henninger *et al.* 2017; Dehmani and Abouarnadasse 2020; Iwuozor *et al.* 2022; Zhao *et al.* 2020; Susianti *et al.* 2022; Choi *et al.* 2021; Vivekh *et al.* 2018; Vu *et al.* 2013). The hysteresis loop of type III isotherms is a characteristic feature observed in adsorption and desorption processes of certain materials, typically porous materials such as mesoporous or macroporous solids. This type of isotherm is commonly associated with non-polar adsorbates and adsorbent materials with narrow pore size distributions. The macroporous structure is one of the reasons for the lower moisture uptake capacity of DCD+Clay composite.

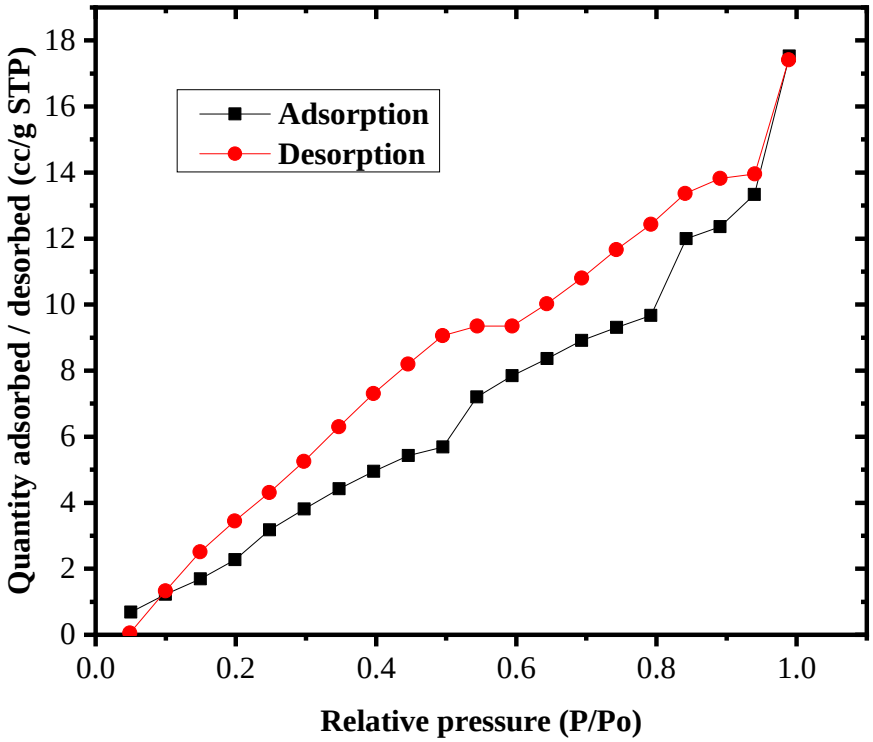

(a)

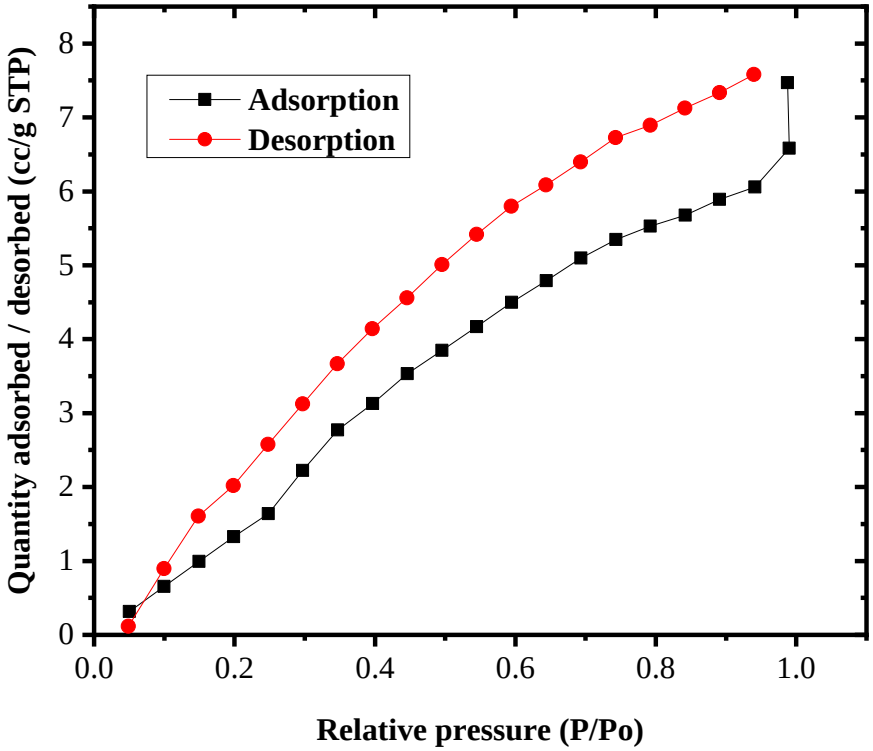

(b)

See the next page for another figure and caption...

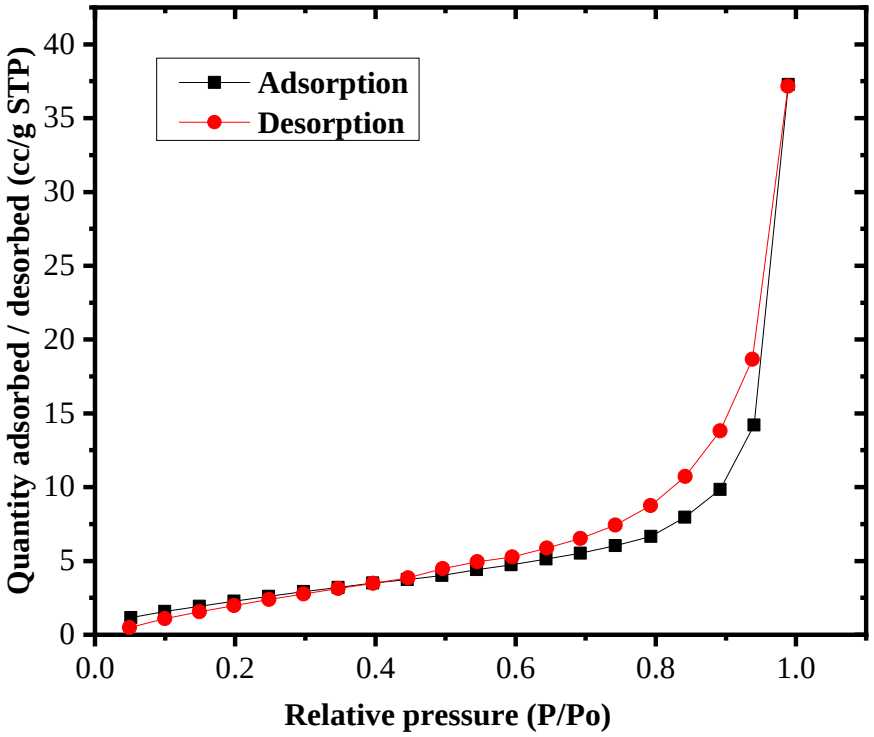

(c)

Figure 4.8: Nitrogen gas adsorption isotherms of (a) DCD, (b) DCD+PVP (3:1) and (c) DCD+Clay (3:1) at standard temperature and pressure conditions.

Table 4.3: Physical properties of desiccants determined by BET and BJH analysis

Desiccants	S_{BET} (m^2/g)	S_{micro} (m^2/g)	S_{micro}/S_{BET}	BJH pore volume (cm^3/g)	D_{avg} (nm)
DCD	21.570	11.408	52.88%	0.022	5.02
DCD + PVP (3:1)	15.157	6.462	42.63%	0.009	2.686
DCD+Clay (3:1)	10.251	11.672	113.82%	0.058	22.85

Table 4.4: Thermal conductivity of DCD + PVP (3:1)

Sl. No.	Temperature (K)	Thermal Conductivity (W/mK)
1	298	0.295
2	323	0.508
3	348	0.561
4	373	0.629

The thermal conductivities of DCD + PVP (3:1) at different temperatures are shown in Table 4.4. At room temperature the thermal diffusivity of composite desiccant is

nearly about 0.3 W/mK. The density is calculated using mass by volume method. Four samples are prepared and weighed. The volume of each sample is found out by measuring the thickness and diameter using Vernier calliper. The average density of this composite desiccant is about 720 kg/m^3. Specific heat is measured using differential scanning calorimeter, which is 7.58 kJ/kgK. Thermal diffusivity is calculated using measured values of thermal conductivity, specific heat and density. The thermal diffusivity of this desiccant is 5.49×10^{-7}m^2/s.

4.5 Exergetic analysis of DCD-based composite desiccants dehumidification systems

Test conditions for each case to calculate the exergy efficiency and power required for these systems are detailed in Table 4.5. Figure 4.9 shows the power required under the different conditions to run the dehumidification system. Cases 1 to 3 represents the DCD at three different inlet conditions i.e., RH = 75%, 85% and 95% respectively. Similarly, cases 4 to 6 for DCD+PVP and cases 7 to 9 for DCD+Clay. The humidity, as well as temperature values at the inlet and exit of the test section are also shown. Power consumption is smaller at lower RH and higher at higher RH conditions because the difference between specific humidity ($\Delta\omega$) at the inlet and outlet increase with RH. The exergy efficiencies are plotted in Fig 4.10. The exergy efficiency of the DCD+PVP dehumidification system is 1.8% and 3.6% higher compared to DCD and DCD+Clay systems at 299 K and 85% RH conditions. The average exergy efficiency of DCD, DCD+PVP and DCD+Clay dehumidification systems is 0.40, 0.43, and 0.35 respectively. Moisture uptake capacity of the DCD+PVP dehumidification system is to 5.3% and 18.77% higher compared to DCD and DCD+Clay systems respectively.

4.6 Total heat load reduction by DCD-based composite desiccants dehumidification systems

Sensible and latent heat loads are calculated for different relative humidity values and corresponding values are tabulated in Table 4.6. It can be seen that the decrease in

Table 4.5: The test conditions for DCD based dehumidification systems.

Desiccants → / Parameters ↓	DCD			DCD+PVP			DCD+Clay		
Cases →	1	2	3	4	5	6	7	8	9
T_1 (K)	299	299	299	299	299	299	299	299	299
ω_1 (g/kg)	15.5	18	20.4	15.5	18	20.4	15.5	18	20.4
h_1 (kJ/kg)	66	72.3	77.6	66	72.3	77.6	66	72.3	77.6
T_2 (K)	302.3	303.5	304.5	302.8	303	303.9	301.1	301.5	301.9
ω_2 (g/kg)	14.5	14.6	14.8	15.1	15.3	15.6	15	14.9	15
h_2 (kJ/kg)	65.0	65.8	69.5	68.0	67.8	70.0	65.9	65.7	66.5
$\Delta\omega$ (g/kg)	1	3.4	5.6	0.93	2.7	4.8	0.91	3.1	5.4

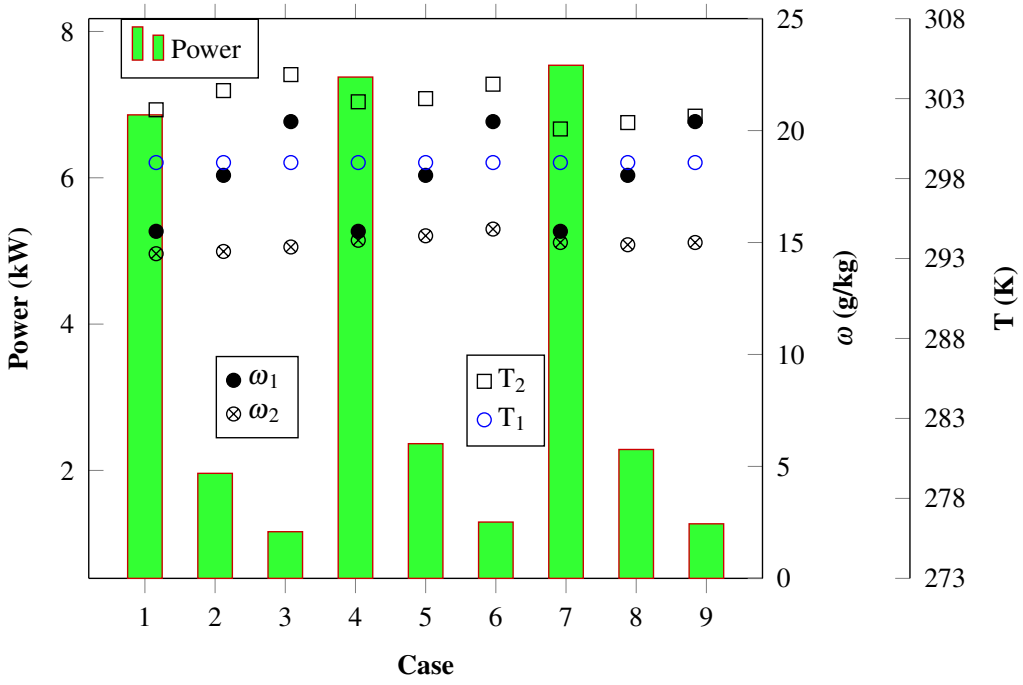

Figure 4.9: Comparison of power required by the three different materials under various operating conditions. Case 1-3 for DCD, 4-6 for DCD+PVP and 7-9 for DCD+Clay

latent heat load surpasses the increase in sensible heat load. Hence the overall heat load of the cooling system will decrease. It is observed that the total heat load reduction is high for DCD+PVP, and this is true for all the RH values. This implies that the moisture removal capacity of DCD+PVP is high compared to other desiccants. Total heat load reduction is less for the DCD+Clay humidification system compared to the other two systems, due to less moisture uptake capacity of the material, which is shown in Table

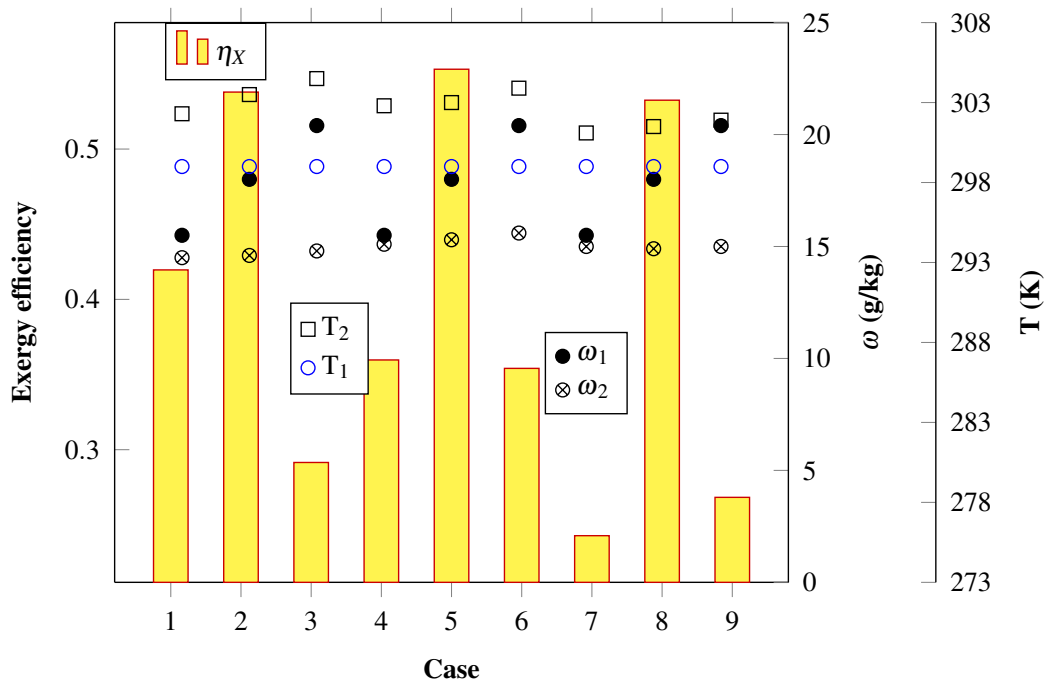

Figure 4.10: Comparison of exergy efficiency of three different materials under various operating conditions. Case 1-3 for DCD, 4-6 for DCD+PVP and 7-9 for DCD+Clay

Table 4.6: Total heat load (sensible + latent heat load) reduction by different materials in various conditions.

Sl. No.	Desiccants ↓	Q_s (kJ/kg)	Q_l (kJ/kg)			Net decrease in THL (Q_l-Q_s) (kJ/kg)		
	Test conditions →		75% RH	85% RH	95% RH	75% RH	85% RH	95% RH
1	DCD	20.93	32.77	38.42	42.94	11.83	17.48	22.05
2	DCD+PVP	20.09	33.90	39.55	45.20	13.80	19.45	25.10
3	DCD+Clay	12.14	22.60	27.23	31.64	10.46	15.09	19.50

4.6. However, the DCD+Clay desiccant performs well in terms of reducing the sensible heat load. The total heat load reduction of the DCD+PVP dehumidification system is 13.6% and 22.3% higher compared to the DCD and DCD+Clay dehumidification systems respectively.

4.7 Summary

- BET and BJH analyses were conducted on selected composite desiccants.

- The desiccants DCD and DCD+PVP exhibited type IV isotherms, while DCD+Clay showed a type III isotherm.
- The DCD+PVP composite desiccant had the highest moisture uptake capacity compared to DCD and DCD+Clay.
- At 299 K and 95% RH, the maximum moisture uptake capacities were 14.42 g/100 g for DCD, 14.72 g/100 g for DCD+PVP, and 4.53 g/100 g for DCD+Clay.
- Polyvinyl pyrrolidone (PVP) and clay acted as binders for DCD, reducing the loss of desiccant material during sorption-desorption.
- The optimal binding ratio based on the isotherm test was found to be 3:1 (DCD:PVP).
- The addition of PVP increased the life cycle of DCD-based composite desiccants.
- PVP is found to have a higher moisture uptake capacity than clay.
- Exergy analysis showed that DCD+PVP had better exergy efficiency compared to DCD and DCD+Clay dehumidification systems.
- The total heat load reduction in the DCD+PVP dehumidification system was 13.6% and 22.3% higher than DCD and DCD+Clay systems, respectively.
- Desorption times for DCD, DCD+PVP, and DCD+Clay were 13, 17, and 15 minutes, respectively.
- Moisture content remaining in DCD+PVP desiccants after desorption was approximately 15% and 35% lower than DCD and DCD+Clay, respectively.
- The proposed methods and calculations in the study had an error range of ±1.5-5%, which is comparable to accepted uncertainties.

CHAPTER 5

METAL EMBEDDED NATURAL COMPOSITE DESICCANT DEHUMIDIFICATION SYSTEM

This chapter focuses on metal-embedded natural composite desiccant (DCD+PVP with 3:1 ratio) with a different thickness ratio. A natural composite desiccant, in which the unutilised portion of the spherical desiccant material is replaced with different diameters of stainless steel balls to optimize the thickness ratio of metal embedded natural composite desiccants (MENCDs). Analysis of moisture uptake capacity, rate of moisture uptake and desorption of MENCDs with different thickness ratios are carried out under various humid conditions. The effect of thickness ratio on temperature rise during sorption, maximum moisture uptake and moisture uptake rate for MENCDs have been analysed. Along with this, the total heat load reduction and exergetic efficiency of MENCDs-based dehumidification systems are also calculated.

5.1 Effect of thickness ratio on maximum moisture uptake capacity and rate

Metal-embedded natural composite desiccants (MENCDs) are prepared with different thickness ratios to investigate the moisture uptake capacity under different humid conditions to find the optimum thickness ratio. Figure 5.1 shows the variation of moisture uptake capacity and rate of moisture uptake of MENCDs with a different ratio under different relative humidity conditions. The moisture uptake rate is determined by measuring the quantity of moisture absorbed during a 5-minute interval and the maximum amount of moisture sorbed until the composite desiccant becomes saturated.

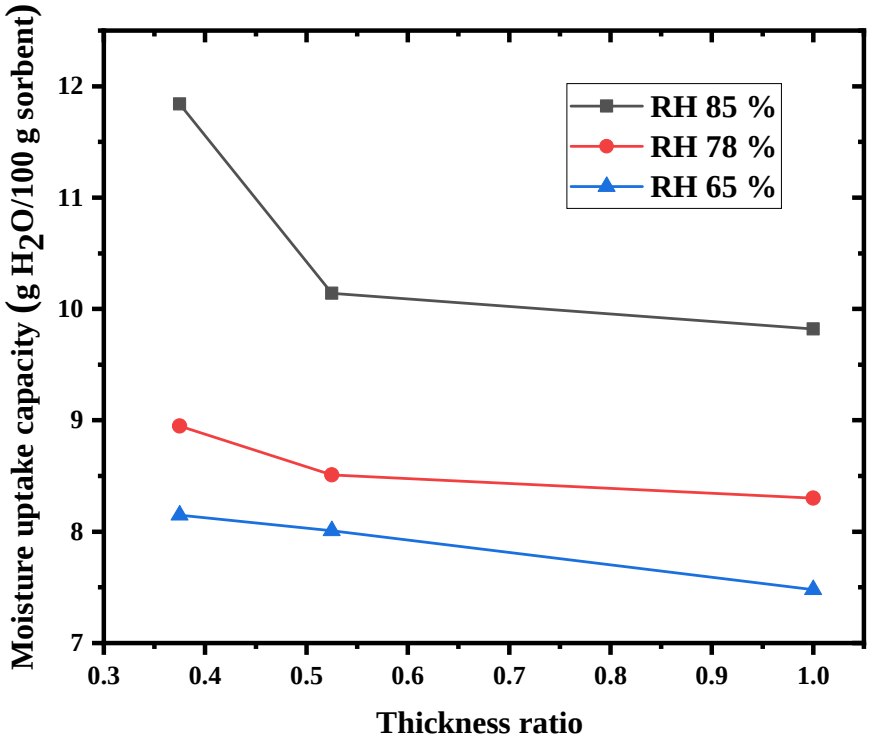

(a)

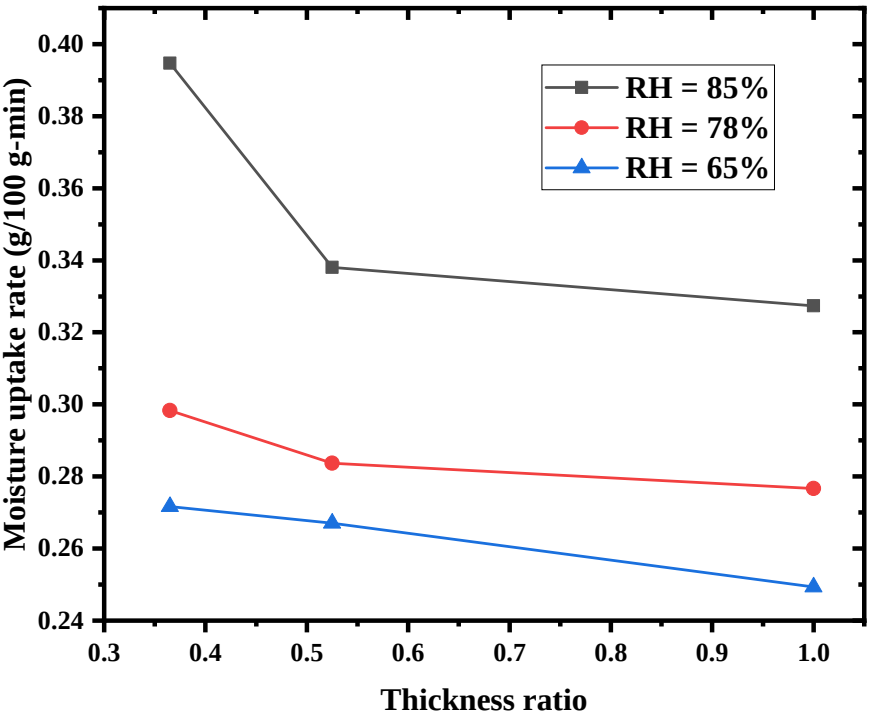

(b)

Figure 5.1: Comparison of (a) moisture uptake capacity and (b) moisture uptake rate of MENCDs of different thickness ratios at various inlet RH

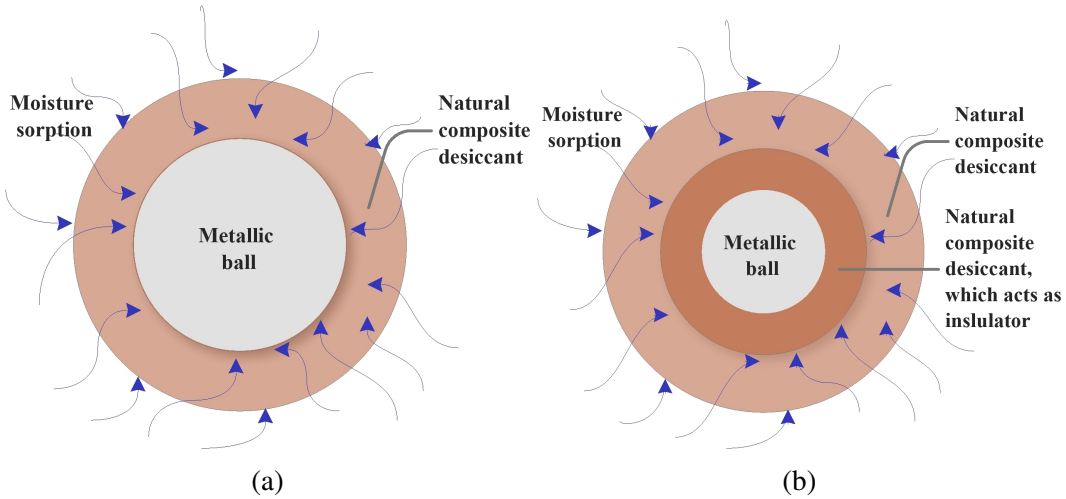

Figure 5.2: Pictorial representation of moisture sorption by natural composite desiccant with (a) TR = 0.365 and (b) TR = 0.525 (acts as insulator)

From Fig. 5.1, it can be observed that total moisture sorbed is expected to be high in between 0.3 and 0.5 thickness ratios of MENCDs. The optimum thickness ratio for MENCDs is found to be 0.365. For a thickness ratio of 0.365, at the end of the sorption process, the maximum moisture uptake capacity is 16.94% higher than the natural composite desiccant (i.e., TR = 1) without metallic balls at 85% RH and 301 K. At same condition, the moisture uptake rate is 20.57% higher for thickness ratio is equal 0.365 compared to thickness ratio equal to 1, which can be observed from Fig. 5.1 (b). Moisture uptake capacity of MENCDs with TR = 0.365 is 8.15, 9, 11.45 g/100 g at 65, 78, and 85% RH respectively. A theoretical study on the thickness ratio of MENCDs conducted by Kadoli *et al.* (2011) shows that the moisture uptake capacity is maximum for thickness ratio equal to 0.2. Although the composite desiccant is made of silica and inert material, current experimental study shows the thickness ratio is closer to that analysis. The current study has prepared the same thickness ratio of MENCDs and tested it under different humid conditions. The preparation of MENCDs with thickness ratio of 0.2 is a difficult process. Moreover, these MENCDs will not be stable during the sorption and desorption process. Maximum moisture uptake capacity and moisture uptake rate is even less for thickness ratio of 0.215, compared to a thickness ratio of 1 in all the conditions. This is because of less amount of natural composite desiccant

deposited on metallic balls. If the thickness ratio of natural composite desiccant is less than 0.365 and more than 0.525, then the maximum moisture uptake reduces, it can be observed from Fig. 5.1 (a). This is because the natural composite desiccant act as insulator, due to less thermal conductive of the composite desiccant. Embedment of metallic ball with optimum thickness ratio increase the thermal conductivity of natural composite desiccant. The pictorial representation of this process is shown in Fig. 5.2a and Fig. 5.2b.

5.2 Variation of outlet relative humidity and moisture uptake with respect to time

Figure 5.3 shows the variation of outlet relative humidity (RH) under different inlet RH conditions for different thickness ratios of MENCDs with respect to time. The tests are conducted for 30 minutes because the reduction of outlet relative humidity is not significant after 10 minutes of the sorption process. This indicates that the composite desiccant material needs to be regenerated periodically if it is used in the desiccant wheel. From these figures, it can be observed that the moisture reducing capacity is more for MENCDs with TR = 0.365, at different inlet relative humidity conditions. MENCDs with a TR = 0.365 can bring the relative humidity from 85% to below 60%, which is nearly 13.33% more than that of the natural composite desiccants (i.e., TR = 1). Figures 5.4 (a), (b), and (c) show the comparison of moisture sorption for different thickness ratios of MENCDs at different inlet conditions along with time. Maximum moisture sorption for MENCDs with TR = 0.365 is 11.45, 9, and 8.15 g/100 g of the sorbent at a constant temperature of 301 K, and 85%, 78%, and 65% RH, respectively. The increase of maximum moisture sorption for MENCDs with TR = 0.365 is 20.57%, 8.4%, and 8.9% more compared to TR = 1 at constant temperature of 301 K, and 85%, 78%, and 65% RH, respectively. This indicates that the optimum thickness ratio for MENCDs will be equal to 0.365.

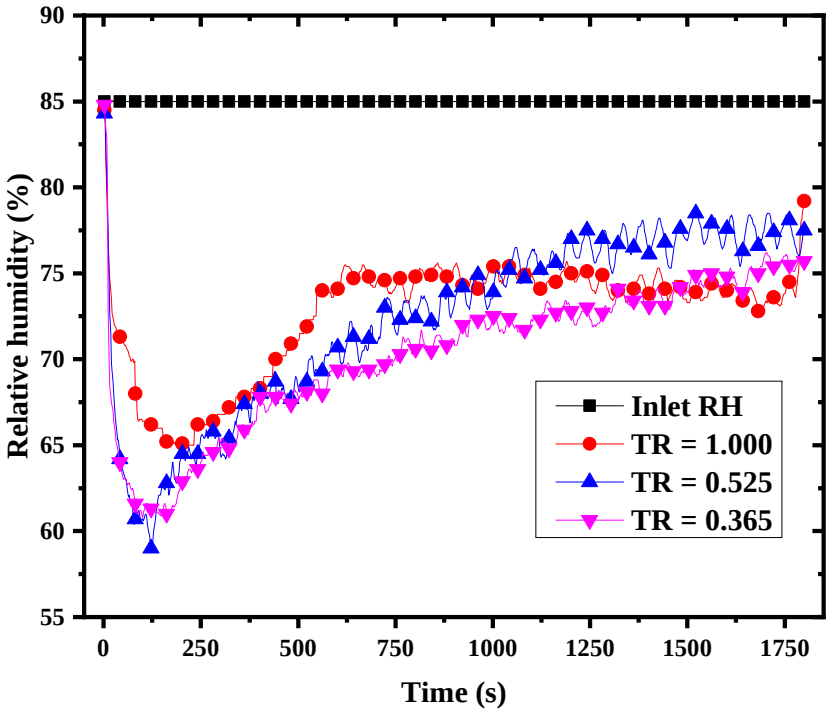

(a)

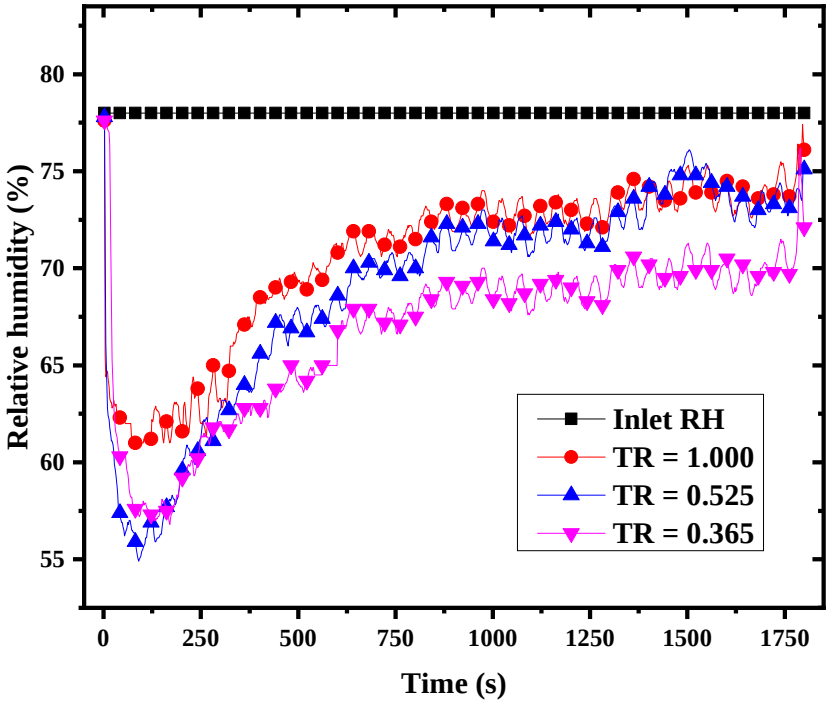

(b)

See the next page for another figure and caption...

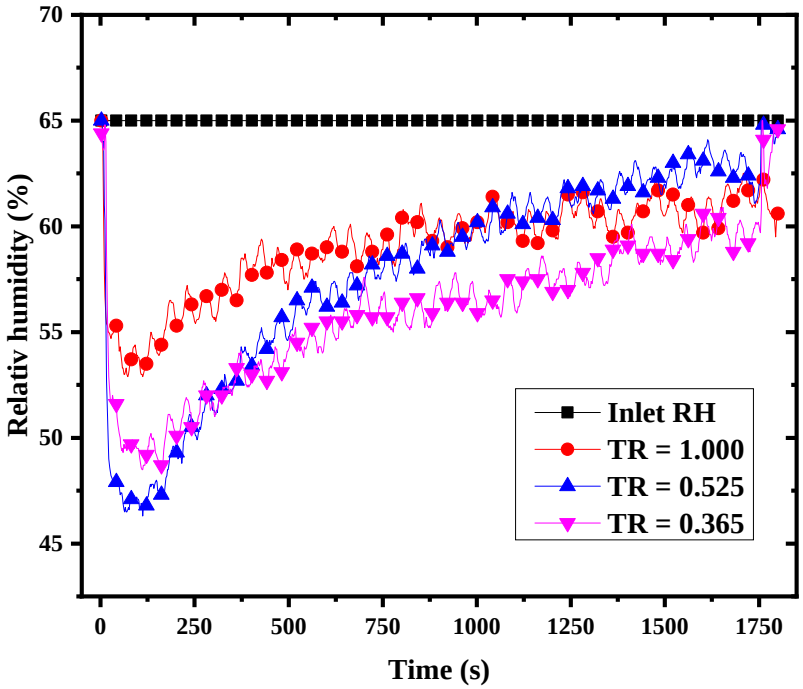

(c)

Figure 5.3: Comparison of outlet relative humidity variation for MENCDs of different thickness ratio at an inlet conditions of (a) 85% RH (b) 78% RH and (c) 65% RH

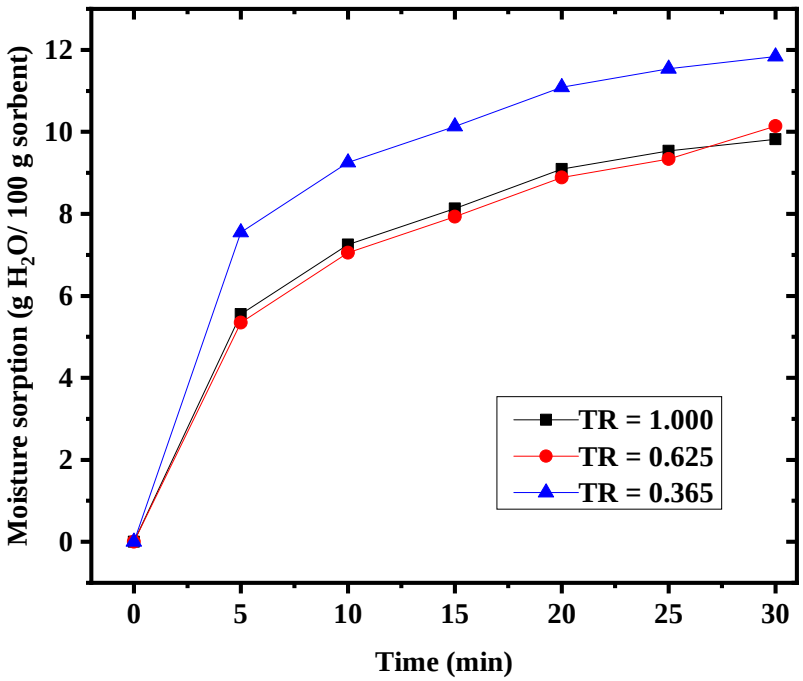

(a)

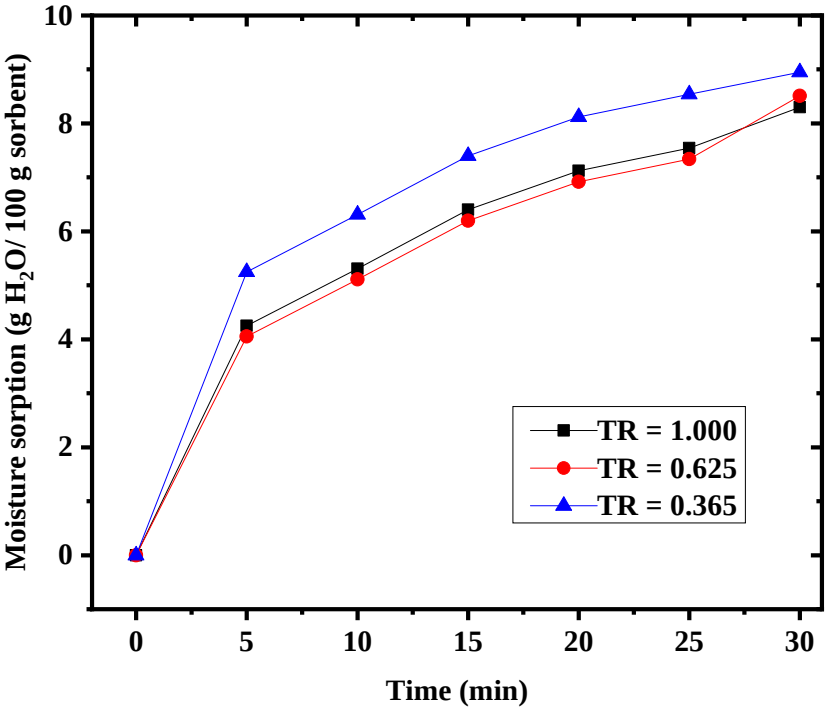

(b)

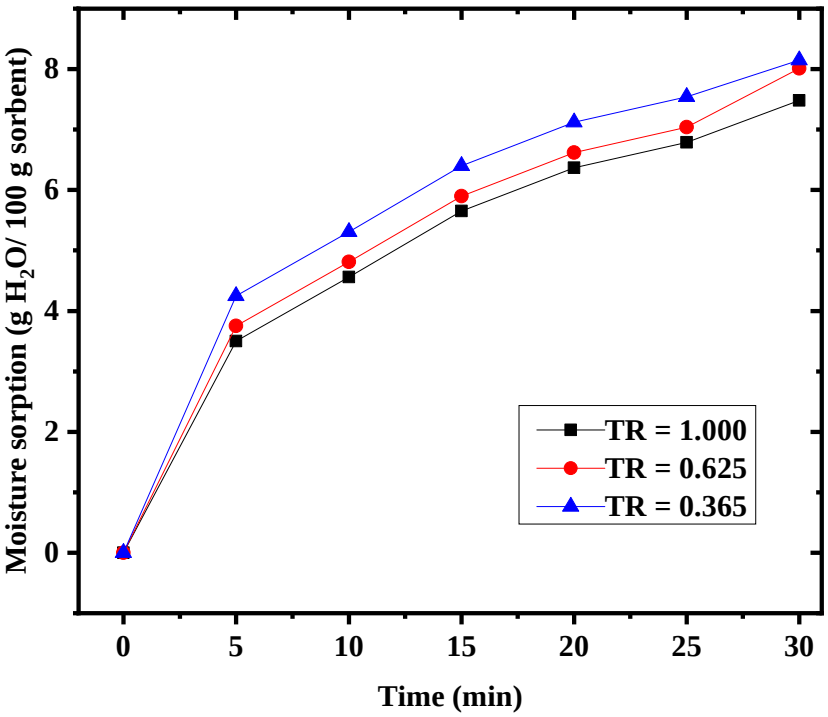

(c)

Figure 5.4: Comparison of moisture sorption for different thickness ratio of MENCDs at various inlet RH (a) 85% RH, (b) 78% RH, and (c) 65% RH

5.3 Study on moisture desorption rate

Moisture desorption tests are conducted at 328 K and 5% RH conditions for all the metal embedded natural composite desiccants. Figures 5.5 (a), (b), and (c) show the variation of moisture desorption rate (MDR) for the tests conducted after sorption process at 85, 78, and 65% RH, respectively. MDR is defined as the amount moisture desorbed at an interval of 5 minutes. From these figures, it can be observed that the MDR is high for lower thickness ratio MENCDs and less for higher thickness ratios. With fixed desorption (regeneration) temperature, MENCDs with a TR = 1 has less MDR compared to TR = 0.365. Additionally, in comparison with total moisture sorbed and moisture sorption rate of MENCDs with a TR = 0.365 has a high performance compared to MENCDs with a TR = 1. The MDR for MENCDs with a TR = 0.365 compared to TR = 1 is more in all three cases. This indicates that the use of MENCDs-based composite desiccants will increase the rate of desorption as well as the rate of sorption.

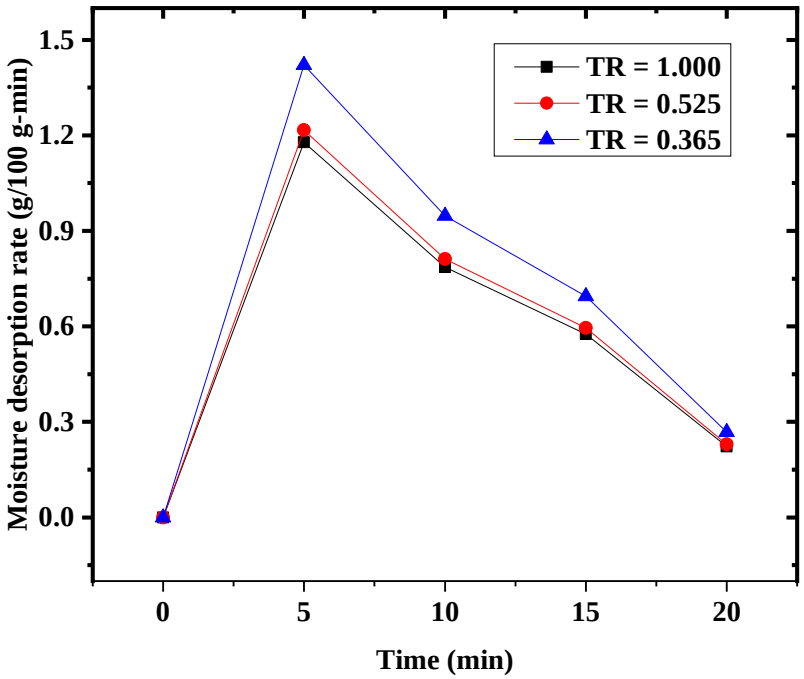

(a)

See the next page for two more figures and caption...

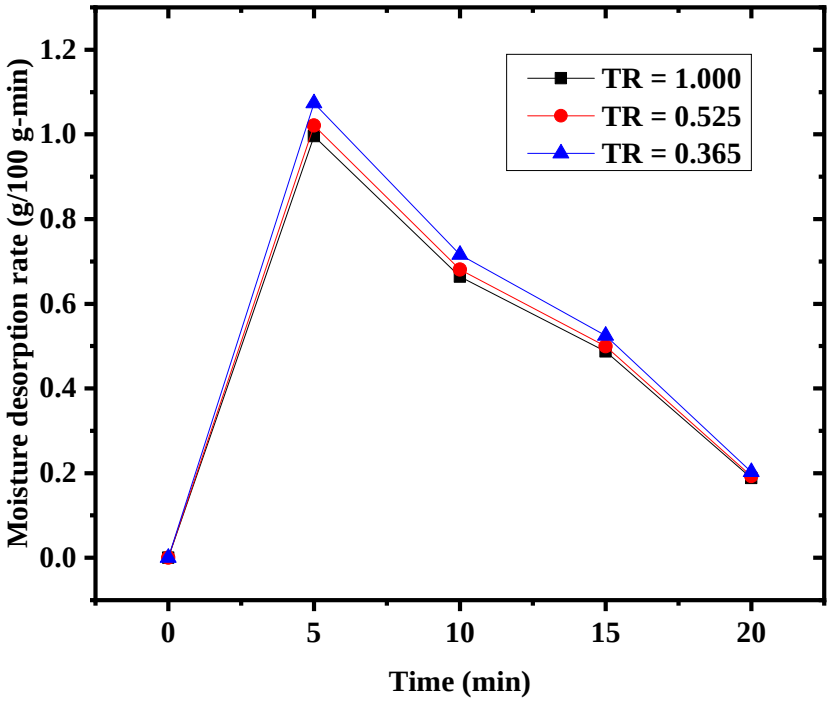

(b)

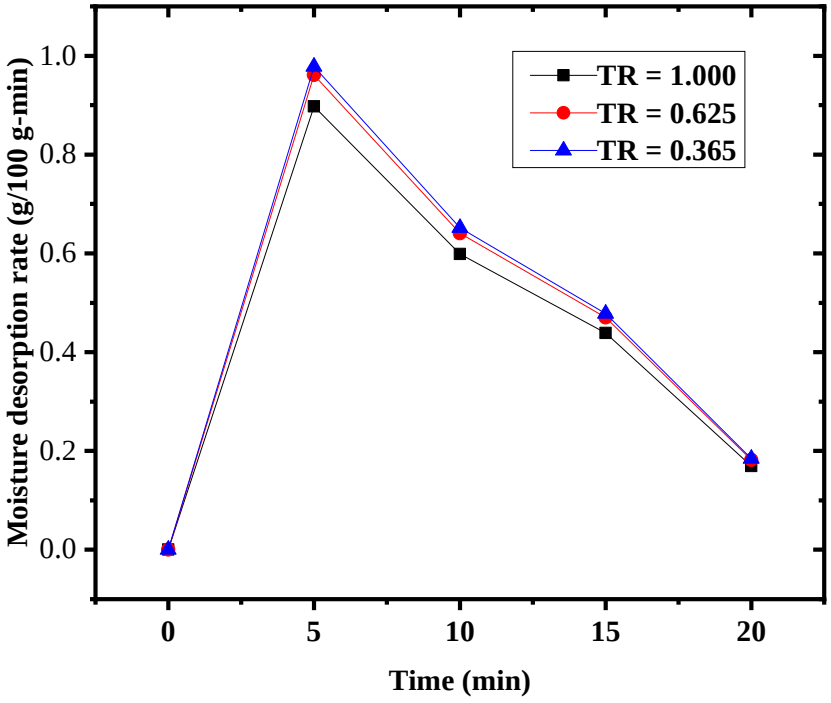

(c)

Figure 5.5: Comparison of moisture desorption rate at 328 K and 5% RH for different thickness ratio of MENCDs after sorption at (a) 85% RH, (b) 78% RH, and (c) 65% RH

5.4 Exergetic analysis of MENCDs dehumidification systems

Test conditions for each case to calculate the exergy efficiency and power required for MENCDs-based dehumidification systems are detailed in Table 5.1. Cases 1 to 3 represents the MENCDs with TR = 1, at three different inlet conditions i.e., RH= 85, 78, and 65% with constant temperature, respectively. Similarly, cases 4 to 6 for a TR = 0.525, and cases 7 to 9 for a TR = 0.365 at 65%, 78%, and 85% RH respectively. The humidity ratio, as well as temperature values at the inlet and exit of the test section, are also shown in Table 5.1. Figure 5.6 shows the power required under the different conditions to run the dehumidification system. The average power required for MENCDs-based dehumidification system with a TR = 1, 0.525, and 0.365 is 4.7, 2.3, and 1.8 kW respectively. The average power required in all the different inlet conditions for MENCDs with a TR = 0.365 is 63% less compared to TR = 1. Power consumption will be more as the difference between specific humidity ($\Delta\omega$) at the inlet and outlet is smaller. A large difference in the specific humidity reflects higher exergy efficiency. The exergy efficiency for all cases is plotted in Fig. 5.7. The average exergy efficiency in all the different conditions for MENCDs-based dehumidification system with a TR = 1, 0.525, and 0.365 is 57%, 63%, and 62% respectively. The average exergy efficiency for TR = 0.365 is 9.64% higher compared to TR = 1.

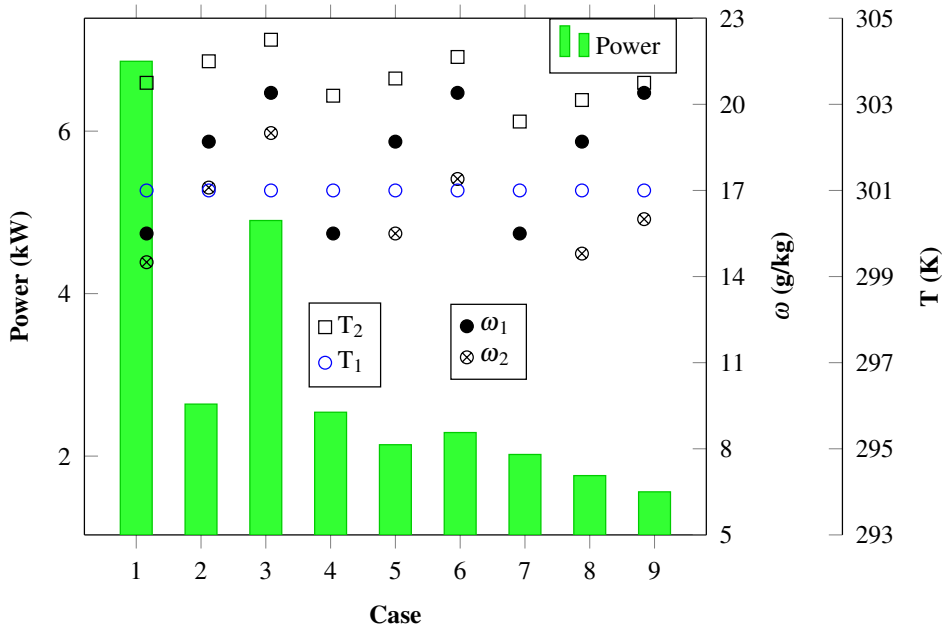

Figure 5.6: Comparison of power required for MENCDs-based dehumidification system under under different relative humidity (RH = 65%, 78%, and 85%) and at a constant temperature (301 K). Cases 1 to 3 for MENCDs with TR = 1, cases 4 to 6 for TR = 0.525, and cases 7 to 9 for TR = 0.365

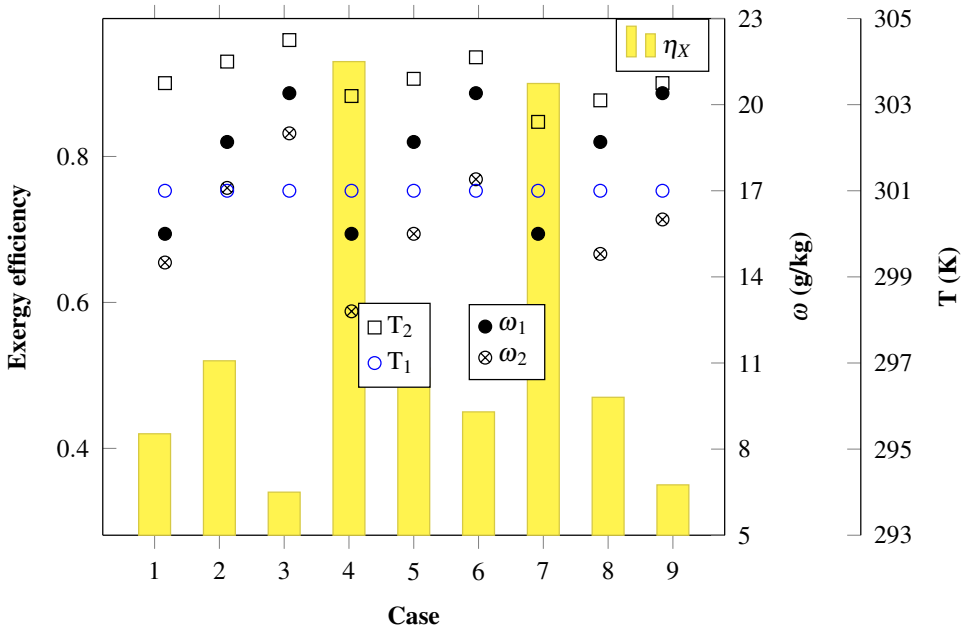

Figure 5.7: Comparison of exergy efficiency of MENCDs-based dehumidification system under different relative humidity (RH = 65%, 78%, and 85%) and at a constant temperature (301 K). Cases 1 to 3 for MENCDs with TR = 1, cases 4 to 6 for TR = 0.525, and cases 7 to 9 for TR = 0.365

5.5 Total heat load reduction by MENCDs dehumidification systems

Sensible and latent heat loads are calculated for different RH values at a constant temperature. The values are tabulated in Table 5.2. It can be seen that the reduction of latent heat load surpasses the increase in sensible heat load. Hence the overall heat load of the evaporative cooling system will decrease. It is observed that the total heat load reduction is high for MENCDs-based dehumidification system with a TR = 0.365, and this is true for all the RH values. This implies that the moisture removal capacity of MENCDs with TR = 0.365 is high compared to all other MENCDs. Total heat load reduction by MENCDs (TR = 0.365) based dehumidification system is 23.9% higher compared to TR = 1, at 85% RH.

Table 5.1: The test conditions of MENCDs dehumidification systems

MENCDs TR → **Parameters ↓**	**TR = 1**			**TR = 0.525**			**TR = 0.365**		
Cases →	1	2	3	4	5	6	7	8	9
RH (%)	65	78	85	65	78	85	65	78	85
T_1 (K)	301	301	301	301	301	301	301	301	301
ω_1(g/kg)	15.5	18.7	20.4	15.5	18.7	20.4	15.5	18.7	20.4
h_1(kJ/kg)	67.65	75.79	80.19	67.65	75.79	80.19	67.65	75.79	80.19
T_2(K)	302.8	303	303.2	303.1	303.6	304	303.8	304.1	304.5
ω_2 (g/kg)	14.1	15.2	17.6	12.7	15.5	17.3	13	15.7	16.9
h_2(kJ/kg)	66	69.08	75.44	62.75	70.4	75.45	64.13	71.34	74.97
$\Delta\omega$ (g/kg)	1.4	3.5	2.8	2.8	3.2	3.1	2.5	3	3.5
T_0 (K)	298	298	298	298	298	298	298	298	298
ω_0 (g/kg)	16.1	16.1	16.1	16.1	16.1	16.1	16.1	16.1	16.1

Table 5.2: Total heat load (sensible + latent heat load) reduction by different MENCDs-based dehumidification system at different RH and constant temperature (301 K)

Sl. No.	**MENCDs TR ↓**	**Q_s (kJ/kg)**	**Q_L (kJ/kg)**			**Net decrease in THL (Q_L-Q_s) (kJ/kg)**		
	Test conditions →		65% RH	78% RH	85% RH	65% RH	78% RH	85% RH
1	1	9.21	31.64	67.80	63.28	22.42	58.58	54.06
2	0.525	12.97	56.50	72.32	70.06	43.52	59.34	57.08
3	0.365	14.65	63.28	79.10	79.10	48.62	64.44	64.44

5.6 Summary

- From the experimental results, it is confirmed that the optimum thickness ratio (TR) is 0.365. The moisture uptake capacity of MENCDs with a TR of 0.365 is 11.84 g/100 g, which is 20.57% higher compared to natural composite desiccants (TR = 1) at 85% RH. This is because the moisture diffusion rate decreases compared to that of moisture convection when the thickness ratio of MNECDs increases.

- The maximum moisture uptake rate (MUR) for MENCDs with a TR = 0.365 is 1.8 g/100 g·min, which is 50% higher compared to TR =1. The total MSR is 0.4 g/100 g·min, which is 25% higher for same the TR. Moisture desorption rate (MDR) for MENCDs with TR = 0.365 is 16.66% higher compared to TR = 1.

- The average power required in all the different inlet conditions for MENCDs with a TR = 0.365 is 2.33 kW, which is 24.91% less compared to TR = 1. The average exergy efficiency of the MENCDs (TR=0.365) system is 62%, which is 9.65% higher compared to TR = 1.

- The total heat load reduction for MENCDs (TR = 0.365) is 23.9% higher compared to TR = 1 at 85% RH. For initial 5 minutes, the rise in temperature due to heat of sorption for TR = 0.365 is 0.13 K/ g of moisture sorbed is less compared to TR = 1.

- The experimental study concluded that the MENCDs will help to increase sorption and desorption rate, and enhance the utilization of a composite desiccant with an optimized thickness ratio. Improvements in these parameters help to increase the total heat load reduction for evaporative cooling systems and the exergetic efficiency of MENCDs-based dehumidification systems.

CHAPTER 6

NATURAL COMPOSITE DESICCANT COATED ON STAGGERED HEXAGONAL ALUMINIUM CHANNEL DEHUMIDIFICATION SYSTEM

In this chapter, a thorough investigation is presented on the enhanced utilization of natural composite desiccant (NCD) coated on hexagonal aluminium channels. The study investigates and contrasts the pressure loss, moisture sorption, and desorption characteristics of a hexagonal aluminium channel bed coated with NCD against a traditional packed bed dehumidification system. The utilization of hexagonal channels in sorption systems is anticipated to yield superior performance compared to other geometries.

6.1 Moisture uptake capacity & moisture uptake rate

Moisture uptake capacity (MUC) is the amount of moisture the composite desiccant can sorb for a certain period until it reaches saturation (g/100 g of sorbent). Moisture uptake rate (MUR) is the amount of moisture sorbed per minute (g/100 g·min). MUR is calculated as the total amount of moisture sorbed for five minutes then averaged. Figure 6.1 (a) shows the maximum moisture uptake (MMU) at different relative humidities (85, 75, and 65%) and temperatures (300 and 304 K). The MMU at a constant temperature of 300 K and relative humidities 85, 75, and 65% is 14.31, 13.13, and 10.2 g/100 g of sorbent respectively. The MMU is higher at high RH due to the larger availability of water vapour in the moist air. The MMU at a constant temperature of 304 K and relative humidities 85, 75, and 65% is 12.97, 10.78, and 8.43 g/100 g of sorbent

respectively. The MMU is less at a temperature of 304 K compared to 300 K for the same relative humidities. This is because the moisture sorption capacity reduces with increase in temperatures. Due to sorption being an exothermic process, the moisture sorption capacity is reduced with an elevation in temperature in accordance with the Le-Chatelier principle. Figure 6.1 (b) and (c) represents the amount of moisture sorbed or isotherms (300 & 304 K) and rate of moisture uptake respectively. The amount of moisture sorbed is more at lower temperatures and higher relative humidity, and it is less at higher temperatures and lower relative humidity (Fig. 6.1b). The saturation time of NCD-coated SHACs dehumidification bed at RH (85%, 75%, and 65%) & 300 K, and RH 85% & 304 K is between 50 and 55 minutes due to high moisture content. Whereas, At RH (75 & 65%) and temperature (304 K) is between 30 and 35 minutes due to less moisture content and higher temperature. Higher temperatures reduces the moisture uptake capacity, however increase the MSR. This can be observed from Fig. 6.1 (c). The average MSR at temperature of 300 K is 0.26, 0.24, 0.20, g/100 g·min under RH 85%, 75%, and 65% respectively. Whereas, at temperature of 304 K, it is 0.26, 0.31, and 0.28 g/100 g·min under RH 85%, 75 %, and 65% respectively.

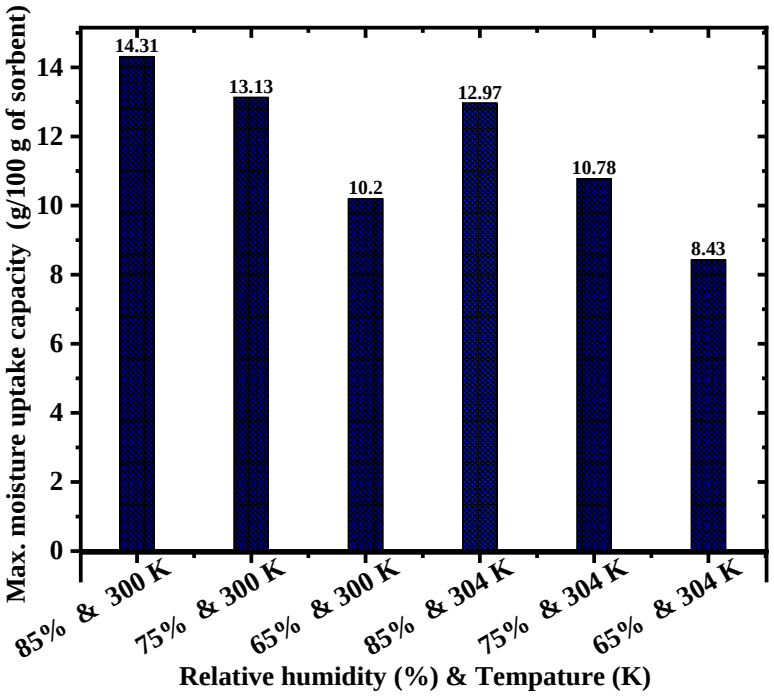

(a)

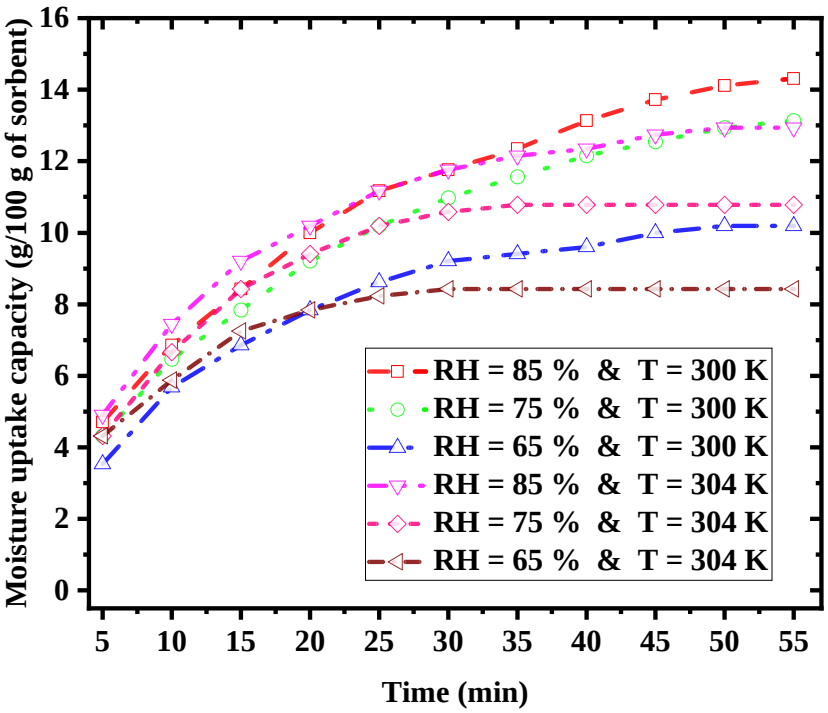

(b)

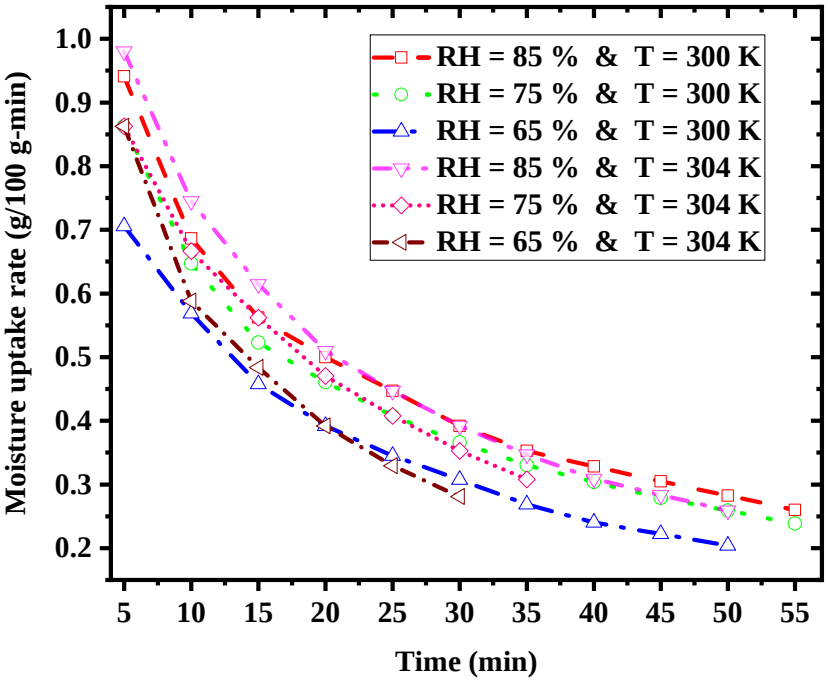

(c)

Figure 6.1: Variation of (a) maximum moisture uptake, (b) amount of moisture uptake, and (c) moisture uptake rate at different relative humidities and temperatures along with time

6.2 Variation of relative humidity and temperature during sorption process

Figures 6.2 (a) and (b) show the variation of outlet relative humidity (RH) and temperature (K) respectively, under different inlet RH & temperature for NCDs-coated SHACs dehumidification bed with respect to time. The tests are conducted until the composite desiccant reaches the saturation level. In all the inlet conditions the dehumidification bed brings relative humidity well below 60% for initial 8-10 minutes, along with, the dehumidification outlet temperature rises due to the heat of sorption. The spikes in between both the Figures 6.2 (a) and (b) are due to the experiments being stopped every 5 minutes to measure the moisture sorption capacity (i.e., weigh the dehumidification bed). This will cause a drop in temperature due to heat loss. During this period the relative humidity and temperature tend to move back to the inlet condition. The temperature rise is high for initial 8-10 minutes as the moisture sorption capacity is high. The maximum temperature rise at inlet temperature of 300 K is 4.8, 4.3, and 4.0 K under RH 85, 75, and 65% respectively. Whereas, at inlet temperature of 304 K it is 6.0, 5.5, and 4.0 K under RH 85, 75, and 65% respectively.

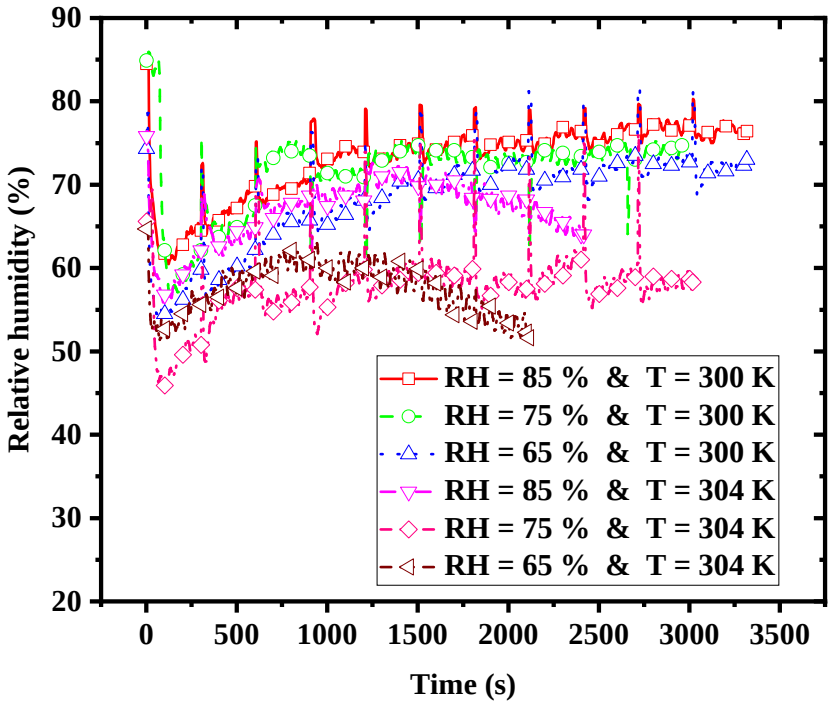

(a)

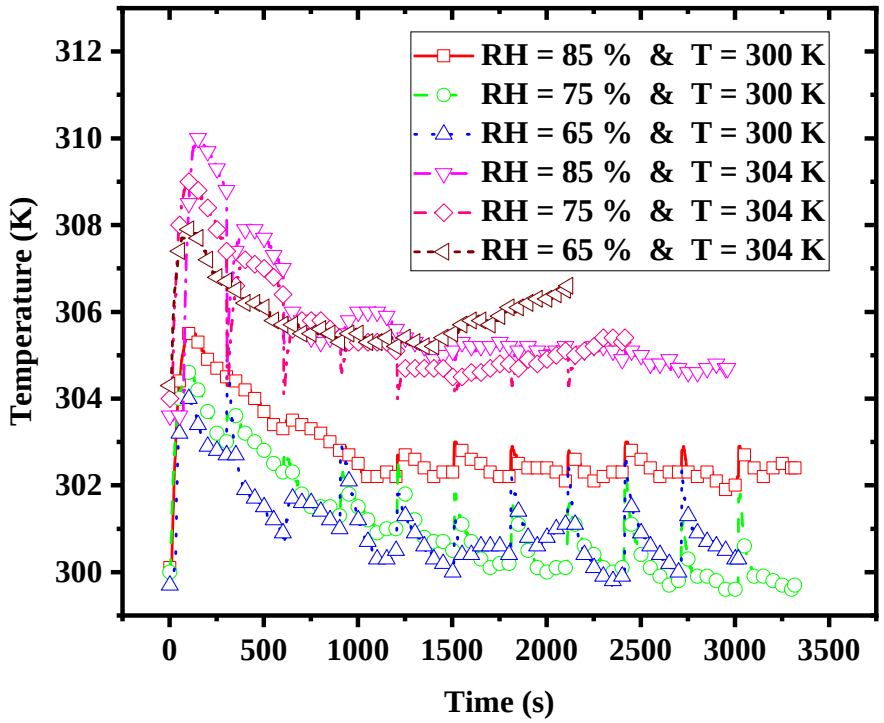

(b)

Figure 6.2: Variation of outlet (a) relative humidity and (b) temperature at fixed inlet relative humidities and temperatures along with time

6.3 Moisture desorption and pressure drop

Figures 6.3 (a) and (b) show the variation of the amount of moisture desorption and moisture desorption rate (MDR) respectively, at 323 K after sorption at different relative humidities and temperatures with respect to time. This temperature helps to maintain sorption process above 85% after regeneration to reduce the moisture lock. The desorption time of NCD-coated SHACs dehumidification bed is between 20 and 25 minutes. The average MDR after sorption at 300 K is 0.57, 0.53, 0.51 g/100 g·min under RH 85, 75, and 65% respectively. Wherae as, sorption at 304 K, it is 0.52, 0.54, and 0.42 g/100 g·min under RH 85, 75, and 65% respectively. The pressure drop is calculated for NCD-coated SHACs and NCDs-packed dehumidification beds using a digital U-tube manometer. The test is conducted for the same bed length (10 cm) and velocity (2.5 m/s). The moisture removal capacity of NCD-coated SHACs bed is in-

creased from 9.01 g/100 g to 14.31 g/ 100g compared NCD-packed bed at 299-300 K and 85% RH, which is 58.8% increase in moisture removal capacity. The pressure drop for the NCD-packed bed and the NCD-coated SHACs bed is found to be 0.45 and 0.13 kPa respectively. This accounts for the reduction of 71.11% pressure drop across NCD-coated SHACs bed compared to the packed bed, which indicates that fan energy can be saved up to 71.11%.

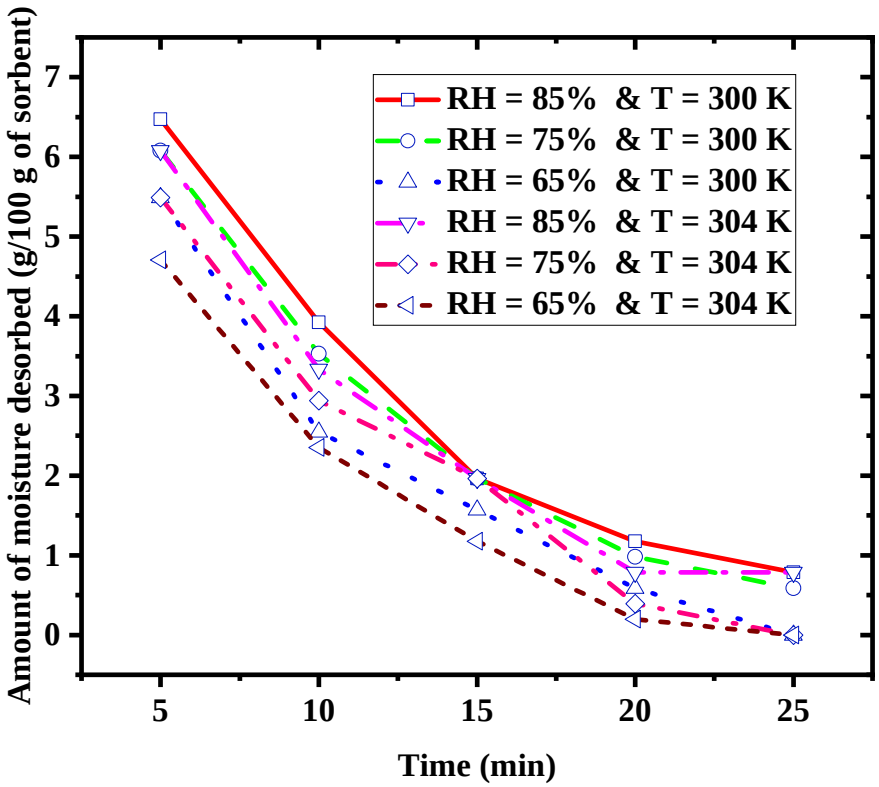

(a)

See the next page for another figure and caption...

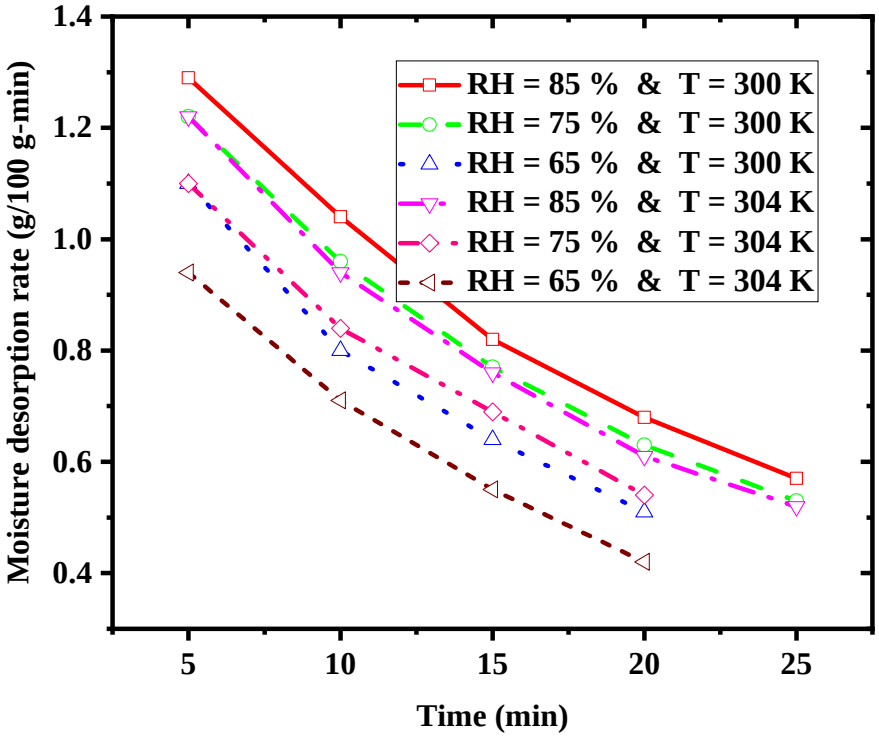

(b)

Figure 6.3: Variation of (a) moisture desorption and (b) moisture desorption rate at 323 K after sorption at different relative humidities and temperatures with respect to time

6.4 Total heat load reduction of MENCDs dehumidification systems

The Table 6.1 shows the test conditions of NCD-coated SHACs dehumidification system at different relative humidities (85, 75, and 65%) and temperatures (300 and 304 K). Sensible and latent heat loads were computed for varying relative humidities and temperatures, and the resulting values are presented in Table 6.2 for temperatures of 300 K and 304 K across different RH levels. The computed values indicate that the reduction in latent heat load (Q_L) outweighs the increase in sensible heat load (Q_s), resulting in a decrease in the overall heat load of the evaporative cooling system. Specifically, the NCD-coated SHACs dehumidification system exhibits a total heat load reduction (THLR) of 14.05, 23.09, and 5.01 kJ/kg at RH levels of 85%, 75%, and 65%, respectively, at 300 K. Similarly, at 304 K, the THLR is 23.85, 60.01, and 1.25 kJ/kg at RH levels of 85%, 75%, and 65%, respectively.

Table 6.1: The test conditions of NCD-coated SHACs dehumidification system.

Temperature → **Parameters ↓**	**300 K**			**304 K**		
RH (%)	85	75	65	85	75	65
T_1 (K)	300	300	300	304	304	304
ω_1(g/kg)	19.2	16.9	14.6	24.4	21.4	18.5
h_1(kJ/kg)	76.09	70.19	64.31	93.56	85.98	78.43
T_2(K)	304.8	304.3	304	310	309.5	308
ω_2 (g/kg)	17.8	15.1	15.6	22.4	17.8	19.5
h_2(kJ/kg)	77.62	72.75	70.99	94.71	82.33	80.79
$\Delta\omega$ (g/kg)	1.4	1.8	1	2	3.6	1
T_0 (K)	298	298	298	298	298	298
ω_0 (g/kg)	16.1	16.1	16.1	16.1	16.1	16.1

Table 6.2: Total heat load (sensible + latent heat load) reduction by NCD-coated SHACs dehumidification bed at different RHs and temperatures

Sl. No.	**Inlet temp (K) ↓**	**Q_s (kJ/kg)**	**Q_L (kJ/kg)**			**Net decrease in THL (Q_L-Q_s) (kJ/kg)**		
	RH (%) →		85	75	65	85	75	65
1	300	17.59	31.64	40.68	22.60	14.05	23.09	5.01
2	304	21.35	45.20	81.36	22.60	23.85	60.01	1.25

6.5 Exergetic analysis of NCD-coated SHACs dehumidification systems

The power required for NCD-coated SHACs dehumidification systems is studied at different inlet conditions. Figure 6.4 shows comparison of power required for NCD-coated SHACs dehumidification system under different relative humidity (RH = 85%, 75%, and 65%) and temperature (300 & 304 K). The test conditions for this analysis are tabulated in Table 6.1. The average power required in all the different inlet conditions for MENCDs with a TR = 0.365 is 63% less compared to TR = 1. Power consumption will be more as the difference between specific humidity ($\Delta\omega$) at the inlet and outlet is less. The higher the change in specific humidity reflects higher exergy efficiency. The exergy efficiency for all cases is plotted in Fig. 5.7. The average exergy efficiency in all the different conditions for MENCDs-based dehumidification system with a TR = 1, 0.525, and 0.365 is 57%, 63%, and 62% respectively. The average exergy efficiency for TR = 0.365 is 9.64% higher compared to TR = 1.

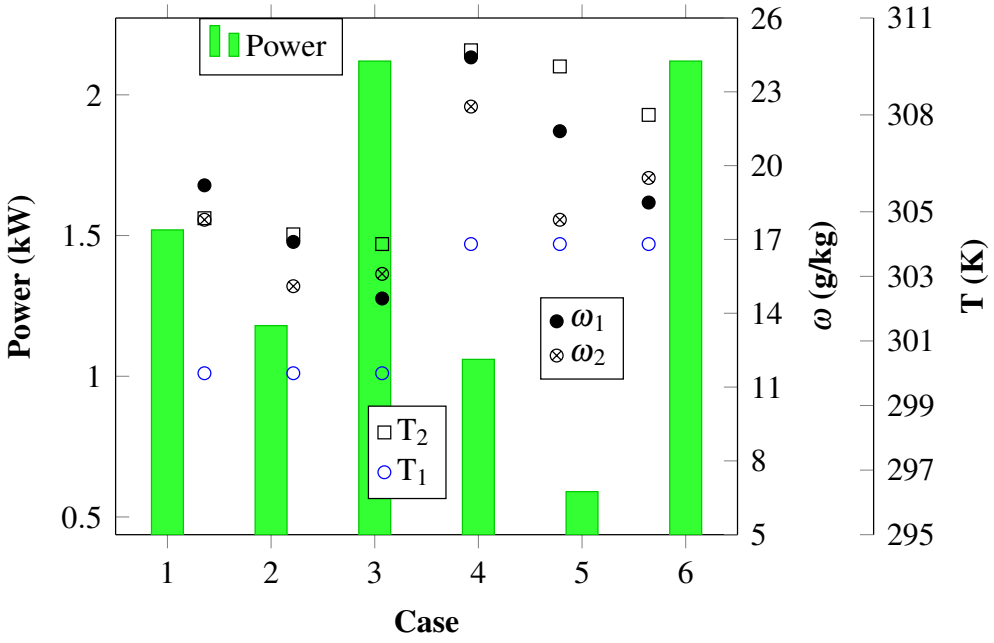

Figure 6.4: Comparison of power required for NCD-coated SHACs dehumidification system under different relative humidity (RH = 85, 75, and 65%) and temperature (300 & 304 K).

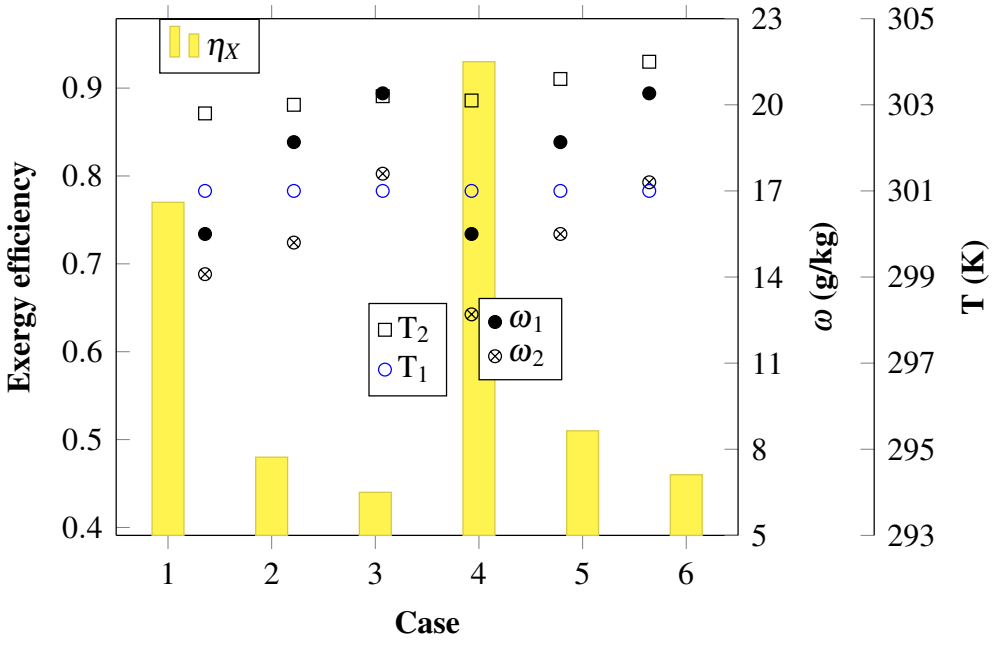

Figure 6.5: Comparison of exergy efficiency of MENCDs-based dehumidification system under different relative humidity (RH = 85, 75, and 65%) and constant temperatures (300 & 304K).

6.6 Summary

- The maximum moisture uptake capacity (MUC) reached 14.31, 13.13, and 10.2 g/100 g at RH 85, 75, and 65% and temperature of 300 K respectively. Whereas at higher temperature of 304 K, MMU gets reduced to 12.97, 10.78, and 8.34 g/100 g for the RH at 85, 75, and 65%, respectively.

- The average moisture uptake rate (MUR) of the NCD-coated SHACs dehumidification system is 0.26 g/100g·min, while the moisture desorption rate (MDR) reached 0.51 g/100 g·min. The desorption time of this system is about 20-25 minutes.

- The maximum moisture uptake (MMU) of NCD-coated SHACs dehumidification bed is 60.7% higher compared to cow dung balls packed bed at 300-301 K and 85%. Similarly, at 300-301 K and 65% RH, the MMU is 85% high.

- The natural composite desiccants featuring staggered hexagonal channels exhibited a significantly lower pressure drop compared to the desiccant-packed bed made of natural composite material. This resulted in a 71.11% reduction in energy consumption by the fans. Moreover, the average exergy efficiency was approximately 28%.

- The average heat load reduction of NCD-coated SHACs dehumidification system at different RH conditions with temperatures of 300 K and 304 K is about 14.02 and 32.12 kW respectively.

- Dried cow dung, a natural desiccant, is an excellent choice for residential dehumidification systems due to its affordability, environmentally-friendly production processes utilizing low temperatures and low-pressure drop when used with SHACs.

CHAPTER 7

CONCLUSIONS AND FUTURE SCOPE

7.1 Conclusions

In this work, an experimental investigation has been carried out to understand the sorption and desorption characteristics of a new composite desiccant based on a natural material. Dried cow dung (DCD) is chosen as the base natural material. DCD and its two composites, DCD+PVP (polyvinyl pyrrolidone), DCD+clay, and their dehumidification systems viz., metal embedment natural composite desiccant dehumidification system and natural composite desiccant coated dehumidification system with hexagonal channels are tested in different compositions and humid conditions.

The BET and BJH analysis of the selected composite desiccants is carried out to understand the type of isotherms, pore volume, BET surface area and pore diameter. DCD and DCD+PVP desiccants follow the type IV isotherm, whereas DCD+Clay desiccant follows the type III isotherm. The maximum moisture uptake capacity of DCD+PVP composite desiccant is observed to be higher than DCD and DCD+Clay composite desiccant. The maximum moisture uptake capacity of DCD, DCD+PVP and DCD+Clay is 9.87, 9.01 and 5.12 g/100 g respectively at 299 K and 85% RH. The exergy analysis reveals that the DCD+PVP has better exergy efficiency compared to DCD and DCD+Clay dehumidification systems. The total heat load reduction of the DCD+PVP dehumidification system is 13.6% and 22.3% higher compared to the DCD and DCD+Clay dehumidification systems respectively. Desorption time for DCD,

DCD+PVP and DCD+Clay is 13, 17 and 15 minutes respectively. However, after the desorption, moisture content remained in DCD+PVP desiccants almost 15% and 35% lower than DCD and DCD+Clay desiccants respectively. The methods and calculations proposed in this study have an error of ±1.5–5%, which is comparable to the accepted uncertainties. The polyvinyl pyrrolidone and clay act as binders to the DCD and reduce the loss of desiccant material during the sorption-desorption process. Based on the isotherm test the optimum binding ratio is found to be 3:1 (DCD:PVP). The addition of PVP increases the life cycle of DCD-based composite desiccants. The PVP is found to be better than clay due to its higher moisture uptake capacity.

The maximum moisture uptake of MENCDs with a TR of 0.365 is 11.84 g/100 g, which is 20.57% higher compared to natural composite desiccants (thickness ratio = 1) at 85% RH. This is because the moisture diffusion rate decreases compared to that of moisture convection when the thickness ratio of MNECDs increases. The maximum moisture uptake rate for MENCDs with a TR = 0.365 is 1.8 g/100 g·min, which is 50% higher compared to TR =1. The total MSR is 0.4 g/100 g·min, which is 25% higher for same the TR. The moisture desorption rate (MDR) for MENCDs with TR = 0.365 is 16.66% higher compared to TR = 1. The average power required in all the different inlet conditions for MENCDs with a TR = 0.365 is 2.33 kW, which is 24.91% less compared to TR = 1. The average exergy efficiency of the MENCDs (TR=0.365) system is 62%, which is 9.65% higher compared to TR = 1. The total heat load reduction for MENCDs (TR = 0.365) is 23.9% higher compared to TR = 1 at 85% RH. For the initial 5 minutes, the rise in temperature due to heat of sorption for TR = 0.365 is 0.13 K/ g of moisture sorbed is less compared to TR = 1. The maximum moisture uptake capacity reached 14.31, 13.13, and 10.2 g/100 g at RH 85, 75, and 65% and a temperature of 300 K respectively. Whereas at a higher temperature of 304 K, MMU gets reduced to 12.97, 10.78, and 8.34 g/100 g for the RH at 85, 75, and 65%, respectively. The maximum moisture uptake capacity of NCD-coated SHACs dehumidification bed is 60.7% higher compared to cow dung balls packed bed at 300-301 K and 85% RH. The optimum thickness ratio (TR) is 0.365.

The natural composite desiccants featuring staggered hexagonal channels exhibited a significantly lower pressure drop compared to the desiccant-packed bed made of natural composite material. This resulted in a 71.11% reduction in energy consumption by the fans. Moreover, the average exergy efficiency is improved approximately by 28%. The average heat load reduction of NCD-coated SHACs dehumidification system at different RH conditions with temperatures of 300 K and 304 K is about 14.02 and 32.12 kW respectively.

7.2 Scope of future work

These natural composite desiccants can be used in desiccant wheels, which is used in evaporative cooling systems. The possible applications of this biomaterial are the removal of pollutants from aqueous media, tertiary wastewater treatment, chemical oxygen demand removal from municipal leachate, biomass densification, biogas and fertilizer production, and it can be converted into electrode material for other energy storage and conversion systems such as Li-ion batteries and fuel cells.

The composite desiccant with SHACs dehumification systems for desiccant wheel evaporative cooling stands out as a promising contender for commercialization due to its performance and sustainable technology product. The composite desiccant with staggered hexagonal channels system leading to a remarkable decrease in pressure drop when compared to the desiccant-packed bed crafted from natural composite material. Consequently, this advancement translates into an impressive reduction in energy consumption by the fans, which are used blow the humidified and dehumidified air

APPENDIX

Uncertainty Analysis

Uncertainty pertains to the level of imprecision or deviation that arises when measuring and computing the performance or physical characteristics of a system. This analysis yields an assessment of the accuracy of the measured data and computed parameters. The physical attributes are measured using calibrated devices, the specifics of which are described in Table 1. However, some physical parameters such as specific humidity, exergy efficiency, and power required for dehumidification cannot be directly measured but are instead calculated based on measurements of relative humidity, temperature, and air velocity. To evaluate the level of imprecision or deviation in these calculated parameters, an uncertainty analysis is conducted using the propagation of the error formula (Su *et al.* 2021; Sun *et al.* 2021; Liu *et al.* 2022).

$U = f(Z_1, Z_2, Z_3.....)$

$$\partial U = \sqrt{\left(\frac{\partial U}{\partial Z_1}\delta Z_1\right)^2 + \left(\frac{\partial U}{\partial Z_2}\delta Z_2\right)^2 + \left(\frac{\partial U}{\partial Z_3}\delta Z_3\right)^2 + \cdots} \tag{1}$$

The notation for the total uncertainty attributed to the parameter U is δU, whereas the notation for the total uncertainty related to parameters $Z1....Z3$ is $\delta Z1....Z3$. Table 2 presents the uncertainty values for exergy efficiency and change in humidity (g/kg) of NCD-coated SHACs dehumidification system.

Table 1: Uncertainty of experimental measurements

Sl. No.	Quantity	Instrument	Uncertainty
1	Temperature	Hygrometer (Testo 605i)	$\delta T = \pm 0.5$ K
2	Velocity	Anemometer	$\delta V = 0.04$ m/s
3	Relative humidity	Hygrometer (Testo 605i)	$\delta RH = \pm 3\%$
4	Mass of desiccant	Electronic weighing machine	$\delta M_d = 0.001$ g
5	Time	Stop watch	$\delta t = 0.01$ s
6	Pressure drop	Digital U-tube manometer (HTC, PM-6025)	$\delta P = \pm 0.2$ Pa

Table 2: Uncertainty of calculated parameters for NCD-coated SHACs dehumidification system at 300 K

Sl. No.	RH (%)	$\Delta\omega$ (g/kg)	Exergy efficiency (-)
1	85	1.4 ± 0.0399	0.20 ± 0.0060
2	75	1.8 ± 0.0441	0.14 ± 0.0188
3	65	1.0 ± 0.0497	0.14 ± 0.0343

Calibration Certificates

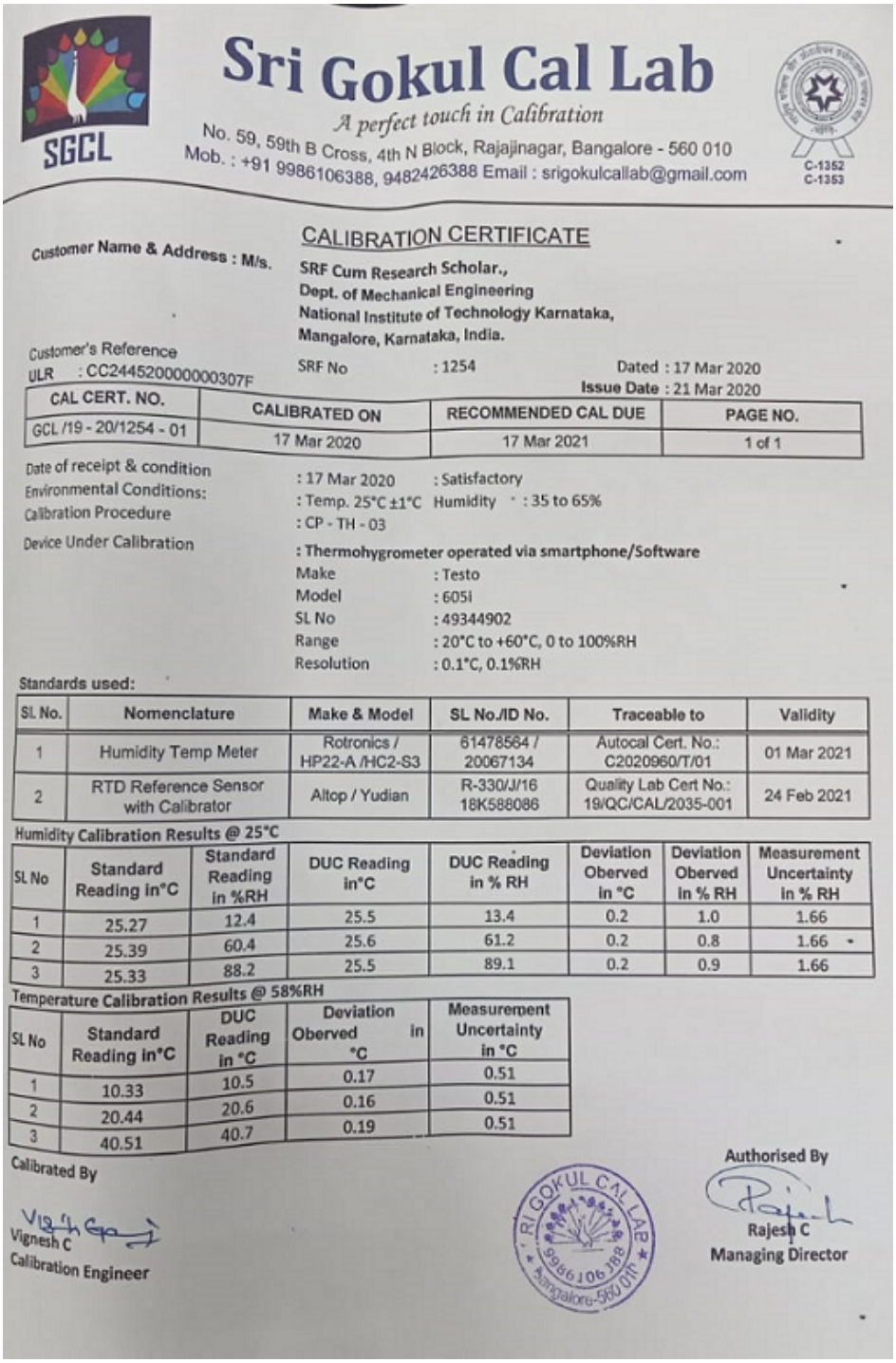

Sri Gokul Cal Lab

A perfect touch in Calibration

No. 59, 59th B Cross, 4th N Block, Rajajinagar, Bangalore - 560 010
Mob. : +91 9986106388, 9482426388 Email : srigokulcallab@gmail.com

C-1352
C-1353

CALIBRATION CERTIFICATE

Customer Name & Address : M/s.

SRF Cum Research Scholar.,
Dept. of Mechanical Engineering
National Institute of Technology Karnataka,
Mangalore, Karnataka, India.

Customer's Reference
ULR : CC244520000000307F

SRF No : 1254

Dated : 17 Mar 2020
Issue Date : 21 Mar 2020

CAL CERT. NO.	CALIBRATED ON	RECOMMENDED CAL DUE	PAGE NO.
GCL /19 - 20/1254 - 01	17 Mar 2020	17 Mar 2021	1 of 1

Date of receipt & condition : 17 Mar 2020 : Satisfactory
Environmental Conditions: : Temp. 25°C ±1°C Humidity : 35 to 65%
Calibration Procedure : CP - TH - 03
Device Under Calibration : Thermohygrometer operated via smartphone/Software
Make : Testo
Model : 605i
SL No : 49344902
Range : 20°C to +60°C, 0 to 100%RH
Resolution : 0.1°C, 0.1%RH

Standards used:

SL No.	Nomenclature	Make & Model	SL No./ID No.	Traceable to	Validity
1	Humidity Temp Meter	Rotronics / HP22-A /HC2-S3	61478564 / 20067134	Autocal Cert. No.: C2020960/T/01	01 Mar 2021
2	RTD Reference Sensor with Calibrator	Altop / Yudian	R-330/J/16 18K588086	Quality Lab Cert No.: 19/QC/CAL/2035-001	24 Feb 2021

Humidity Calibration Results @ 25°C

SL No	Standard Reading in°C	Standard Reading in %RH	DUC Reading in°C	DUC Reading in % RH	Deviation Oberved in °C	Deviation Oberved in % RH	Measurement Uncertainty in % RH
1	25.27	12.4	25.5	13.4	0.2	1.0	1.66
2	25.39	60.4	25.6	61.2	0.2	0.8	1.66
3	25.33	88.2	25.5	89.1	0.2	0.9	1.66

Temperature Calibration Results @ 58%RH

SL No	Standard Reading in°C	DUC Reading in °C	Deviation Observed in °C	Measurement Uncertainty in °C
1	10.33	10.5	0.17	0.51
2	20.44	20.6	0.16	0.51
3	40.51	40.7	0.19	0.51

Calibrated By
Vignesh C
Calibration Engineer

Authorised By
Rajesh C
Managing Director

Figure 1: Calibration of thermohygrometer on 17^{th} Mar 2020

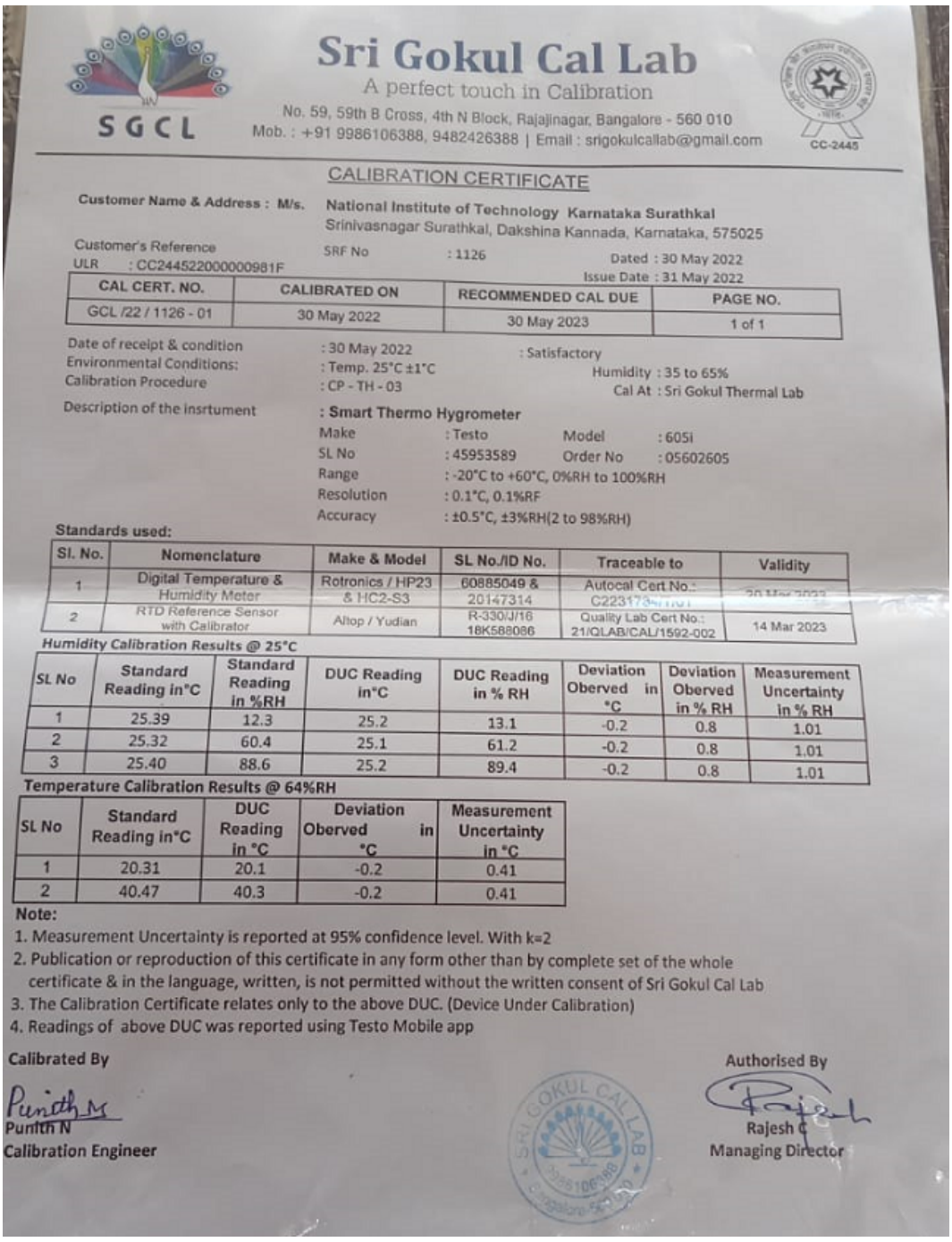

Sri Gokul Cal Lab

A perfect touch in Calibration

SGCL

No. 59, 59th B Cross, 4th N Block, Rajajinagar, Bangalore - 560 010
Mob. : +91 9986106388, 9482426388 | Email : srigokulcallab@gmail.com

CC-2445

CALIBRATION CERTIFICATE

Customer Name & Address : M/s. National Institute of Technology Karnataka Surathkal
Srinivasnagar Surathkal, Dakshina Kannada, Karnataka, 575025

Customer's Reference
ULR : CC244522000000981F

SRF No : 1126

Dated : 30 May 2022
Issue Date : 31 May 2022

CAL CERT. NO.	CALIBRATED ON	RECOMMENDED CAL DUE	PAGE NO.
GCL /22 / 1126 - 01	30 May 2022	30 May 2023	1 of 1

Date of receipt & condition : 30 May 2022 : Satisfactory
Environmental Conditions: : Temp. 25°C ±1°C Humidity : 35 to 65%
Calibration Procedure : CP - TH - 03 Cal At : Sri Gokul Thermal Lab

Description of the insrtument : **Smart Thermo Hygrometer**

Make : Testo Model : 605i
SL No : 45953589 Order No : 05602605
Range : -20°C to +60°C, 0%RH to 100%RH
Resolution : 0.1°C, 0.1%RF
Accuracy : ±0.5°C, ±3%RH(2 to 98%RH)

Standards used:

Sl. No.	Nomenclature	Make & Model	SL No./ID No.	Traceable to	Validity
1	Digital Temperature & Humidity Meter	Rotronics / HP23 & HC2-S3	60885049 & 20147314	Autocal Cert No.: C223178	[illegible]
2	RTD Reference Sensor with Calibrator	Altop / Yudian	R-330/J/16 18K588086	Quality Lab Cert No.: 21/QLAB/CAL/1592-002	14 Mar 2023

Humidity Calibration Results @ 25°C

SL No	Standard Reading in°C	Standard Reading in %RH	DUC Reading in°C	DUC Reading in % RH	Deviation Oberved in °C	Deviation Oberved in % RH	Measurement Uncertainty in % RH
1	25.39	12.3	25.2	13.1	-0.2	0.8	1.01
2	25.32	60.4	25.1	61.2	-0.2	0.8	1.01
3	25.40	88.6	25.2	89.4	-0.2	0.8	1.01

Temperature Calibration Results @ 64%RH

SL No	Standard Reading in°C	DUC Reading in °C	Deviation Oberved in °C	Measurement Uncertainty in °C
1	20.31	20.1	-0.2	0.41
2	40.47	40.3	-0.2	0.41

Note:

1. Measurement Uncertainty is reported at 95% confidence level. With k=2
2. Publication or reproduction of this certificate in any form other than by complete set of the whole certificate & in the language, written, is not permitted without the written consent of Sri Gokul Cal Lab
3. The Calibration Certificate relates only to the above DUC. (Device Under Calibration)
4. Readings of above DUC was reported using Testo Mobile app

Calibrated By

Punith N
Punith N
Calibration Engineer

Authorised By

Rajesh C
Rajesh C
Managing Director

Figure 2: Calibration of thermohygrometer on 30^{th} May 2022

REFERENCES

Ahmed, M., N. Kattab, and M. Fouad (2005). Evaluation and optimization of solar desiccant wheel performance. *Renewable Energy*, 30(3), 305–325.

Al-Sharqawi, H. S. and N. Lior (2007). The effect of flow-duct geometry on solid desiccant dehumidification. *Heat Transfer Summer Conference*, 42762, 209–226.

Arens, E. *et al.* (2017). Ansi/ashrae standard 55-2017 thermal environmental conditions for human occupancy. *Atlanta: ASHRAE*.

Barčauskaitė, K., Z. Brazienė, D. Avižienytė, M. Silva, D. Drapanauskaite, K. Honer, K. Gvildienė, R. Slinksiene, K. Jancaitiene, R. Mazeika, *et al.* (2020). Mechanochemically synthesized gypsum and gypsum drywall waste cocrystals with urea for enhanced environmental sustainability fertilizers. *Journal of Environmental Chemical Engineering*, 8(4), 103965.

Barrett, E. P., L. G. Joyner, and P. P. Halenda (1951). The determination of pore volume and area distributions in porous substances. i. computations from nitrogen isotherms. *Journal of the American Chemical society*, 73(1), 373–380.

Bejan, A., *Advanced engineering thermodynamics*. John Wiley & Sons, 2016.

Bhabhor, K. and D. Jani (2021). Performance analysis of desiccant dehumidifier with different channel geometry using cfd. *Journal of Building Engineering*, 44, 103021.

Birol, F. (2018). The future of cooling: opportunities for energy-efficient air conditioning. *International Energy Agency*.

Brunauer, S., P. H. Emmett, and E. Teller (1938). Adsorption of gases in multimolecular layers. *Journal of the American chemical society*, 60(2), 309–319.

Chen, C. H., C. Y. Hsu, C. C. Chen, and S. L. Chen (2015). Silica gel polymer composite desiccants for air conditioning systems. *Energy and buildings*, 101, 122–132.

Chen, C.-H., C.-Y. Hsu, C.-C. Chen, Y.-C. Chiang, and S.-L. Chen (2016). Silica gel/polymer composite desiccant wheel combined with heat pump for air-conditioning systems. *Energy*, 94, 87–99.

Cho, W., S. Kato, R. Ooka, Y.-S. Tsay, M. Koganei, N. Shoda, and K. Kawamoto, Study on dehumidification performance of fam-z rotor. *In the 6th international conference on indoor air quality, ventilation & energy conservation in buildings IAQVEC*. 2007.

Choi, D., J. Shin, and Y. Park (2021). Effects of $cacl_2$ on cyclic carbonation-calcination kinetics of cao-based composite for potential application to solar thermochemical energy storage. *Chemical Engineering Science*, 230, 116207.

Chua, K. J., S. K. Chou, and M. R. Islam (2018). On the experimental study of a hybrid dehumidifier comprising membrane and composite desiccants. *Applied Energy*, 220, 934–943.

Courbon, E., P. D'Ans, A. Permyakova, O. Skrylnyk, N. Steunou, M. Degrez, and M. Frère (2017). Further improvement of the synthesis of silica gel and $cacl_2$ composites: Enhancement of energy storage density and stability over cycles for solar heat storage coupled with space heating applications. *Solar Energy*, 157, 532–541.

Cui, S., M. Qin, A. Marandi, V. Steggles, S. Wang, X. Feng, F. Nouar, and C. Serre (2018). Metal-organic frameworks as advanced moisture sorbents for energy-efficient high temperature cooling. *Scientific reports*, 8(1), 1–9.

Czanderna, A. W. and H. Neidlinger (1990). Polymers as advanced materials for desiccant applications, 1988. Technical report, Solar Energy Research Inst., Golden, CO (USA).

Dai, L., Y. Yao, F. Jiang, X. Yang, X. Zhou, and P. Xiong (2017). Sorption and regeneration performance of novel solid desiccant based on pva-licl electrospun nanofibrous membrane. *Polymer Testing*, 64, 242–249.

Davis, L., P. Gertler, S. Jarvis, and C. Wolfram (2021). Air conditioning and global inequality. *Global Environmental Change*, 69, 102299.

De Antonellis, S., E. Bramanti, L. Calabrese, B. Campanella, and A. Freni (2022). A novel desiccant compound for air humidification and dehumidification. *Applied Thermal Engineering*, 214, 118857.

De Antonellis, S., L. Colombo, A. Freni, and C. Joppolo (2021). Feasibility study of a desiccant packed bed system for air humidification. *Energy*, 214, 119002.

Dehmani, Y. and S. Abouarnadasse (2020). Study of the adsorbent properties of nickel oxide for phenol depollution. *Arabian Journal of Chemistry*, 13(5), 5312–5325.

Dhawan, V., N. Shah, G. Dreyfuss, D. Zaelke, Z. Osho, A. Murphy, and S. Seth (2023). Low carbon development pathways for cooling: Leveraging kigali amendment across residential applications.

Duong, X. Q., N. V. Cao, W. S. Lee, M. Y. Park, J. D. Chung, K. J. Bae, and O. K. Kwon (2021). Effect of coating thickness, binder and cycle time in adsorption cooling applications. *Applied Thermal Engineering*, 184, 116265.

Fagerlund, G. (1973). Determination of specific surface by the bet method. *Matériaux et Construction*, 6, 239–245.

Florides, G. A., S. A. Tassou, S. A. Kalogirou, and L. Wrobel (2002). Review of solar and low energy cooling technologies for buildings. *Renewable and Sustainable Energy Reviews*, 6(6), 557–572.

Gao, Z., V. C. Mei, and J. J. Tomlinson (2005). Theoretical analysis of dehumidification process in a desiccant wheel. *Heat and mass transfer*, 41, 1033–1042.

Garba, J., W. A. Samsuri, R. Othman, and M. S. A. Hamdani (2019). Evaluation of adsorptive characteristics of cow dung and rice husk ash for removal of aqueous glyphosate and aminomethylphoshonic acid. *Scientific reports*, 9(1), 17689.

Ge, F. and C. Wang (2020). Exergy analysis of dehumidification systems: A comparison between the condensing dehumidification and the desiccant wheel dehumidification. *Energy Conversion and Management*, 224, 113343.

Ge, T., R. Hao, Y. Dai, R. Wang, and H. Yan (2017). Experimental investigation on anti-condensation characteristic of desiccant coated metal cabinet. *Renewable Energy*, 113, 835–845.

Hall, M. and D. Allinson (2009). Analysis of the hygrothermal functional properties of stabilised rammed earth materials. *Building and Environment*, 44(9), 1935–1942.

Han, H., P. Pang, N. Zhong, Q. Luo, Y. Ma, and Y. Gao (2020). The pore characteristics and gas potential of the jurassic continental shales in the middle-small basins, northwest china. *Journal of Petroleum Science and Engineering*, 188, 106873.

Hashemi, S. M., M. Mohamedali, M. H. Sedghkerdar, and N. Mahinpey (2022). Stability of cao-based sorbents under realistic calcination conditions: Effect of metal oxide supports. *ACS Sustainable Chemistry & Engineering*.

Henninger, S. K., S.-J. Ernst, L. Gordeeva, P. Bendix, D. Frohlich, A. D. Grekova, L. Bonaccorsi, Y. Aristov, and J. Jaenchen (2017). New materials for adsorption heat transformation and storage. *Renewable Energy*, 110, 59–68.

Hiremath, C. and R. Kadoli (2022). Adsorption and desorption through packed and fluidized clay-based composite desiccant beds: a comparison study. *Journal of the Brazilian Society of Mechanical Sciences and Engineering*, 44(4), 1–19.

Hiremath, C., R. Kadoli, and V. Katti (2018). Experimental and theoretical study on dehumidification potential of clay-additives based $CaCl_2$ composite desiccants. *Applied Thermal Engineering*, 129, 70–83.

Hiremath, C., V. Katti, and R. Kadoli (2014). Experimental determination of specific heat and thermal conductivity of clay+ additives-cacl$_2$ composite desiccant. *Procedia Materials Science*, 5, 188–197.

Hiremath, C. R. and K. Ravikiran (2021). Experimental analysis of low-temperature grain drying performance of vertical packed clay and clay-additives composite desiccant beds. *Sādhanā*, 46(1), 1–16.

Hyland, R. W. and C. W. Hurley (1983). General guidelines for the on-site calibration of humidity and moisture control systems in buildings. *Building science series*, (157).

Intini, M., M. Goldsworthy, S. White, and C. M. Joppolo (2015). Experimental analysis and numerical modelling of an aqsoa zeolite desiccant wheel. *Applied Thermal Engineering*, 80, 20–30.

Iwuozor, K. O., E. C. Emenike, C. O. Aniagor, F. U. Iwuchukwu, E. M. Ibitogbe, O. B. Temitayo, P. E. Omuku, and A. G. Adeniyi (2022). Removal of pollutants from aqueous media using cow dung-based adsorbents. *Current Research in Green and Sustainable Chemistry*, 100300.

Jia, C., Y. Dai, J. Wu, and R. Wang (2006). Experimental comparison of two honeycombed desiccant wheels fabricated with silica gel and composite desiccant material. *Energy Conversion and Management*, 47(15-16), 2523–2534.

Kadoli, R., T. A. Babu, and K. A. Ramzy (2011). Improved utilization of desiccant material in packed bed dehumidifier using composite particles. *Renewable energy*, 36(2), 732–742.

Kadoli, R., T. A. Babu, *et al.* (2012). Performance studies on the desiccant packed bed with varying particle size distribution along the bed. *International journal of refrigeration*, 35(3), 663–675.

Kurlov, A., A. M. Kierzkowska, T. Huthwelker, P. M. Abdala, and C. R. Müller (2020).

Na_2CO_3-modified cao-based co_2 sorbents: the effects of structure and morphology on co_2 uptake. *Physical Chemistry Chemical Physics*, 22(42), 24697–24703.

Lee, J. and D. Y. Lee (2012). Sorption characteristics of a novel polymeric desiccant. *International journal of refrigeration*, 35(7), 1940–1949.

Lee, K. C., J. H. Her, and S. K. Kwon (2008). Red clay composites reinforced with polymeric binders. *Construction and Building Materials*, 22(12), 2292–2298.

Li, X., J. Chen, X. Sun, Y. Zhao, C. Chong, Y. Dai, and C.-H. Wang (2021). Multi-criteria decision making of biomass gasification-based cogeneration systems with heat storage and solid dehumidification of desiccant coated heat exchangers. *Energy*, 233, 121122.

Liu, Z., C. Cheng, J. Han, Z. Zhao, and X. Qi (2022). Experimental evaluation of the dehumidification performance of a metal organic framework desiccant wheel. *International Journal of Refrigeration*, 133, 157–164.

Ma, Q. and X. Zheng (2022). Preparation and characterization of thermo-responsive composite for adsorption-based dehumidification and water harvesting. *Chemical Engineering Journal*, 429, 132498.

Majumdar, P. (1998). Heat and mass transfer in composite desiccant pore structures for dehumidification. *Solar energy*, 62(1), 1–10.

Narayanan, R. (2017). Investigation of geometry effects of channels of a silica-gel desiccant wheel. *Energy Procedia*, 110, 20–25.

Ng, K. C., H. Chua, C. Chung, C. Loke, T. Kashiwagi, A. Akisawa, and B. B. Saha (2001). Experimental investigation of the silica gel-water adsorption isotherm characteristics. *Applied Thermal Engineering*, 21(16), 1631–1642.

Sing, K. S. (1985). Reporting physisorption data for gas/solid systems with special reference to the determination of surface area and porosity (recommendations 1984). *Pure and applied chemistry*, 57(4), 603–619.

Singh, A., S. Kumar, and R. Dev (2019). Studies on cocopeat, sawdust and dried cow dung as desiccant for evaporative cooling system. *Renewable Energy*, 142, 295–303.

Strobel, M., U. Jakob, W. Streicher, and D. Neyer (2023). Spatial distribution of future demand for space cooling applications and potential of solar thermal cooling systems. *Sustainability*, 15(12), 9486.

Su, M., X. Han, D. Chong, J. Wang, J. Liu, and J. Yan (2021). Experimental study on the performance of an improved dehumidification system integrated with precooling and recirculated regenerative rotary desiccant wheel. *Applied Thermal Engineering*, 199, 117608.

Subramanyam, N., M. Maiya, and S. S. Murthy (2004). Application of desiccant wheel to control humidity in air-conditioning systems. *Applied thermal engineering*, 24(17-18), 2777–2788.

Sun, X., J. Chen, Y. Zhao, X. Li, T. Ge, C. Wang, and Y. Dai (2021). Experimental investigation on a dehumidification unit with heat recovery using desiccant coated heat exchanger in waste to energy system. *Applied Thermal Engineering*, 185, 116342.

Susianti, B., I. Warmadewanthi, and B. V. Tangahu (2022). Characterization and experimental evaluation of cow dung biochar + dolomite for heavy metal immobilization in solid waste from silica sand purification. *Bioresource Technology Reports*, 101102.

Tashiro, Y., M. Kubo, Y. Katsumi, T. Meguro, and K. Komeya (2004). Assessment of adsorption-desorption characteristics of adsorbents for adsorptive desiccant cooling system. *Journal of materials science*, 39(4), 1315–1319.

Thommes, M., K. Kaneko, A. V. Neimark, J. P. Olivier, F. Rodriguez-Reinoso, J. Rouquerol, and K. S. Sing (2015). Physisorption of gases, with special reference to the evaluation of surface area and pore size distribution (iupac technical report). *Pure and applied chemistry*, 87(9-10), 1051–1069.

Tian, H., L. Pan, X. Xiao, R. W. Wilkins, Z. Meng, and B. Huang (2013). A preliminary study on the pore characterization of lower silurian black shales in the chuandong thrust fold belt, southwestern china using low pressure N_2 adsorption and fe-sem methods. *Marine and Petroleum Geology*, 48, 8–19.

Touloumet, Q., G. Postole, L. Silvester, L. Bois, and A. Auroux (2022). Hierarchical aluminum fumarate metal-organic framework-alumina host matrix: Design and application to $cacl_2$ composites for thermochemical heat storage. *Journal of Energy Storage*, 50, 104702.

Tretiak, C. and N. B. Abdallah (2009). Sorption and desorption characteristics of a packed bed of clay–$CaCl_2$ desiccant particles. *Solar Energy*, 83(10), 1861–1870.

Tso, C. Y. and C. Y. Chao (2012). Activated carbon, silica-gel and calcium chloride composite adsorbents for energy efficient solar adsorption cooling and dehumidification systems. *International journal of refrigeration*, 35(6), 1626–1638.

Valarezo, A. S., X. Sun, T. Ge, Y. Dai, and R. Wang (2019). Experimental investigation on performance of a novel composite desiccant coated heat exchanger in summer and winter seasons. *Energy*, 166, 506–518.

Vivekh, P., M. Kumja, D. Bui, and K. Chua (2018). Recent developments in solid desiccant coated heat exchangers–a review. *Applied energy*, 229, 778–803.

Vu, D. H., K. S. Wang, B. H. Bac, and B. X. Nam (2013). Humidity control materials prepared from diatomite and volcanic ash. *Construction and Building Materials*, 38, 1066–1072.

Wang, C., B. Yang, X. Ji, R. Zhang, and H. Wu (2022). Study on activated carbon/silica gel/lithium chloride composite desiccant for solid dehumidification. *Energy*, 251, 123874.

Yefeng, L. and W. Ruzhu (2003). Pore structure of new composite $SiO_2 \cdot xH_2O \cdot yCaCl_2$ with uptake of water air. *Sci. China, Ser. E: Technol. Sci*, 46, 551–559.

Younes, M. M., I. I. El-sharkawy, A. Kabeel, K. Uddin, A. Pal, S. Mitra, K. Thu, and B. B. Saha (2019). Synthesis and characterization of silica gel composite with polymer binders for adsorption cooling applications. *International Journal of Refrigeration*, 98, 161–170.

Yu, N., R. Wang, Z. Lu, and L. Wang (2014). Development and characterization of silica gel–licl composite sorbents for thermal energy storage. *Chemical engineering science*, 111, 73–84.

Zhang, H., W. Gu, M. Li, Z. Li, Z. Hu, and W. Tao (2014). Experimental study on the kinetics of water vapor sorption on the inner surface of silica nano-porous materials. *International Journal of Heat and Mass Transfer*, 78, 947–959.

Zhang, H., Y. Yuan, Q. Sun, X. Cao, and L. Sun (2016). Steady-state equation of water vapor sorption for $cacl_2$-based chemical sorbents and its application. *Scientific reports*, 6(1), 1–8.

Zhang, L.-Z. (2015). Transient and conjugate heat and mass transfer in hexagonal ducts with adsorbent walls. *International Journal of Heat and Mass Transfer*, 84, 271–281.

Zhang, X. and L. Qiu (2007). Moisture transport and adsorption on silica gel–calcium chloride composite adsorbents. *Energy conversion and management*, 48(1), 320–326.

Zhang, X., K. Sumathy, Y. Dai, and R. Wang (2006). Dynamic hygroscopic effect of the composite material used in desiccant rotary wheel. *Solar energy*, 80(8), 1058–1061.

Zhang, Z. and Z. Yang (2013). Theoretical and practical discussion of measurement accuracy for physisorption with micro-and mesoporous materials. *Chinese Journal of Catalysis*, 34(10), 1797–1810.

Zhao, H., S. Jia, J. Cheng, X. Tang, M. Zhang, H. Yan, and W. Ai (2017). Experimental investigations of composite adsorbent $13X/CaCl_2$ on an adsorption cooling system. *Applied Sciences*, 7(6), 620.

Zhao, H., Z. Wang, Q. Li, T. Wu, M. Zhang, and Q. Shi (2020). Water sorption on composite material zeolite 13*X* modified by licl and $cacl_2$. *Microporous and Mesoporous Materials*, 299, 110109.

Zheng, X., T. Ge, L. Hu, and R. Wang (2015*a*). Development and characterization of mesoporous silicate-licl composite desiccants for solid desiccant cooling systems. *Industrial & engineering chemistry research*, 54(11), 2966–2973.

Zheng, X., T. Ge, Y. Jiang, and R. Wang (2015*b*). Experimental study on silica gel-licl composite desiccants for desiccant coated heat exchanger. *International journal of refrigeration*, 51, 24–32.

Zheng, X., R. Wang, and W. Ma (2020). Dehumidification assessment for desiccant coated heat exchanger systems in different buildings and climates: Fast choice of desiccants. *Energy and Buildings*, 221, 110083.

Zhou, B. and Z. Chen (2016). Experimental study on the hygrothermal performance of zeolite-based humidity control building materials. *Int J Heat & Tech*, 34(3), 407–414.

PUBLICATIONS BASED ON THIS THESIS

Journal Papers

1. **Dasar SR,** Boche AM, Yadav AK, Anish S. *"Sorption–desorption characteristics of dried cow dung with PVP and clay as composite desiccants: Experimental and exergetic analysis"* Renewable Energy. 2023 Jan 1;202:394-404. **(SCI, IF - 8.634)** available from: https://doi.org/10.1016/j.renene.2022.11.094

2. **Dasar SR,** Anish S, Kadoli R, Yadav AK. *"Experimental study on sorption-desorption characteristics of natural composite desiccant with metal embedment"* Applied Thermal Engineering. 2023 Apr 5:120516. **(SCI, IF - 6.465)** Available from: https://doi.org/10.1016/j.applthermaleng.2023.120516

3. **Dasar SR,** Naveen KB, Sonu KS, Anish S, Yadav AK. *"Experimental study on sorption-desorption characteristics of a natural composite desiccant coated on staggered hexagonal aluminium channels"* (To be submitted)

Conference Papers/Posters

1. **Sangappa R. Dasar,** Ajay K. Yadav, Anish S. "*Experimental investigation on sorption and desorption of silica gel based composite desiccants*" Proceedings of the 25^{th} National and 3^{rd} International ISHMT-ASTFE Heat and Mass Transfer Conference (IHMTC-2019), December 28-31, 2019, IIT Roorkee, Roorkee, India.

CURRICULUM VITAE

SANGAPPA R. DASAR

Kesapura (village), Alur (post)

Muddebihal (taluk), Vijayapura (district)

Karnataka - 586129

Contact: +91 89434 58659

Email: sangappadasar@gmail.com

EDUCATIONAL QUALIFICATIONS

(PhD): Mechanical Engineering

NITK, Surathkal, 2023

CGPA: 5.75

B.Tech: Mechanical Engineering

SJCIT Chickballapur, KA, 2013

67.85%

M.Tech: Energy Engineering and Management

NIT Calicut, Kerala, 2015

CGPA: 6.75

10+2 (PUC): Science

Seshadripuram Independent P U College

Seshadripuram, Bengaluru, KA, 2009

53.66%

10th (SSLC): NA

Govt. High School Alur, Vijayapura, KA,

2007

87.36%

WORK EXPERIENCE

- Ad-hoc faculty at department of mechanical engineering, NIT Calicut, India from January 2016 to May 2017
- Project Associate at Maire Tecnimont Centre for Clean Energy and Circular Econ-

omy, NITK Surathkal, India from 12^{th} December 2022 to present date.

TECHNICAL SKILLS

- Technical background in Thermodynamics, Heat transfer, Fluid mechanics and CFD
- Skilled in Modelling software: SolidWorks, Ansys-Design Modeller/Space claim
- Analytical software: Ansys Fluent
- Typesetting and presentation software: LaTeX, Beamer, MS Word, MS Excel and MS PPT
- Familiar with MATLAB®

RESEARCH AREA INTEREST

- Fluid Flow and Heat Transfer in Porous Media
- Computational Fluid Dynamics
- Heating, Ventilation, Air Conditioning, and Refrigeration

WORKSHOP/PROGRAMS ATTENDED

- Global Initiative of Academic Networks (GAIN) 2 week course on Advances in Renewable energy Technology. held at NIT Calicut, 02-13 January 2017.
- Two days national workshop on "MATLAB and its applications" held at NIT Calicut, 07-09 March 2017.

LANGUAGES

- Kannada, English and Hindi
